EVALUATION OF NAVICULAR SYNDROME HORSES WITH MAGNETIC RESONANCE IMAGING TO IDENTIFY STRUCTURES INVOLVED, PREVALENCE AND LOCATION OF INJURY, AND EVALUATION OF A SURGICAL APPROACH FOR TRANSECTION OF THE COLLATERAL SESAMOIDEAN LIGAMENT

By

SARAH NASEECHIS SAMPSON

A dissertation submitted in partial fulfillment of
the requirements for the degree of

DOCTOR OF PHILOSOPHY

WASHINGTON STATE UNIVERSITY
College of Veterinary Medicine

DECEMBER 2008

To the Faculty of Washington State University:

The members of the Committee appointed to examine the dissertation of SARAH NASEECHIS SAMPSON find it satisfactory and recommend that it be accepted.

_____
Chair

_____

_____

_____

ACKNOWLEDGMENT

This thesis was a group effort, and it is with sincere appreciation and respect that I thank my committee for having the courage to undertake this project and then to provide the assistance needed to complete it. To my committee chair, Dr. Patrick Gavin, who has my heartfelt gratitude for his patience with my endless questions on the finer points of magnetic resonance imaging and the finer points of being a doctoral candidate. To Dr. Bob Schneider, for the guidance that helped me finish this project, and the day to day support with the clinical aspects of this project-as well as continuous, at times never-ending it seemed, review of the manuscripts contained herein. I cannot thank you enough for the many years of support and the faith you had that I would finish this. To Dr. Bob Mealey, for your willingness to be a part of this project and help in any way needed, your humor and enthusiasm were appreciated on many days. To Dr. Warwick Bayly, who has always come through for me, even when you don't have the time. Your support and excellent advice over the years, many more than you probably want to count, and your tireless efforts on my behalf never went unnoticed.

I also must thank Dr. Tim Baszler, who made the time to spend many hours with me in the pathology laboratory when I know he had other pressing duties. Your enthusiasm and interest in this project was appreciated and I am grateful to have had access to your expertise. And to Dr. Russ Tucker, who had faith in me long before I began this project, and has helped and encouraged and given me opportunities I wouldn't have had otherwise. I admire all of you in so many different ways, and it has been an honor to work with each of you.

The day to day running of theses projects included many people over several years and I must thank Caryn Rumble, Lethea Hunter, Molly Bellefieulle, Jillian Connolly, Chad Whetzel, and Astan Lucenti for their excellent assistance with the daily care and examination of the horses. I appreciated the kindness you showed these horses as they made much of this research possible. I must also thank Vicki Mitzemburg for freely giving her time to help with the imaging of the horses-many days went much smoother because of her assistance. And lastly, I should really thank the horses, as that is what this project is really all about, both now and in the future.

This research was supported in part by a grant from the American Quarter Horse Foundation and Victoria Cavallero.

EVALUATION OF NAVICULAR SYNDROME HORSES WITH MAGNETIC RESONANCE IMAGING TO IDENTIFY STRUCTURES INVOLVED, PREVALENCE AND LOCATION OF INJURY, AND EVALUATION OF A SURGICAL APPROACH FOR TRANSECTION OF THE COLLATERAL SESAMOIDEAN LIGAMENT

Abstract

by Sarah Naseechis Sampson, Ph.D.
Washington State University
December 2008

Chair: Patrick R. Gavin

The first goal of this study was to develop optimal, standardized magnetic resonance imaging protocols for the foot of the horse using a 1 Tesla magnet. The optimal magnetic resonance imaging evaluation was determined to contain proton density, T2-weighted, short tau inversion recovery, and gradient echo sequences in axial, sagittal, and coronal image planes. This enabled detailed examination of the front feet of horses with lameness localized to this area. The second goal of this study was to examine horses with recent and chronic onset of navicular syndrome to test the hypothesis that the pathologic changes found in the feet of these two groups of horses would be similar when evaluated with magnetic resonance imaging. These results provided evidence that the location, severity, and prevalence of structures affected is different in these two groups of horses and determinations could be made as to the likelihood of specific pathology based on the specific group the horse was in. The horses with chronic signs of navicular disease had an increased likelihood of having multiple structures affected within the foot and the

overall prevalence of injury to each structure was increased. The third goal of this study was to determine if a surgical treatment involving desmotomy of the collateral sesamoidean ligament in normal horses could be a viable treatment option for use in horses with navicular syndrome that were clinically affected with pathologic change in this ligament. This surgical procedure did not cause long term lameness in normal horses and was determined to be a possible treatment option for horses clinically affected with pathologic change in the collateral sesamoidean ligament.

TABLE OF CONTENTS

Page

LIST OF TABLES

Chapter 1

Chapter 2

Chapter 4

LIST OF FIGURES

Chapter 1

Chapter 2

Chapter 3

Chapter 4

Dedication

This thesis is dedicated to my husband Scott, my sons Lucas & Turner, my father Jim Haggarty, my mother Donyne & second father John Gray, and to my second mother Ann Sampson - your love and support, year after year, made this all possible.

CHAPTER ONE

MAGNETIC RESONANCE IMAGING IN THE HORSE

Routine Image Acquisition

In horses, magnetic resonance (MR) enables the generation of high resolution, thin cross-sectional images of the extremities and head. These images can be acquired in any desired orientation and are commonly acquired in transverse, sagittal, and dorsal planes. The number of slices and thickness of the slices can be varied to cover a region of interest or focus on a specific structure.

There are 3 gradient coils surrounding the bore of the magnet, named according to the axis along which they act. The Z gradient (transverse) affects the magnetic field along the long axis, the Y gradient (dorsal) affects the magnetic field along the vertical axis, and the X gradient (sagittal) affects the magnetic field along the horizontal axis. The isocenter of the magnet is the intersection of all 3 gradients, within the center point of the bore of the magnet and is the optimal position for imaging. Slice selection is based on selectively exciting protons in a given area by applying a radiofrequency (RF) pulse at exactly the resonant frequency of the protons in that area. The resonant frequency is determined by the magnetic field gradient produced within the magnet. Slice thickness is altered by changing the slope of the chosen gradient, to result in either thinner (steep slope) or thicker (shallow slope) slices.

Magnetic resonance examinations are typically composed of several sequences which are selected by the MR operator based on developed study protocols providing the most diagnostic information in the shortest imaging times. Each selected sequence should yield unique anatomic and physiologic information. The appearance of different tissues will vary according to the type of sequence. Examples of pathologic changes seen with

different MR imaging sequences can be found in several recent publications.[1-21] It is necessary to use several sequences, in multiple image planes, to accurately identify normal and pathologic conditions. Several new MR sequences are being evaluated in human imaging which may provide additional information for future equine musculoskeletal applications. The physics of MR sequences is complex and beyond the scope of this review. A more in depth understanding is available in suggested references.[22-23]

The following routine sequences have proven useful at our institution, with a typical MR examination producing several hundred images to review (Table 1). Optimal imaging protocols will vary between institutions based on the type of MR system available and clinical experience. The following explanations are brief introductions to the common sequences currently used in equine musculoskeletal examinations.

The common categories of conventional MR sequences include Spin Echo (SE) and Turbo Spin Echo (TSE), Gradient Echo (GE), and Inversion Recovery (IR). The fundamental differences in these sequences are the method and timing of how the RF signals are pulsed into the tissues and subsequently collected to generate the images. Under the influence of the magnetic field (measured in Tesla, a unit of magnetic strength) the available hydrogen protons will absorb the introduced RF pulses and change in magnetic orientation. As the RF pulse is discontinued, the protons will return ("relax") back to their original orientation. During this relaxation phase, the emitted signal is collected to create the MR image. The MR sequences yield differing signal characteristics for each tissue based on specific relaxation characteristics under the selected imaging parameters. Two fundamental parameters which determine the sequence

type are the repetition time (TR) and echo time (TE), both measured in milliseconds. TR dictates the time interval between the RF pulses introduced into the tissues. TE determines the time interval between the introduction of the RF pulse and the time of signal collection.

T1 Weighted Sequences (T1)

One important aspect of the MR signal is the characteristic relaxation of individual tissues along the longitudinal magnetic axis. Longitudinal relaxation (T1 relaxation) becomes progressively greater in magnitude after the RF pulse is turned off. It is the time required for the net magnetization to grow to 63% of its final amplitude. It is generally accepted that at a time equal to five times the specific T1 relaxation of any specific tissue, longitudinal relaxation is complete. T1 relaxation results in the recovery of longitudinal magnetization due to energy dissipation into the surrounding tissue lattice. The appearance of the different T1 relaxations can be highlighted by using pulse sequence parameters that yield T1-weighted images (short TR, short TE). T1-weighted images highlight differences in tissues due to their differences in T1 characteristics. T1-weighted images are characterized by bright (hyperintense) fat and dark (hypointense) fluid. T1-weighted sequences are useful for bone and soft tissue evaluation and produce high resolution anatomic images with relatively good signal strength. T1-weighted sequences are also used to view paramagnetic contrast (gadolinium) enhanced imaging, such as MR arthrography or bursal injections.

T2 Weighted Sequences (T2)

Another important aspect of MR tissue signal is the characteristic relaxation between protons transverse to the longitudinal axis. Transverse relaxation (T2 relaxation)

occurs when the RF pulse is applied, and the influenced protons become “in phase”. T2 relaxation is defined as the time at which the transverse magnetization has decayed to 37% of its full value, which is the time of one elapsed “T2 period”. Transverse decay is essentially over by five times the specific T2 relaxation time of any specific tissue. T2 relaxation results in the loss of transverse magnetization due to interactions between the magnetic fields of adjacent nuclei. A signal is only induced if there is magnetization within the in-phase transverse plane. T2 weighted images (long TR, long TE) are characterized by bright fluid and bright fat. T2-weighted sequences are useful for bone and soft tissue evaluation and readily demonstrate most fluid accumulations.

Proton Density Sequences (PD)

Proton Density (PD) refers to differences in signal intensity between tissues due to the relative number of protons. Tissues that have a high free proton density have a large transverse component of magnetization, resulting in a high signal (ie. fat). Tissues with a low number of available protons have a small transverse component of magnetization, resulting in low signal (ie. cortical bone). Proton density weighted images (long TR, short TE) are characterized by bright areas of high proton density and dark areas of low proton density. Proton density sequences are useful for bone and soft tissue evaluation and provide high resolution of anatomic information.

Gradient Echo Sequences (GE)

Gradient Echo (GE) refers to a fast imaging sequence that uses very short repetition times, making the typical spin-echo RF pulses too long to use. Because of the short TR, it is necessary to superimpose a magnetic field gradient over the existing external magnetic field. This magnetic field gradient is switched on and off for short

intervals which produces peak signal intensities that are collected by the receiver coil. 3D GE sequences are highly susceptible to magnetic field inhomogeneities (such as residual metal fragments and rust within horseshoe nail tracts) because of the uneven magnetic environment, but can be acquired much faster than spin echo sequences. 3D GE sequences can provide the opportunity to view very thin anatomic sections and are used to evaluate bone and soft tissues.

Short Tau Inversion Recovery Sequences (STIR)

The STIR sequence employs an inversion time (typically100-175 ms, depending on magnet field strength) that corresponds to the time it takes fat to recover from full inversion to the transverse plane, resulting in no longitudinal magnetization and, therefore, no signal corresponding to fat. The images created are called “fat suppression” scans because no/low signal is present from fat. This can highlight fluid in areas high in fat content (ie. medullary cavity). Conventional STIR sequence scan times can be reduced by using them in conjunction with fast spin echo.

As previously stated, it is important to understand that the imaging protocols that are used by differing institutions will vary according to the type of MR system employed and clinical experience at each site. The following protocols are based on over 10 years of experience attempting to obtain the most useful information, both anatomic and physiologic, in the shortest total scan time. We routinely image both right and left limbs to allow critical comparison between the suspected lesion(s) and the contralateral limb, or to diagnose bilateral pathology. A standard MR examination will result in hundreds of images in several sequences and slice planes that will require careful evaluation. It is therefore essential to acquire standard image planes and sequences to allow for critical

review between the limbs of an individual horse and between different horses. Excessive imaging, or deviation from established protocols, will frequently complicate interpretation and can lead to misdiagnosis or missed lesions.

Symmetrical, repeatable images are most easily obtained by keeping the distal limb to be imaged in a neutral position that is neither flexed nor extended (dorsal cortices alignment). This is usually possible in the front limb, but can be more difficult in the hind limb due to the reciprocal apparatus. Foam padding can be used to obtain this alignment during MR examinations, with care taken to avoid deformation of the soft tissues by putting excessive pressure on the area of interest with the positioning pads. Dorsal cortices alignment also localizes the potential for the "magic angle" artifact which occurs most commonly in the foot when the deep digital flexor tendon is at a 55 degree angle from the constant magnetic field.[24-26] If an external labeling marker is desired, vitamin E capsules taped to the lateral aspect of the limb seem to be the most inexpensive and are easily applied.

Image Orientation & Sequence Selection

Foot

Imaging of the distal pastern and foot of the horse is completed using a selection of imaging sequences to obtain the most accurate information regarding pathologic change. Proton density, T2, and STIR sequences are used to obtain slices in the sagittal (Figure 1), transverse (Figure 2), and dorsal (Figure 3) planes that span from the insertion of the straight distal sesamoidean ligament on the proximopalmar/plantar middle phalanx to the tip of the distal phalanx. The 3D GE sequence is used to obtain thin slices centered over the navicular bone in the transverse and dorsal planes. The transverse navicular bone

slices are obtained from the proximal aspect of the navicular suspensory ligament to the insertion of the deep digital flexor tendon on the palmar/plantar aspect of the distal phalanx (Figure 4). These slices are aligned perpendicular to the long axis of the navicular bone, based on a sagittal reference slice. The dorsal navicular bone slices are obtained by centering the slices over the navicular bone and distal phalanx and aligning the slice plane with the proximal to distal axis of the navicular bone (Figure 5) and at the same time centering the slices over the navicular bone and aligning the slice plane with the flexor cortex of the bone. Setup for all imaging sequences is referenced to the other two slice planes to produce the most symmetrical images in sagittal, transverse, and dorsal planes. Depending on the specific lesions suspected or lesions found during imaging, new slice planes or additional sequences can be added to better visualize the area of concern.

Pastern

Imaging of the pastern of the horse is completed using sequences similar to those used for the foot. Proton density, T2, and STIR sequences are used to obtain slices in the sagittal and transverse planes from the metacarpo/tarsophalangeal joint to the heel bulbs. The sagittal slices are obtained from the metacarpo/tarsophalangeal joint to the proximal aspect of the second phalanx and aligned with the long axis of the distal limb, perpendicular to the palmar/plantar cortex of the distal aspect of the first phalanx (Figure 6). The transverse slices are obtained from the metacarpo/tarsophalangeal joint to the proximal aspect of the second phalanx (Figure 7) and must be aligned parallel to the proximal interphalangeal joint space, or the distal articular surface of the first phalanx or the proximal articular surface of the second phalanx to obtain the most symmetrical slices

through the joint. The 3D GE sequence is used to obtain thin slices in the dorsal plane as it is helpful to assess joint pathology. The dorsal slices are aligned perpendicular to the distal joint surface on the sagittal slice and parallel to the palmar/plantar aspect of the proximal phalanx on the transverse slice (Figure 8). Depending on the specific lesions suspected or lesions discovered during imaging, new slice planes or additional sequences can be added to better visualize the area of concern.

Types of Equipment

Low-Field and High-Field Magnets

Clinical MR imaging systems operate from magnetic field strengths as low as 0.2 Tesla to as high as 3.0 Tesla, where 1 Tesla is equal to 10,000 Gauss. The fundamental design of any MR system requires the part of the patient to be examined to be placed into a strong magnetic field. This creates a magnetic influence on the available hydrogen protons within the tissue, which are then subjected to multiple radiofrequency (RF) pulses, ultimately emitting a RF signal collected to generate the images.

The strength of the magnetic field is determined by the inherent system design and type of magnet employed. By using large permanent magnets, it is possible to generate low-field strength MR systems. These systems are less expensive to purchase and maintain, but are restricted to low-field strengths, typically 0.2-0.3 Tesla. This field-strength yields lower image resolution and tissue signal, and requires longer acquisition times. Use of low-field magnets has been reported in the horse and examples of pathology visible with these magnets are available.[17, 27]

The high-field magnets are super conducting electromagnets that are cylindrical structures open at each end. Signal strength and resolution increases with higher magnetic

field strength. Consequently, high-field magnets yield more detailed images, tissue differentiation, and signal strength than low-field magnets. Research magnets can have strong magnetic field strengths up to 11 T, but have very small bore sizes limiting their use to imaging only small tissue samples. The cost of clinical MR system purchase and maintenance increases with magnetic field strength. The high-field strength magnets also require close attention to the safety precautions around the magnetic field with any ferromagnetic materials.

Magnetic field strength is most uniform in closed magnets which are those that are cylindrical, with openings at one or both ends. Open magnets are those that have an open design of the magnet, typically using permanent magnets supported by pedestals. Open magnets do not maintain a uniform magnetic field as well as closed magnetic designs and image signal strength and resolution is decreased from that of closed, high-field magnets.

Imaging horses with high-field MR systems requires that the horse be placed under general anesthesia and some type of non-magnetic patient support system be used that is capable of positioning the horse adjacent to the magnet bore. Most high-field magnet systems are able to image forelimbs of horses from the foot to the distal radius, hindlimbs from the foot to distal tibia, and the entire head, including the first cervical vertebrae. It is also possible to image shoulders and stifles of miniature horses and foals, as the limiting factor is the size of the openings at the end of the magnet and the overall bore diameter.

Standing Magnets

A low-field magnetic resonance imaging system is now available that can image the distal limbs of standing horses. These have become very popular because of the lower cost of these units compared to high-field magnets, as well as the ability to image sedated horses standing, instead of under general anesthesia. Presently, there are low-field strength magnets of 0.2-0.3 T field strength.

Horses are sedated during scanning, but limb motion continues to be a challenge. Motion correction software has been developed for the standing magnets, and this continues to improve image quality, but image resolution is inherently inferior to images obtained on higher field strength systems with the horse under general anesthesia. Low-field strength systems also require larger acquisition times because of less tissue signal being generated.

Images obtained with currently available low-field magnets on standing horses cover a much smaller field of view. Small structures such as the impar ligament and the navicular suspensory ligament are more difficult to adequately visualize and evaluate with current low-field imaging. The flexor tendons and collateral ligaments are visible, but their edges are much less defined than with high-field imaging systems. The inversion recovery sequences (fat suppression) are very low signal/noise quality, so subtle lesions within the subchondral and medullary bone which require uniform fat suppression may be missed.

The standing magnetic systems require operation in a stable temperature environment. Additionally, because of the open design of the magnet, there is a tendency towards a non-uniform magnetic field which causes artifacts within the images produced. It is necessary for the continued refinement and improvement of low-field standing

magnet systems before they will be universally accepted as an accurate imaging modality relative to high-field strength systems. It is critical to appreciate the limitations of low-field magnets in regard to MR of equine limbs, or diagnoses may be concluded without sufficient anatomic and physiologic resolution or detail.

References

1. Busoni V, Heimann M, Trenteseaux J, *et al*: Magnetic resonance imaging findings in the equine deep digital flexor tendon and distal sesamoid bone in advanced navicular disease-an ex vivo study. *Vet Rad & Ultrasound* 46(4):279-286, 2005.

2. Dyson S, Murray R, Schramme M: Lameness associated with foot pain: results of magnetic resonance imaging in 199 horses (January 2001-December 2003) and response to treatment. *Equine Vet J* 37(2):113-121, 2005.

3. Dyson S, Murray R, Schramme M, *et al*: Magnetic resonance imaging of the equine foot: 15 horses. *Equine Vet J* 35:18-26, 2003.

4. Dyson SJ, Murray RC, Schramme MC, *et al*: Collateral desmitis of the distal interphalangeal joint in 18 horses (2001-2001). *Equine Vet J* 36(2):160-166, 2004.

5. Dyson SJ, Murray RC, Schramme MC, *et al*: Magnetic resonance imaging in 18 horses with palmar foot pain. *AAEP proceedings* 48:145-154, 2002.

6. Dyson SJ, Murray RC, Schramme MC, *et al*: Lameness in 46 horses associated with deep digital flexor tendonitis in the digit: diagnosis confirmed with magnetic resonance imaging. *Equine Vet J* 35(7):681-690, 2003.

7. Sampson SN, Schneider RK, Tucker RL: Magnetic Resonance Imaging of the Equine Distal Limb, in Auer JA and Stick JA (eds): Equine Surgery (ed 3). Philadelphia, PA, Saunders, 2005, pp 946-963.

8. Mehl ML, Tucker RL, Ragle CA, *et al*: The use of MRI in the diagnosis of equine limb disorders. *Equine Pract* 20:14-17, 1998.

9. Murray RC, Dyson SJ, Schramme MC, *et al*: Magnetic resonance imaging of the equine digit with chronic laminitis. *Vet Rad & Ultrasound* 44:609-617, 2003.

10. Murray R, Roberts BL, Schramme MC, *et al*: Quantitative evaluation of equine deep digital flexor tendon morphology using magnetic resonance imaging. *Vet Rad & Ultrasound* 45(2):103-111, 2004.

11. Anastasiou A, Skioldebrand E, Ekman S, *et al*: *Ex vivo* magnetic resonance imaging of the distal row of equine carpal bones: assessment of bone sclerosis and cartilage damage. *Vet Rad & Ultrasound* ;44(5):501-512, 2003.

12. Zubrod CJ, Farnsworth KD, Tucker RL, *et al*: Injury of the collateral ligaments of the distal interphalangeal joint diagnosed by magnetic resonance. *Vet Rad & Ultrasound* 46(1):11-16, 2005.

13. Zubrod CJ, Schneider RK, Tucker RL, *et al*: Use of magnetic resonance imaging for identifying subchondral bone damage in horses: 11 cases (1999-2003). *JAVMA* 224:411-418, 2004.

14. Zubrod CJ, Schneider RK, Tucker RL: Use of magnetic resonance imaging to identify suspensory desmitis and adhesions between exostoses of the second metacarpal bone and the suspensory ligament in four horses. *JAVMA* 224(11):1815-1820, 2004.

15. Tapprest J, Audigie F, Radier C, *et al*: Magnetic resonance imaging for the diagnosis of stress fractures in a horse. *Vet Rad & Ultrasound* 44(4):438-442, 2003.

16. Tucker RL, Sande RD: Computed tomography and magnetic resonance imaging in equine musculoskeletal conditions. *Vet Clin North Am (Equine Pract)* 17:145-157, 2001.

17. Mair TS, Kinns J: Deep digital flexor tendonitis in the equine foot diagnosed by low-field magnetic resonance imaging in the standing patient: 18 cases. *Vet Rad & Ultrasound* 46(6):458-466, 2005.

18. Ferrell EA, Gavin PR, Tucker RL, et al: Magnetic resonance for evaluation of neurologic disease in 12 horses. *Vet Rad & Ultrasound* 43(6):510-516, 2002.

19. Spoormakers TJP, Ensink JM, Goehring LS, *et al*: Brain abscesses as a metastatic manifestation of strangles: symptomatology and the use of magnetic resonance imaging as a diagnostic aid. *Equine Vet J* 35(2):146-151, 2003.

20. Audigie F, Tapprest J, George C, *et al*: Magnetic resonance imaging of a brain abscess in a 10 month old filly. *Vet Rad & Ultrasound* 45(3):210-215, 2004.

21. Sanders SG, Tucker RL, Bagley RS, *et al*: Magnetic resonance imaging features of equine nigropallidal encephalomalacia. *Vet Rad & Ultrasound* 42(4):291-296, 2001.

22. Tidwell AS, Jones JC: Advanced Imaging Concepts: a pictorial glossary of CT and MRI technology, in Murtaugh RJ (ed): Clinical Techniques in Small Animal Practice 14(2):65-111, 1999.

23. Kraft SL, Gavin PR:Physical principles and technical considerations for equine computed tomography and magnetic resonance imaging. *Vet Clin North Am (Equine Pract)* 17:115-130, 2001.

24. Erickson SJ, Cox IH, Hyde JS, *et al*: Effect of tendon orientation on magnetic resonance imaging signal intensity: a manifestation of the “magic angle” phenomenon. *Radiology* 389-392, 1991.

25. Erickson SJ, Prost RW, Timins ME: The “magic angle” effect: background physics and clinical relevance. *Radiology* 188:23-25, 1993.

26. Busoni V, Snaps F. Effect of deep digital flexor tendon orientation on magnetic resonance imaging signal intensity in isolated equine limbs-the magic angle effect. *Vet Rad & Ultrasound* 43(5):428-430, 2002.

27. Murray R, Mair TS: Use of magnetic resonance imaging in lameness diagnosis in the horse. *Eq Pract* 27:138-146, 2005.

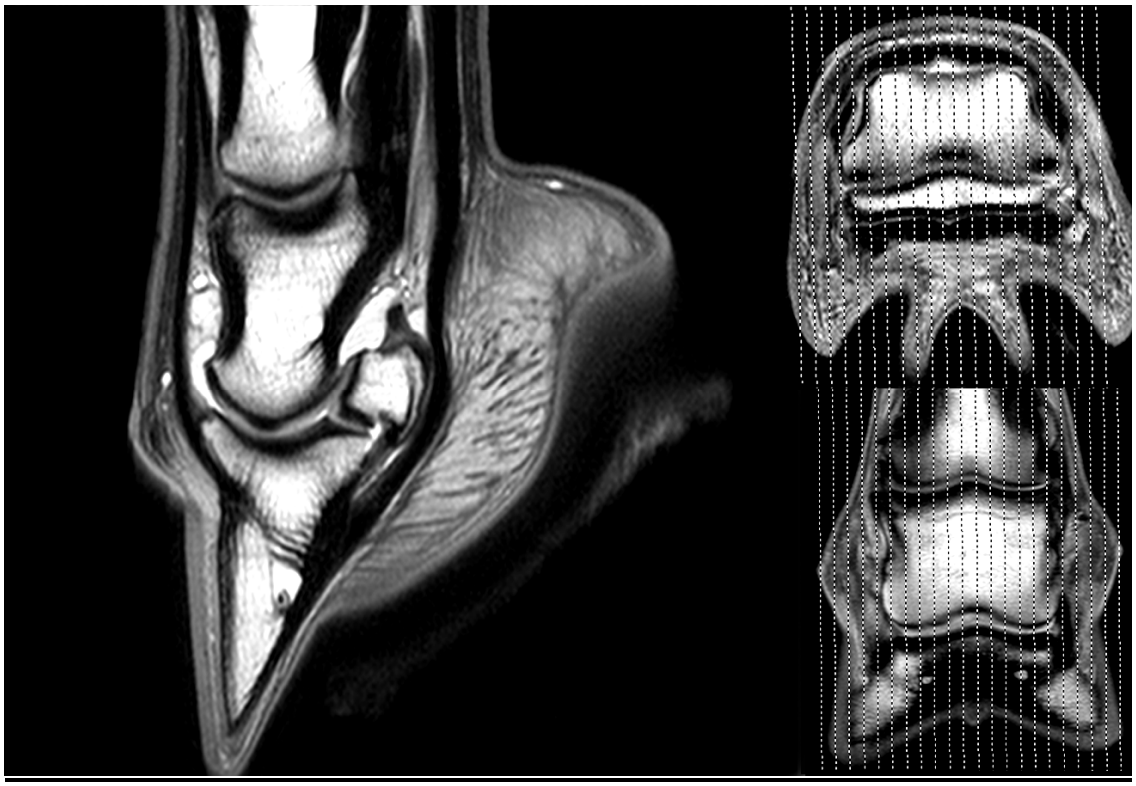

Figure 1: Slice Planes for Sagittal Foot Images. The sagittal slice is shown on the left with the transverse (upper right) and dorsal (lower right) reference set up images.

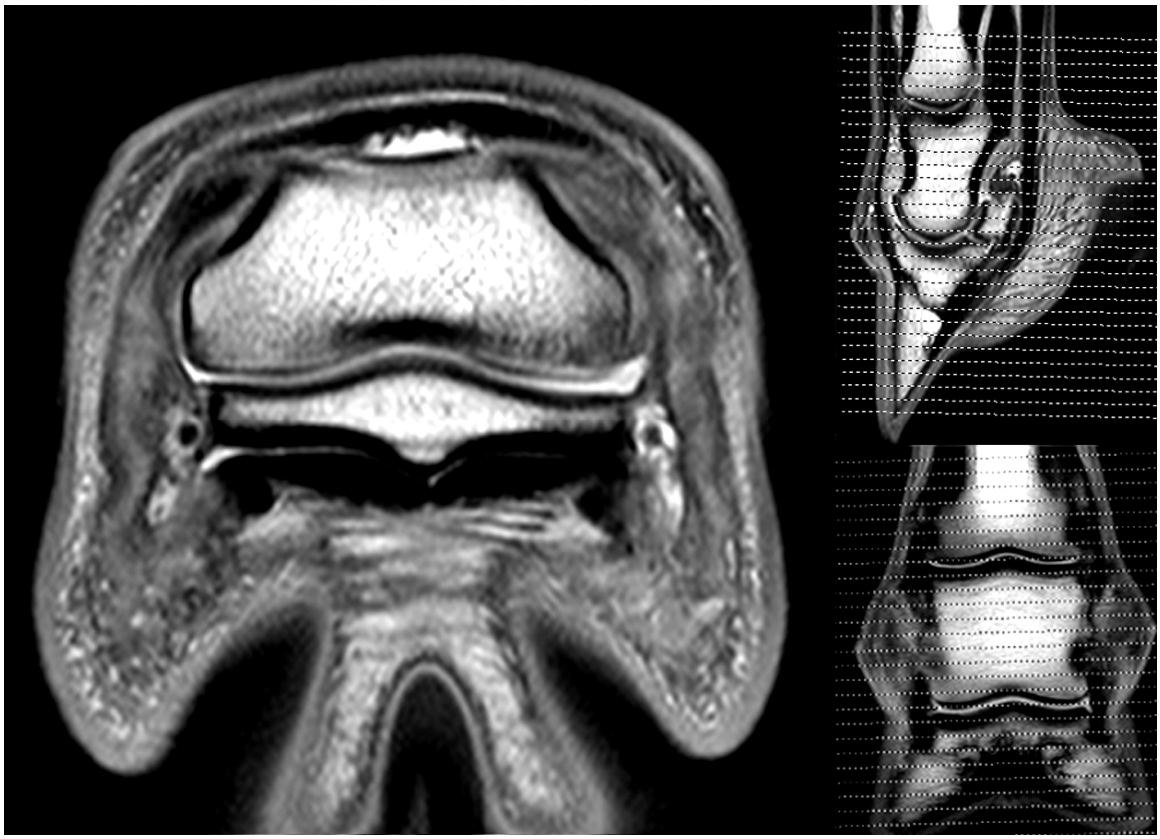

Figure 2: Slice Planes for Transverse Foot Images. The transverse slice is shown on the left with the sagittal (upper right) and dorsal (lower right) reference set up images.

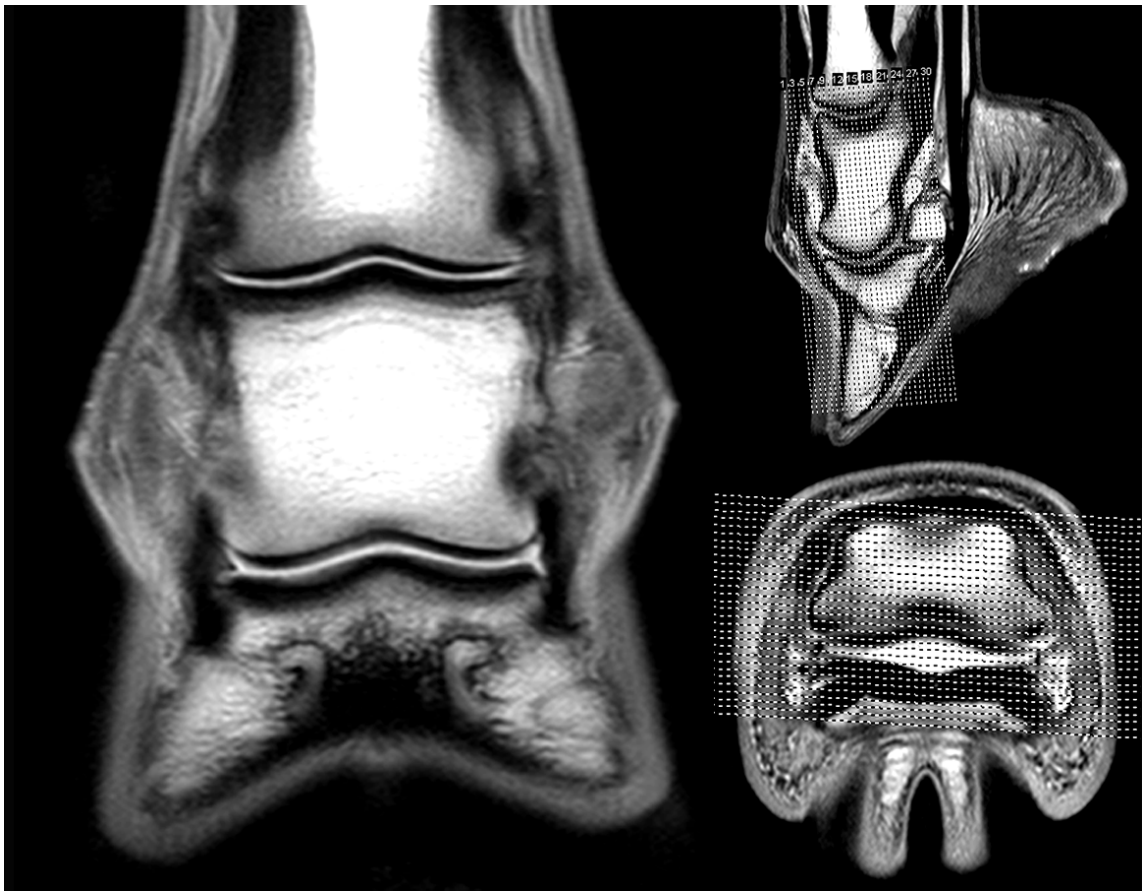

Figure 3: Slice Planes for Dorsal Foot Images. The dorsal slice is shown on the left with the sagittal (upper right) and transverse (lower right) reference set up images.

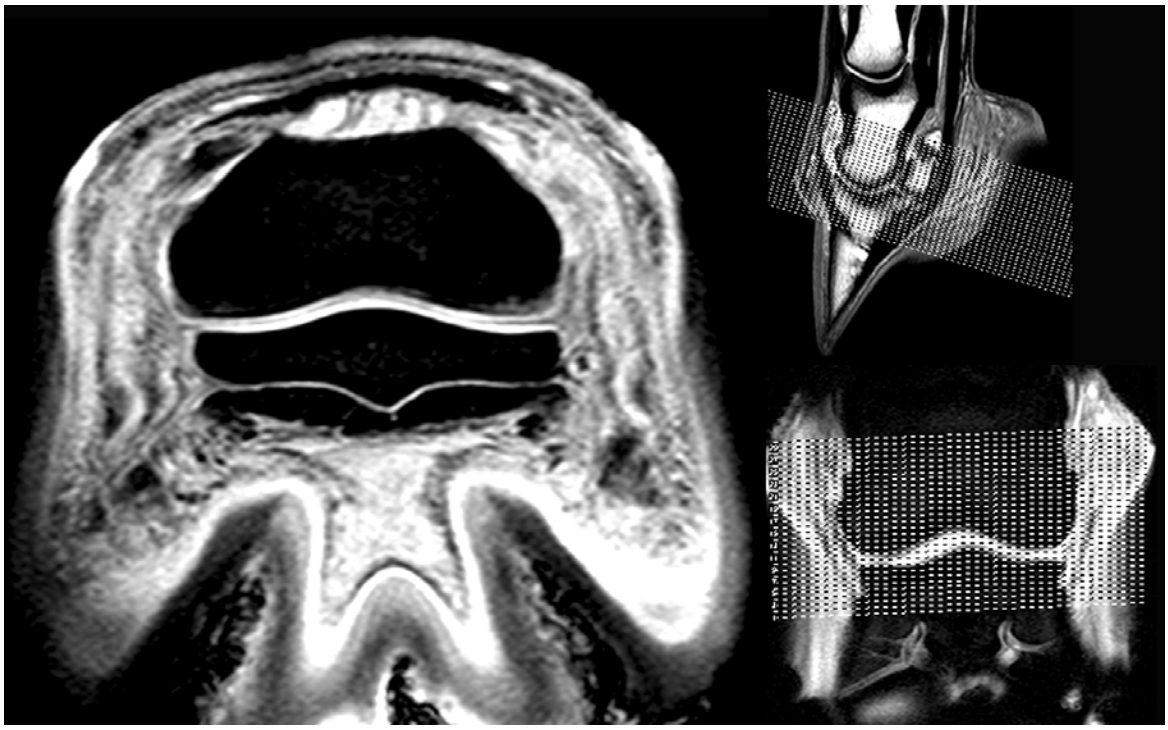

Figure 4: Slice Planes for Transverse Navicular Images. The transverse slice is shown on the left with the sagittal (upper right) and dorsal (lower right) reference set up images.

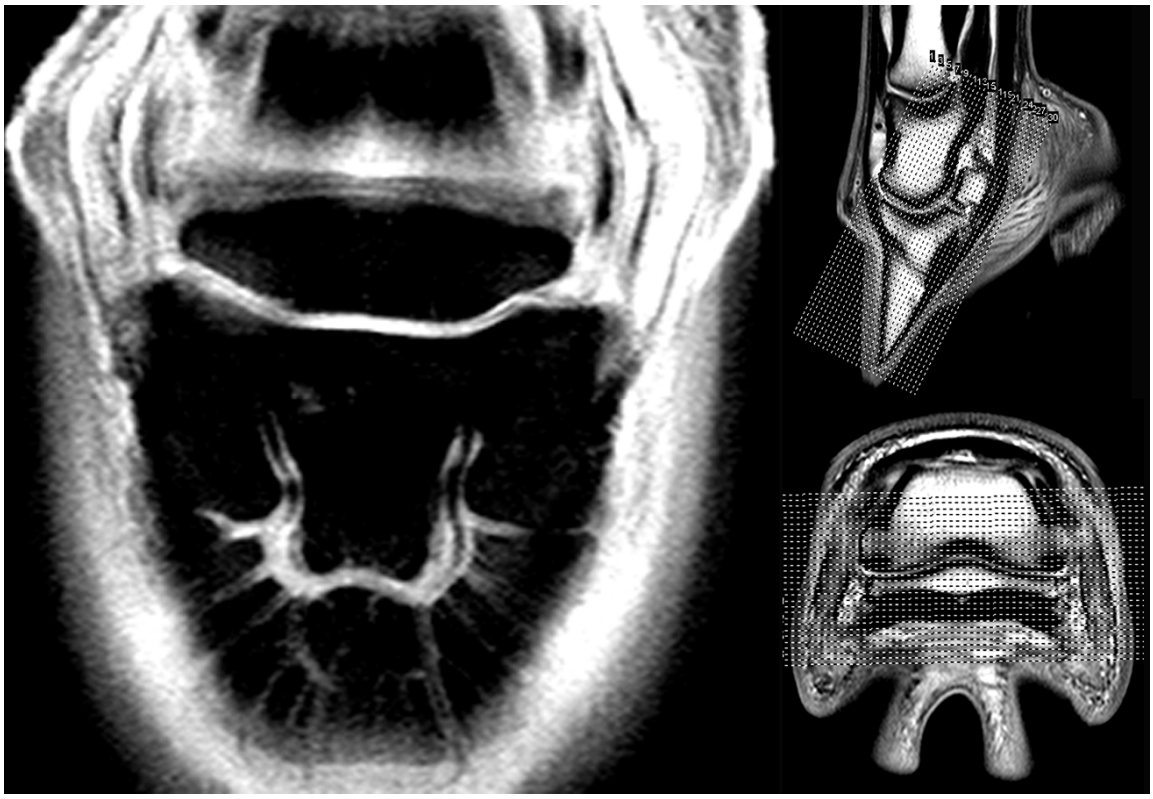

Figure 5: Slice Planes for Dorsal Navicular Images. The dorsal slice is shown on the left with the sagittal (upper right) and transverse (lower right) reference set up images.

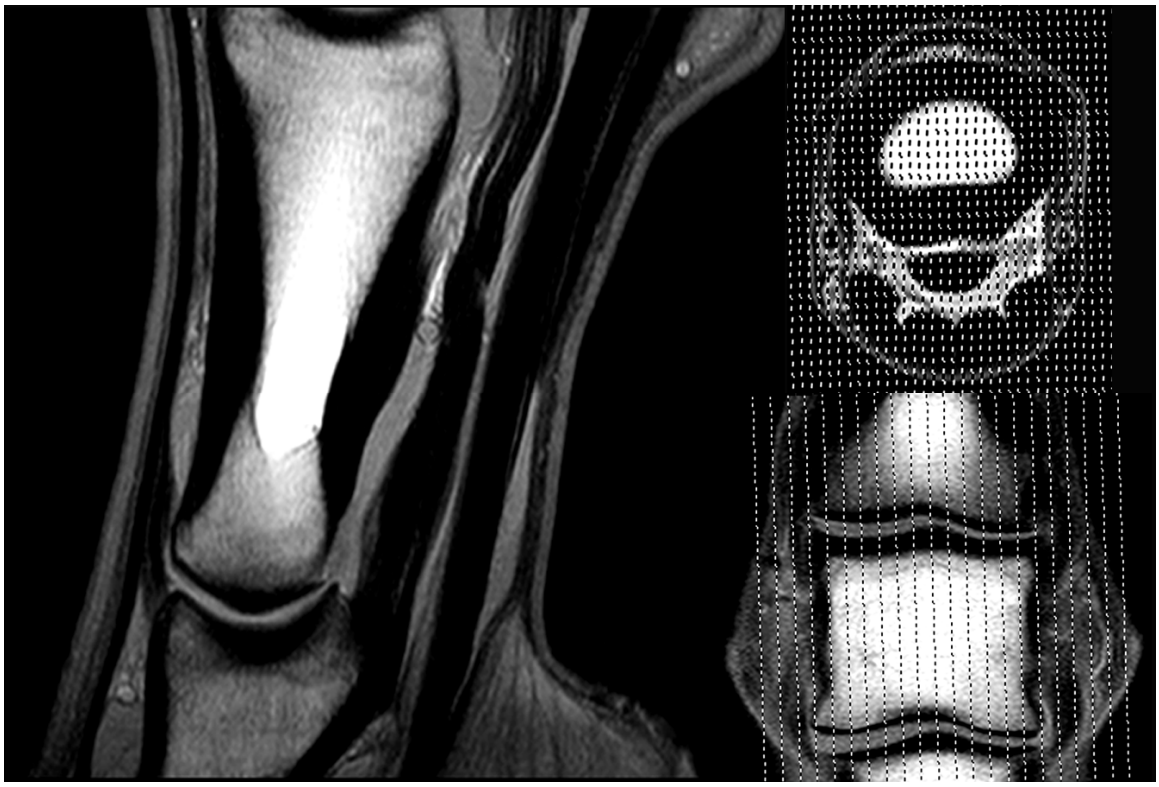

Figure 6: Slice Planes for Sagittal Pastern Images. The sagittal slice is shown on the left with the transverse (upper right) and dorsal (lower right) reference set up images.

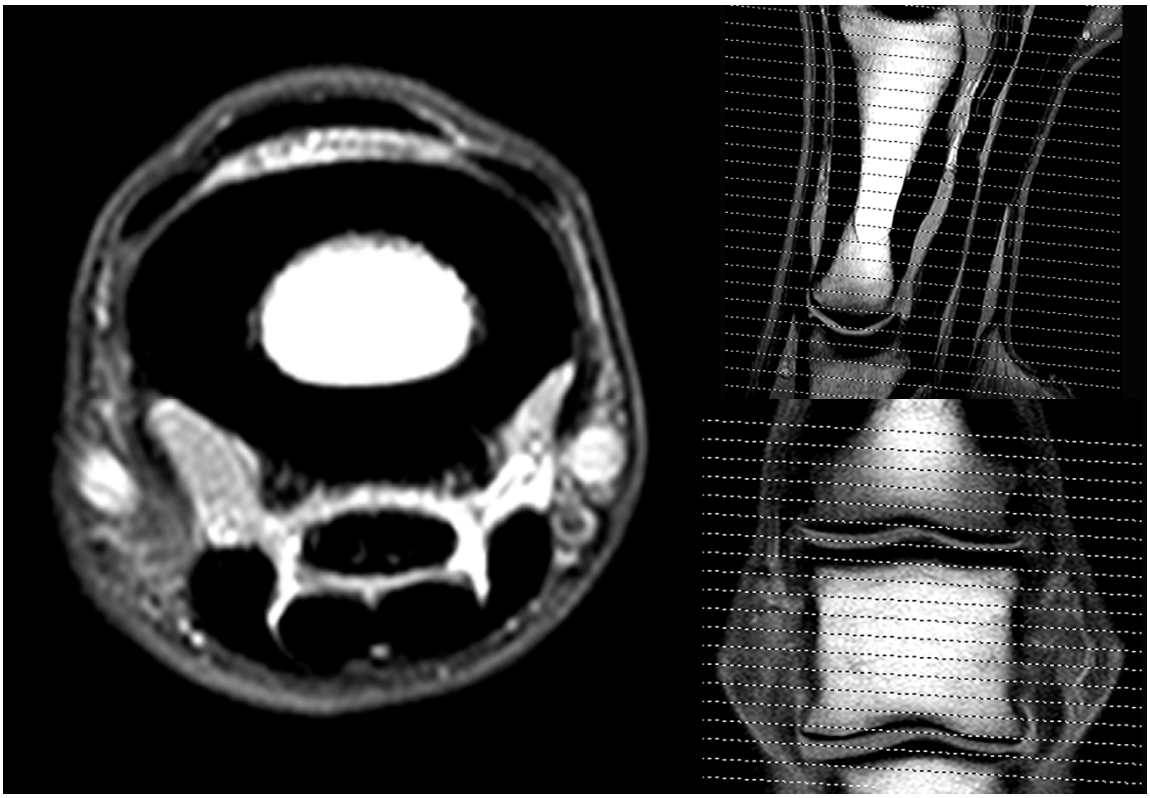

Figure 7: Slice Planes for Transverse Pastern Images. The transverse slice is shown on the left with the sagittal (upper right) and dorsal (lower right) reference set up images.

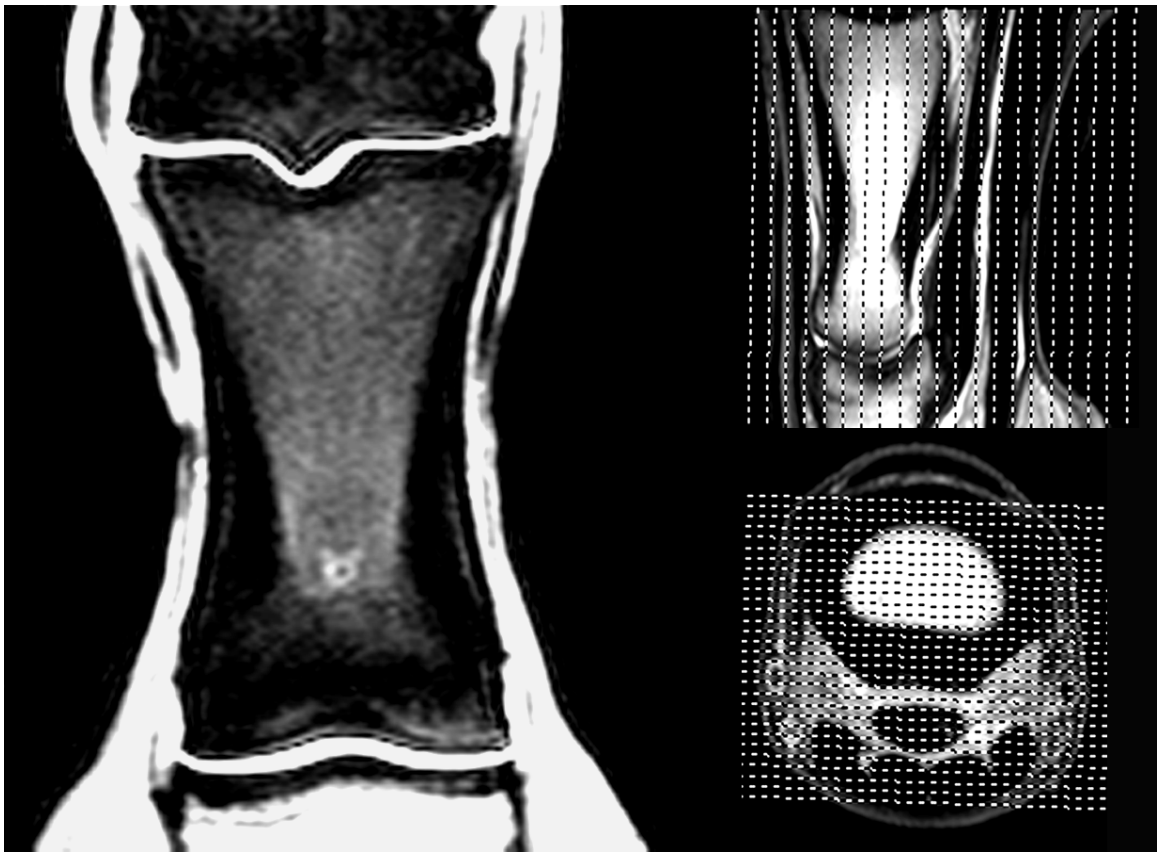

Figure 8: Slice Planes for Dorsal Pastern Images. The dorsal slice is shown on the left with the sagittal (upper right) and transverse (lower right) reference set up images.

Table 1: 1.0 Tesla Magnetic Resonance Imaging Protocols for the Horse. This table outlines the basic MR imaging sequences used for the horse's foot and pastern in a closed super-conducting 1.0 Tesla magnet.

Slice Plane	Sequence	TR (msec)	TE (msec)	FA	FOV/ rFOV	Matrix Size	Slice #/ Width	Gap (mm)	Time (min)
Foot									
Transverse	TSE T2	2116	100	90	15/10.5	256x512	30/4mm	0.5	5:08
Transverse	TSE PD	2116	11	90	15/10.5	256x512	30/4mm	0.5	**
Transverse	STIR*	1725	35	90	15/10.5	192x256	30/3.5mm	1.0	4:42
Transverse	3D GE	47	9	25	10/10	192x256	30/1.5mm	-1.5	3:13
Sagittal	TSE T2	3395	110	90	14/10	256x512	22/4mm	0.5	2:21
Sagittal	TSE PD	3395	14	90	14/10	256x512	22/4mm	0.5	2:21
Sagittal	STIR*	1500	35	90	14/10	256x256	22/3.5mm	0.5	5:48
Dorsal	3D GE	47	9	25	10/10	192x256	30/1.5mm	-1.5	3:13
Pastern									
Transverse	TSE T2	2116	100	90	15/10.5	256x512	30/4.5mm	0.5	3:54
Transverse	TSE PD	2116	10.5	90	15/10.5	256x512	30/4.5mm	0.5	**
Transverse	STIR*	1725	35	90	15/10.5	192x256	30/4mm	1.0	5:17
Sagittal	TSE T2	1738	110	90	12/11	256x512	24/3.2mm	0.4	2:22
Sagittal	TSE PD	1738	13.8	90	12/11	256x512	24/3.2m	0.4	2:22
Sagittal	STIR*	1500	35	90	12/11	192x256	24/3.0mm	0.6	5:12
Dorsal	3D GE	47	8.3	25	12/11	192x256	40/1.5mm	-1.5	4:41

*Inversion time (TI) for STIR sequences is 140 msec
**T2 and PD sequences are collected together during the TSE scan
T1pre = T1 weighted pre contrast
T1post = T1 weighted post contrast
TSE = Turbo spin echo
STIR = Short tau inversion recovery
3D GE = Three dimensional gradient echo
TSE PD = Proton density
TSE T2 = T2-weighted
TR = Repetition Time
TE = Echo time
FA = Flip Angle
FOV/rFOV = Field of view/Relative field of view
Slice # = Number of slices
Width = Thickness of slice
Gap = Space between slices
Time = Actual scanning time for each sequence

CHAPTER TWO

HORSES WITH RECENT ONSET OF NAVICULAR SYNDROME

Introduction

Navicular syndrome is one of the most common causes of forelimb lameness in many types of athletic horses.[1-3] Despite the frequency with which the syndrome occurs, the initiating cause and the pathogenesis of navicular bone degeneration is not clearly understood. Many theories exist about the pathophysiology of navicular syndrome.[4-9] The vascular theory proposes that the pain and degeneration associated with the navicular bone are the result of ischemic necrosis caused by thrombi in the digital arteries.[4] Intimal proliferation and arteriosclerosis of vessels supplying the navicular bone has also been suggested as a cause of ischemic necrosis.[5,6] A biomechanical theory has been proposed based on histopathologic observations of horses with navicular syndrome. Abnormal biomechanical forces that cause chronic sustained pressure of the deep flexor tendon against the navicular bone stimulate an abnormal remodeling process.[7] This bone remodeling leads to increased medullary bone trabeculae, edema, and pain, frequently progressing to degeneration of the bone. Navicular syndrome has also been related to osteoarthritis based on histologic and histomorphometric changes observed in the navicular bone and palmar fibrocartilage that are similar to abnormalities observed in articular hyaline cartilage and subchondral bone of affected joints.[8,9] Regardless of etiology, navicular syndrome is defined as a chronic, progressive bilateral forelimb condition affecting the navicular bone and it's supporting soft tissue structures in the heel of the horse's foot, with or without radiographic abnormalities.[3,8,10]

Most theories about the pathophysiology of this syndrome are based on clinical observations, radiographs, and post-mortem studies of horses with chronic navicular syndrome.[7-9] Post-mortem evaluation of horses with acute clinical signs of navicular syndrome has not been performed because many of these horses can be successfully managed and returned to performance.[3] While post mortem studies have provided useful information about navicular disease, it has been difficult to identify the inciting causes of the pathologic changes. The purpose of this paper is to report abnormalities observed with MR imaging of the front feet in horses that have recently developed clinical signs of navicular syndrome. MRI observations on a group of horses with specific clinical signs of navicular syndrome alone have not been reported, although reports of horses that had pain within one or both front feet have been reported[11-30], but none of these reports focus solely on horses with bilateral forelimb lameness that was abolished by palmar digital nerve blocks.

In human medicine, MRI has proven to be a valuable diagnostic tool for musculoskeletal disease, especially those involving soft tissues.[31-33] Magnetic resonance imaging of live horses has only been available for the last 11 years.[11,34] Multiple MRI studies have been performed on cadaver specimens to evaluate horses with chronic, end-stage navicular syndrome.[13-16,35] None of the post-mortem studies have included horses with recent onset of clinical signs associated with navicular syndrome. MR imaging has allowed us to evaluate the soft tissues associated with the navicular region in live horses.[11,12,17-29,36-40] It also allows us to evaluate horses early in the course of navicular syndrome. The purpose of this study was to evaluate horses with recent onset of bilateral clinical signs of navicular syndrome in order to determine the anatomic location of

pathologic change in affected horses. Our hypothesis was that the initial site of pathologic change would be within the navicular bursa or navicular bone.

Materials and Methods

All 72 horses that had MRI performed on both front feet at Washington State University Veterinary Teaching Hospital between May 1998 and September 2007 because they had developed recent onset of clinical signs of navicular syndrome were included in the study. Inclusion criteria included a bilateral forelimb lameness that was abolished by bilateral palmar digital nerve blocks, with or without a positive response to hoof testers applied to the frog. Lameness was of less than 6 months' duration. There were no detectable radiological abnormalities of the front digits. A thorough lameness evaluation was performed in all horses. Injection of 1.5-2ml local anesthetic over the medial and lateral palmar digital nerves (PDN) of the lame leg proximal to the cartilages of the foot caused each horse to switch to lameness in the opposite forelimb. Injection of local anesthetic over the medial and lateral PDN of the opposite forelimb eliminated the horse's lameness. All horses were examined by the same individual (RKS) and lameness was graded at a trot in a straight line and in small circles in each direction before and after PDN blocks. Lameness grades were 0- no lameness observed, 1- mild lameness without an observed head nod, 2- subtle head nod observed, 3- obvious head nod observed, 4- severe head nod with less than 50% of normal weight supported on the limb, and 5- non-weight bearing on the limb. Radiographs, including a 60 degree dorsopalmar projection, a palmaroproximal to palmarodistal oblique (skyline) projection of the distal sesamoid (navicular) bone, and a lateromedial projection of the digit, were evaluated and found to be normal for the age and use of the horse for all horses included in the study.[41]

Magnetic resonance imaging was performed on both front feet of every horse following general anesthesia. Each horse had a thorough physical examination, including an ECG, CBC, and chemistry profile prior to anesthesia. Anesthesia was induced with ketamine and diazepam and maintained with 2 to 5% isoflurane in oxygen. All horses were placed in right lateral recumbency and their front limbs positioned in a 1.0 Tesla magnet.* A human knee quadrature receiver coil was positioned around the foot being imaged and multiple image sequences were obtained using proton density (PD), T2-weighted (T2W), short tau inversion recovery (STIR), and gradient echo (3DGE) sequences. Axial, sagittal, and dorsal sections were obtained using standard MR protocols for the foot of the horse developed at Washington State University (Table 1).[37]

A standardized format was used to record all MRI observations and images were compared to images previously obtained from normal horses. On all horses, magic angle artifact occurring in any structure(s), most commonly tendons and ligaments, was determined by comparing proton density images and T2 weighted images from the dual echo sequences.[42-45] A primary finding (most severe finding), based on severity and lack of other observed abnormalities, was made in horses where it was clear that one principle abnormality was present. In some horses, a primary location of pathologic change could not be identified because multiple abnormalities of similar severity were observed in different structures. Due to the observations of multiple MRI abnormalities in many horses, an attempt was made to determine the primary abnormality based on the most obvious or severe MRI finding.

Results

There were 51 geldings, 19 mares, and 2 stallions, with an average age of 8.2 years (median 8 years, range 3-17 years). Forty-two were Quarter Horses, 17 were Warmbloods, 7 were Thoroughbreds, 4 were Paints, 1 was an Appaloosa and 1 was an Arabian. Thirty-four were used in western performance events, 15 were used for eventing or jumping, 10 were used as pleasure or show horses, and 9 were used for dressage. The use was unknown in 4 horses. The mean lameness grade was three when the horses were trotted in a straight line and circled in each direction over a smooth hard surface. Lameness was observed on both forelimbs in 76% of horses when the horse was trotted in small circles. All other horses had a unilateral lameness observed prior to the PDN block on the most lame limb.

MRI Observations

Many different abnormalities were observed on MR images of the front feet of the horses in this study (Table 2). Abnormal hyperintensity was observed in the navicular bone on STIR sequences in 108 limbs (62 horses [86%]). Thirty of these limbs (23 horses [38%]) also had abnormal hypointensity in the medullary cavity of the navicular bone. One of these horses had a 3mm navicular bone flexor cortex erosion just medial to the sagittal ridge that was not visible on radiographs. Focal hyperintensity was seen within the proximal, middle, or distal aspect of the navicular bone on the sagittal STIR sequences. This abnormal hyperintensity was located diffusely throughout the medullary cavity, or varied in both signal intensity and location (Figure 1).

Fifteen of 48 (31%) limbs that had the navicular bone sectioned in a coronal plane on gradient echo sequences had bone fragments identified off the distal margin of the navicular bone at the origin of the distal sesamoidean impar ligament. Six horses had

these bilaterally, with 5 having lateral fragments on each foot and 1 horse having medial and lateral fragments on each foot. Three horses had these unilaterally, with 1 horse having a medial fragment and 2 horses having lateral fragments. Two of the unilateral fragments were on the most lame limb and one was on the least lame limb.

Thickening of the collateral sesamoidean ligament was observed in 86 limbs (54 horses [75%]) (Figure 2) and abnormal hyperintensity on STIR and T2-weighted sequences or thickening of the distal sesamoidean impar ligament was observed in 40 limbs (26 horses [36%]) (Figure 3). Nineteen limbs (10 horses [14%]) had abnormalities in the distal sesamoidean impar ligament at its origin from the navicular bone which included abnormal hypointensity of the adjacent medullary cavity on PD images.

Forty nine limbs (32 horses [44%]) had thickening, irregularity and/or abnormal hyperintensity within the deep digital flexor tendon (Figure 4), most commonly located in the tendon proximal to the navicular bone, at the level of the collateral sesamoidean ligament. In some horses, abnormalities extended proximally as far as the horse was imaged (midway in the proximal phalanx). Lesions within the deep flexor tendon were divided into 4 locations: distal to the navicular bone (40% of limbs), at the navicular bone (35% of limbs), proximal to the navicular bone (94% of limbs), and between the pastern and fetlock joint (31% of limbs). Twenty-four limbs (49%) had lesions in more than one region and 25 (51%) limbs had lesions in only one region. Of the 25 limbs that had lesions in only one region, 21 (84%) had lesions proximal to the navicular bone, 2 (8%) had lesions distal to the navicular bone, and 1 (4%) had a lesion at the navicular bone. Twenty-seven (84%) horses with DDF lesions also had enlargement of the collateral sesamoidean ligament.

Seventy-one limbs (36 horses [50%]) had increased synovial fluid observed in the distal interphalangeal joint (Figure 5). All of these horses also had other abnormalities observed in the navicular bone or supporting soft tissue structures, although they may not have been the primary abnormality noted. Fifty-eight limbs (32 horses [44%]) had increased synovial fluid observed in the navicular bursa, although in most horses, a relatively small increase in fluid was observed. In 17 limbs (29%) there was severe bursitis, which included horses with increased fluid with or without hypointense tissue within the bursa; 12 of these (71%) had deep flexor tendonitis within the navicular bursa. Although a severe increase in synovial fluid was observed in the bursa in seventeen horses, a large amount of fluid consistent with bursitis was not considered the primary abnormality in any of these horses, although 1 horse with multiple other chronic lesions and an acute lameness history did have severe fluid in the bursa (Figure 6). Bursitis was determined by evaluation of the bursal fluid signal between the deep digital flexor tendon and collateral sesamoidean ligament as well as the size of the abaxial proximal bursal outpouchings seen best on sagittal STIR sequences. Horses with substantial scar tissue in the proximal bursa between the deep digital flexor tendon and collateral sesamoidean ligament only had fluid visible in the abaxial proximal outpouchings of the bursa.

Areas of hyperintensity on STIR sequences and/or hypointensity on proton density and T2 sequences in the navicular bone were the primary abnormality in 24 (33%) horses. Deep digital flexor tendonitis was the primary abnormality in 13 (18%) horses. Collateral sesamoidean ligament desmitis was the primary abnormality in 11 (15%) horses. Abnormal thickening and/or separation of fibers, seen on proton density sequences, and/or hyperintensity, seen on T2 and STIR sequences, in the distal

sesamoidean impar ligament was the primary abnormality in 7 (10%) horses. Multiple abnormalities were observed in 13 (18%) horses where a primary abnormality could not be determined. Abnormalities were not observed in the navicular bone or it's supporting soft tissues in 4 (6%) horses. Fifty-six horses had obvious differences in severity of pathology between limbs. In 93% (52/56) of horses, the most severe abnormalities occurred in the lamest limb. In 7% (4/56) of horses the worst findings were in the less lame limb.

Abnormalities were not observed in the navicular bone and its supporting soft tissues in 4 horses. One horse had bilateral increased synovial fluid in the proximal interphalangeal joint, best seen on STIR sequences. One horse had thickening of and hyperintensity in the straight distal sesamoidean ligament proximal to its insertion, best seen in proton density and T2 weighted images. One horse had thickening of and heterogenous signal intensity in the distal digital annular ligament bilaterally, best seen on proton density and STIR sequences. One horse had increased thickness and irregularity of the laminae over the medial and lateral palmar processes of the distal phalanx, best seen on proton density sequences, in both front feet without increased signal intensity on T2 or STIR sequences.

Twenty-two (15%) limbs had increased synovial fluid in the digital flexor tendon sheath, best seen on STIR sequences, as a secondary finding. Six limbs had thickening and irregularity of the distal digital annular ligament, best seen on proton density and T2 weighted sequences. Six limbs had increased synovial fluid of the proximal interphalangeal joint, best seen on STIR sequences. Four limbs had abnormal hyperintensity within the distal phalanx seen on STIR sequences. Two horses had

irregularity of the subchondral bone and/or cartilage of the distal interphalangeal joint seen on axial proton density, T2, and STIR sequences in images crossing through the joint spaces. Three horses had smoothly marginated semi-circular defects within the laminar tissue of the medial (1) or lateral (2) quarter, best seen on proton density sequences, and all were found on the most lame limb. One horse had thickening, best seen on proton density and T2 sequences, with abnormal hyperintensity, best seen on T2 and STIR sequences, of the medial collateral ligament of the distal interphalangeal joint.

Discussion

Our hypothesis that the initial site of pathologic change would be within the navicular bursa or navicular bone proved to be false, as multiple abnormalities were observed in the front feet of these horses. The abnormalities seen with MRI were not visible on radiographs, even though the majority of horses had changes involving the navicular bone itself. The term navicular syndrome has been used to describe horses with lameness that is improved by local anesthesia of the palmar digital nerves and that have no radiographic abnormalities.[46] It is clear that clinical signs of navicular syndrome can result from a variety of abnormalities and that abnormalities like distal sesamoidean impar ligament desmitis, collateral sesamoidean ligament desmitis, abnormal hyperintensity and hypointensity in the navicular bone, navicular bursitis, and deep digital flexor tendonitis are likely related and often occur together in the same horse.[11,13-14,17-18,47-48] A specific diagnosis is possible in these horses after evaluation with MRI, and these horses can then be grouped into specific subgroups based on their primary lesions. Because of the variation observed in these horses, MRI will have to be performed on a

large number of horses with clinical signs of navicular syndrome before patterns can be recognized and related to a specific etiology and pathogenesis.

This is the first report of MRI observations in a specific group of horses with consistent recent onset of clinical signs of navicular syndrome. This group of horses had a high percentage of Quarterhorses, of which the majority were western performance horses. This is a different population than that reported in other studies of foot lameness diagnosed with MRI[11-12,14,17,20-22,24,26-29], although many of the previous studies do not report breed and/or use prevalence.[13,15-16,18,25,27,30] This study group was also more specific in that these horses had bilateral forelimb lameness eliminated with local anesthesia of the palmar digital nerves and a history of lameness no longer than 6 months. Previous reports of foot lameness diagnosed with MRI are less specific in that they include either unilateral forelimb and/or hindlimb lameness, and/or lameness that was eliminated with abaxial sesamoid nerve blocks and/or distal interphalangeal joint anesthesia, and do not have a limit on duration of lameness.[11-30]

Magnetic resonance imaging is a sensitive imaging modality for detecting even small amounts of abnormal hyperintensity in tissue using inversion recovery (STIR) sequences. Abnormal signal intensity, most commonly hyperintensity, in the navicular bone was seen in 86% of horses and was the most frequent MRI observation in the horses in this study. The hyperintensity in the navicular bone seen with STIR sequences could be indicative of hemorrhage, synovial fluid, bone necrosis, fibrosis, or fluid that accumulates secondary to inflammation (edema).[13,15-16,39,49] Granulation tissue can appear as hyperintense tissue, but differentiation of granulation tissue was not attempted in this study. Granulation tissue has not been shown to be a component of navicular syndrome

horses unless flexor cortex lesions are present.[50] This difference is relevant at times in determining the components of hyperintensity seen on PD or STIR sequences. Gradient echo sequences are often not reliable in determining true hyperintensity because of their susceptibility to artifacts and distortion which often results in inaccurate depiction of hyperintensity seen on STIR sequences, either as an exaggeration of the signal or as a dilution of the signal when seen on gradient echo sequences. Correlation of MR images with histopathologic observations may help to determine the source of this abnormal hyperintensity in horses with recent onset of signs of navicular syndrome, but this has only been looked at in horses with chronic navicular syndrome.[14-16,39,47,48] Histopathologic correlation with MRI observations in a group of horses with recent onset (<6 months) of clinical signs may improve our understanding of the cause of abnormal hyperintensity in the navicular bone on STIR images.

Tendonitis of the deep digital flexor tendon was previously recognized in horses with adhesion of the tendon to the navicular bone[3] or observed in the area of the tendon over the back of the navicular bone on postmortem studies.[7,8] The observation that deep digital flexor tendonitis occurs as a primary problem in some horses with clinical signs of navicular syndrome is an important observation.[12,17,20] Eighteen percent of horses in this study had deep flexor tendonitis as their primary diagnosis. This is different than a previous report of 33% of horses that had lameness localized to their foot in which deep flexor tendonitis was the most common injury.[17] Reasons for this difference may relate to the study populations. In the previous study, the majority of horses were used for English performance events, whereas in this study the majority of horses competed in western performance events and consisted of a large number of Quarterhorses. One report

provides data that suggest jumping horses are more likely to sustain tendon injury within the digit than non-jumping horses in a population of English performance horses.[12] The different inclusion criteria between studies could also be important because the previous study looked at horses with unilateral and bilateral lameness occurring in either the forelimb or hindlimb.[12] Unilateral lameness and hindlimb lameness are more likely to be caused by a traumatic event than as a result of navicular syndrome, and may be more likely to result in tendon injury that extends into the pastern region. It has been reported in a study of deep flexor tendonitis within the digit, that 24% of the horses had lameness eliminated with a palmar digital nerve block.[12] The present study looks at horses with bilateral forelimb lameness that blocks to the heel of the front feet and is more likely to identify horses with inflammation centered around the navicular region, possibly excluding horses with more severe tendon injury extending into the pastern region. The overall prevalence of horses with deep flexor tendonitis in this study was 44% (34% of limbs) which is different than a previous report of 83%.[18] The most common location of injury in this study was proximal to the navicular bone at the level of the collateral sesamoidean ligament, which agrees with a previous report.[18] Lesion location within the deep flexor tendon was similar at the level of the pastern (31% in this study vs. 29%) and distal to the navicular bone (40% in this study vs. 35-37%), although it differed greatly at the level of the collateral sesamoidean ligament (94% in this study vs. 59%) and the navicular bone (35% in this study vs. 59%) when compared to a previous report.[18]

The observation that inflammation extends proximally in the tendon above the level of the proximal interphalangeal joint affects treatment for some horses. Prior to MRI, rest, rehabilitation, and physical therapy to stretch the deep digital flexor tendon

within the digit had not been routinely used to treat horses with navicular syndrome. Deep digital flexor tendonitis may be a primary cause of lameness in horses with multiple MRI abnormalities as was observed in 13 (18%) of the horses in this study. The report of deep digital flexor tendonitis as a major contributor to lameness in 61% of 75 horses with foot lameness evaluated with MRI further emphasizes the importance of deep digital flexor tendonitis as a cause of lameness in the horse's digit.[12] Extension of the tendonitis proximally into the area covered by the digital flexor tendon sheath makes injection of the sheath a possible diagnostic (local anesthetic injection) or therapeutic technique (steroid and/or hyaluronic acid injection) for these horses.[†,40] Horses with deep digital flexor tendonitis and inflammation in the navicular bursa may be more effectively treated by injection of anti-inflammatory medications into the navicular bursa.[51]

Collateral sesamoidean ligament desmitis was the primary abnormality in 15% of horses, and this has not been reported as a primary cause of injury in a group of horses before. There are two isolated case reports of desmitis within this ligament, one diagnosed by ultrasound and one diagnosed by MRI.[23,52] The prevalence of collateral sesamoidean ligament desmitis in a group of horses has been reported previously (10.5% of limbs), but is much lower than seen was in this study (60% of limbs).[17] In this current study, injury to this ligament was seen often as either one of multiple abnormalities within the navicular region of the foot or as a single injury affecting only this structure.

Distal sesamoidean impar ligament desmitis was a primary injury in 10% of horses in this study which is similar to a previously reported prevalence of 7% in a group of horses with lameness localized to the foot.[17] The overall prevalence of injury to this ligament in this study (28% of limbs) is also similar to a reported prevalence of 38% in a

previous study in which horses had unilateral or bilateral lameness localized to the foot in either the forelimb or hindlimb.[18]

Multiple structures were affected in 18% of horses, and a primary abnormality was not observed. This finding is similar to a previous report of horses with lameness localized to the foot in which 17% of horses had multiple abnormalities.[17]

The hypothesis that navicular syndrome is a continuum that starts as navicular bursitis and progresses to degeneration of the flexor cortex of the navicular bone[7,53] is not supported by the MRI observation in these horses. Increased synovial fluid in the navicular bursa as a primary entity was not observed in any of the horses, making it unlikely that the syndrome starts with initial inflammation of the bursa in most horses. Distension of the navicular bursa, most visible as outpouching of the proximal, abaxial synovial pouches, was most often seen in horses that had pathologic changes within the ligaments or tendon intimately associated with the bursa, and more rarely seen in horses that did not have damage to these soft tissue structures. The amount of increased distension visible on sagittal STIR images of horses in this study ranged from 0.5cm to 2.0cm if measured in a proximal to distal direction at the most distended portion of the bursa on either side of the deep digital flexor tendon. These horses may also have variable amounts of hypointense tissue (scar tissue) within the proximal aspect of the navicular bursa which was more often seen concurrently with deep flexor tendon injury in the region of the tendon covered by the bursa, and in limbs in which the tendon damage extended to the dorsal surface of the tendon covered by the navicular bursa.

Chronic strain on the palmar support structures of the distal interphalangeal joint, including the distal sesamoidean impar ligament, collateral sesamoidean ligament, and

the deep digital flexor tendon, due to repetitive use or poor conformation, may cause mechanical damage and inflammation in these tissues. Hyperextension of the distal interphalangeal joint occurs late in the horse's stride when the horse is pushing off the ground with the foot,[54] and the greater the speed on an uneven surface, the more hyperextension of this joint may occur. Rough uneven surfaces and deep plowed ground can also contribute to hyperextension of this joint. In the authors' opinion, hyperextension could explain the observation of increased fluid in the distal interphalangeal joint observed in some horses. This hyperextension could also result in injury to the deep digital flexor tendon from forces that cause sudden upward pressure on the dorsal aspect of the distal phalanx (on the toe). Horses frequently perform on deep or uneven surfaces, and uneven pressure to the toe of the foot would be frequent. Acute, blunt trauma to the bottom of the foot may also be a cause of navicular bone injury in the horse's foot,[55] particularly when lameness is much more severe on one foot. In one horse in this study, acute lameness was observed on one limb 3 weeks before MRI was performed. This horse had diffuse abnormal high signal intensity in the navicular bone that was much more severe than the opposite limb, possibly due to contusion as a result of severe, direct concussion to the bone. Horses that are already experiencing inflammation within the navicular region may be more susceptible to external trauma to the bottom of the foot than normal, sound horses.

Unfortunately, due to the bilateral nature of lameness associated with the palmar heel region, bilateral forelimb lameness can be difficult for owners to identify early in the disease process. It is impossible to determine accurately how long these horses were experiencing pain. It is possible that the duration of disease was longer than the owners

thought, even though lameness was only noticed by owners or trainers within the last 6 months. Determining the etiology of many of these lesions is difficult as the age of each lesion in horses with multiple pathologic changes can not be determined accurately at this time.

Conclusion

The cause of each specific injury within the heel of the horse's foot remains to be determined. MRI has provided proof in live horses that navicular syndrome is not the same in individual horses.[13-14,17-18,47-48] The presence of abnormalities seen with MRI in the navicular bone and supporting soft tissues in horses with normal radiographs further demonstrates the limitations of radiography for evaluating horses affected with navicular syndrome.[10] Magnetic resonance imaging allows for a more definitive diagnosis in horses with clinical signs of navicular syndrome, and improves selection of specific treatments for individual horses.

Abnormalities observed in the front feet of horses in this study that are bilaterally symmetrical may be the result of use-related remodeling of the navicular bone and its supporting soft tissue structures, however, the findings in these horses are not observed in sound horses.[14,38] Perhaps more important, is the observation that the most obvious abnormalities or most severe changes on MRI occurred in the foot in which the horse was most lame 93% of the time, when horses were more lame in one foot than another. This is evidence that MRI observations correlate with clinical signs, which is something that has not been observed with radiography or any other method of imaging the digit.

Inflammation of several different tissues in the heel of the horse's foot can cause similar clinical signs that are currently diagnosed as navicular syndrome if an MR

evaluation is not done. For this reason, MRI is a valuable technique for evaluating horses with navicular syndrome because a specific diagnosis can be made and a definitive diagnosis can affect the treatment of these horses. More horses need to be evaluated with MRI earlier in the disease process to learn more about navicular syndrome, and especially, to correlate findings with postmortem histopathology to enable evaluation of new diagnostic and treatment methods.

Footnotes

* Philips Gyroscan, Medical Systems, Best, The Netherlands

† Schneider RK. Injection of the digital flexor tendon sheath as a diagnostic and treatment technique for horses with deep digital flexor tendonitis. Unpublished cases. 2001.

References

1. Ackerman N, Johnson JH, Porn CR. Navicular disease in the horse: risk factors, radiographic changes, and response to therapy. J Am Vet Med Assoc 1977;170:183-187.

2. Lowe JE. Sex, breed and age incidence of navicular disease and its treatment. In Pract 1982;4:29.

3. Stashak TS. Lameness. In: Stashak TS, ed. Adams' Lameness in Horses. Philadelphia: Lippinjcott, Williams, & Wilkins, 2002:664-680.

4. Colles C, Hickman J. The arterial supply of the navicular bone and its variations in navicular disease. Equine Vet J 1977;9(3):150-154.

5. Rijkenhuizen ABM, Nemeth F, Dik KJ, et al. The arterial supply of the navicular bone in adult horses with navicular disease. Equine Vet J 1989;21(6):418-424.

6. Fricker C, Riek W, Hugelshofer J. Occlusion of the digital arteries-A model for pathogenesis of navicular disease. Equine Vet J 1982;14(3):203-207.

7. Pool RR, Meagher DM, Stover SM. Pathophysiology of navicular syndrome. In: Yovich JV, ed. Vet Clin of North Am Equine Pract 1989;109-129.

8. Wright IM, Kidd L, Thorp BH. Gross, histological and histomorphometric features of the navicular bone and related structures in the horse. Equine Vet J 1998;30(3):220-234.

9. Doige C, Hoffer MA. Pathological changes in the navicular bone and associated structures of the horse. Can J Comp Med 1983;47:387-395.

10. Turner T, Fessler J. The anatomic, pathologic, and radiographic aspects of navicular disease. Comp Cont Ed 1982;4(8):350-355.

11. Dyson S, Murray R, Schramme M, et al. Magnetic resonance imaging of the equine foot: 15 horses. Equine Vet J 2003;35:18-26.

12. Dyson S, Murray R, Schramme M, et al. Lameness in 46 horses associated with deep digital flexor tendinitis in the digit: diagnosis confirmed with magnetic resonance imaging. Equine Vet J 2003;35(7):681-690.

13. Schramme MC, Murray RC, Blunden TS, et al. A comparison between magnetic resonance imaging, pathology, and radiology in 34 limbs with navicular syndrome and 25 control limbs, in Proceedings. 51st Annu Conv Am Assoc Equine Pract 2005;51:348-358.

14. Murray RC, Schramme MC, Dyson SJ, et al. Magnetic resonance imaging characteristics of the foot in horses with palmar foot pain and control horses. Vet Radiol Ultrasound 2006;47(1):1-16.

15. Murray RC, Blunden TS, Schramme MC, et al. How does magnetic resonance imaging represent histologic findings in the equine digit? Vet Radiol Ultrasound 2006;47(1):17-31.

16. Busoni V, Heimann M, Trenteseaux J, et al. Magnetic resonance imaging findings in the equine deep digital flexor tendon and distal sesamoid bone in advanced navicular disease: an ex vivo study. Vet Radiol Ultrasound 2005;46(4):279-286.

17. Dyson SJ, Murray RC, Schramme MC. Lameness associated with foot pain: results of magnetic resonance imaging in 199 horses (January 2001-December 2003) and response to treatment. Equine Vet J 2005;37(2):113-121.

18. Dyson SJ, Murray R. Magnetic resonance imaging evaluation of 264 horses with foot pain: the podotrochlear apparatus, deep digital flexor tendon and collateral ligaments of the distal interphalangeal joint. Equine Vet J 2007;39(4):340-343.

19. Murray RC, Roberts BL, Schramme MC, et al. Quantitative evaluation of equine deep digital flexor tendon morphology using magnetic resonance imaging. Vet Radiol Ultrasound 2004;45(2):103-111.

20. Mair TS, Kinns J, Jones RD, et al. Magnetic resonance imaging of the distal limb of the standing horse: technique and review of 40 cases of foot lameness, in Proceedings. 49th Annu Conv Am Assoc Equine Pract 2003;49:29-41.

21. Dyson SJ, Murray RC, Schramme MC, et al. Magnetic resonance imaging in 18 horses with palmar foot pain, in Proceedings. 48th Annu Conv Am Assoc Equine Pract 2002;48:145-154.

22. Mair TS, Sherlock CE. Osseous cyst-like lesions in the feet of lame horses: diagnosis by standing low-field magnetic resonance imaging. Equine Vet Educ 2008;20(1):47-56.

23. Kofler J, Kneissl S, Malleczek D. MRI and CT diagnosis of acute desmopathy of the lateral collateral sesamoidean (navicular) ligament and long-term outcome in a horse. Vet Journal 2007;174:410-413.

24. Smith MRW, Wright IM, Smith RKW. Endoscopic assessment and treatment of lesions of the deep digital flexor tendon in the navicular bursae of 20 lame horses. Equine Vet J 2007;39(1):18-24.

25. Dyson S, Murray R. Use of concurrent scintigraphic and magnetic resonance imaging evaluation to improve understanding of the pathogenesis of injury of the podotrochlear apparatus. Equine Vet J 2007;39(4):365-369.

26. Sherlock CE, Kinns J, Mair TS. Evaluation of foot pain in the standing horse by magnetic resonance imaging. Vet Record 2007;161:739-744.

27. Mitchell RD, Ewards RB, Makkreel LD, et al. Standing MRI lesions identified in jumping and dressage horses with lameness isolated to the foot, in Proceedings. 52nd Annu Conv Am Equine Pract 2006;52:422-426.

28. Martinelli MJ, Rantanan NW. Relationship between nuclear scintigraphy and standing MRI in 30 horses with lameness of the foot. 51st Annu Conv Am Assoc Equine Pract 2005;51.

29. Mair TS, Kins J. Deep digital flexor tendonitis in the equine foot diagnosed by low-field magnetic resonance imaging in the standing patient: 18 cases. Vet Radiol Ultrasound 2005;46(6):458-466.

30. Dyson S, Murray R. Verification of scintigraphic imaging for injury diagnosis in 264 horses with foot pain. Equine Vet J 2007;39(4):350-355.

31. Moon KL, Genant HK, Helms CA, et al. Musculoskeletal applications of nuclear magnetic resonance. Radiology 1983;147:161-171.

32. Sabiston CP, Adams ME, Li DKB. Magnetic resonance imaging of osteoarthritis: correlation with gross pathology using an experimental model. J Orthop Res 1987;5:164-172.

33. Poly DW, Callaghan JJ, Sikes, RA, et al. The accuracy of selective magnetic resonance imaging compared with the findings of arthroscopy of the knee. J Bone Joint Surgery 1988;70(2):192-198.

34. Kraft SL and Gavin PR. Physical principles and technical considerations for equine computed tomography and magnetic resonance imaging. Vet Clin North Am Equine Pract 2001;17:115-130.

35. Whitton RC, Buckley C, Donovan T, et al. The diagnosis of lameness associated with distal limb pathology in a horse: a comparison of radiography, computed tomography and magnetic resonance imaging. The Vet Journal 1998;155:223-229.

36. Sanz M, Sampson SN, Schneider RK, et al. Epidermoid cyst in the foot of a horse diagnosed with magnetic resonance imaging. J Am Vet Med Assoc 2006;228:1918-1921.

37. Sampson SN, Schneider RK, Tucker RL. Magnetic resonance imaging of the equine distal limb, in Auer JA and Stick JA, eds. Equine Surgery, 3rd ed. Philadelphia: WB Saunders Co, 2005;946-963.

38. Busoni V, Snaps F, Trenteseaux J, et al. Magnetic resonance imaging of the palmar aspect of the equine podotrochlear apparatus: normal appearance. Vet Radiol Ultrasound 2004;45(3):198-204.

39. Widmer WR, Buckwalter KA, Fessler JF, et al. Use of radiography, computed tomography and magnetic resonance imaging for evaluation of navicular syndrome in the horse. Vet Radiol Ultrasound 2000;41(2):108-116.

40. Schneider RK, Sampson SN, Gavin PR. Magnetic resonance imaging evaluation of horses with lameness problems, in Proceedings. 51st Annu Conv Am Assoc Equine Pract 2005;51:21-34.

41. Dyson SJ. Radiological interpretation of the navicular bone. Equine Vet Educ 2008;20(5):268-280.

42. Erickson SJ, Prost RW, Timins ME. The “magic angle” effect: background physics and clinical relevance. Radiology 1993;188:23-25.

43. Erickson SJ, Cox IH, Hyde JS, et al. Effect of tendon orientation on MR imaging signal intensity: a manifestation of the “magic angle” phenomenon. Radiology 1991;181:389-392.

44. Spriet M, Mai W, McKnight A. Asymmetric signal intensity in normal collateral ligaments of the distal interphalangeal joint in horses with a low-field MRI system due to the magic angle effect. Vet Radiol Ultrasound 2007;48(2):95-100.

45. Busoni V, Snaps F. Effect of deep digital flexor tendon orientation on magnetic resonance imaging signal intensity in isolated equine limbs – the magic angle effect. Vet Radiol Ultrasound 2002;43(5):428-430.

46. Turner T. Diagnosis and treatment of the navicular syndrome in horses. Vet Clin N Am: Equine Pract 1989;5:131-144.

47. Blunden A, Dyson S, Murray R, et al. Histopathology in horses with chronic palmar foot pain and age-matched controls. Part 1: Navicular bone and related structures. Equine Vet J 2006;38(1):15-22.

48. Blunden A, Dyson S, Murray R, et al. Histopathology in horses with chronic palmar foot pain and age-matched controls. Part 2: The deep digital flexor tendon. Equine Vet J 2006;38(1):23-27.

49. Zanetti M, Bruder E, Romero J, et al. Bone marrow edema pattern in osteoarthritic knees: correlation between MR imaging and histologic findings. Radiology 2000;215(3):835-840.

50. Schmid MR, Hodler J, Vienne P, et al. Bone marrow abnormalities of foot and ankle: STIR versus T1-weighted contrast-enhanced fat suppressed spin-echo MR imaging. Radiology 2002;224:463-469.

51. Dabareiner RM, Carter GK, Honnas CM. Injection of corticosteroids, hyaluronate, and amikacin into the navicular bursae in horses with signs of navicular area pain unresponsive to other treatments: 25 cases (1999-2002). J Am Vet Med Assoc 2003;223(10):1469-1474.

52. Jacquet S, Coudry V, Denoix JM. Severe tear of the collateral sesamoidean ligament in a horse. Vet Record 2006;159(24):818-820.

53. Adams OR. Lameness in Horses, 3rd ed. Philadelphia, Lea & Febiger, 1974; 260.

54. Denoix JM. Functional anatomy of the equine interphalangeal joints, in Proceedings. 44th Ann Conv Am Assoc Equine Pract 1999;44:174-177.

55. Barber M, Sampson SN, Schneider RK, et al. Unilateral navicular bone injury diagnosed with magnetic resonance imaging in a horse. J Am Vet Med Assoc 2006;229(5):717-720.

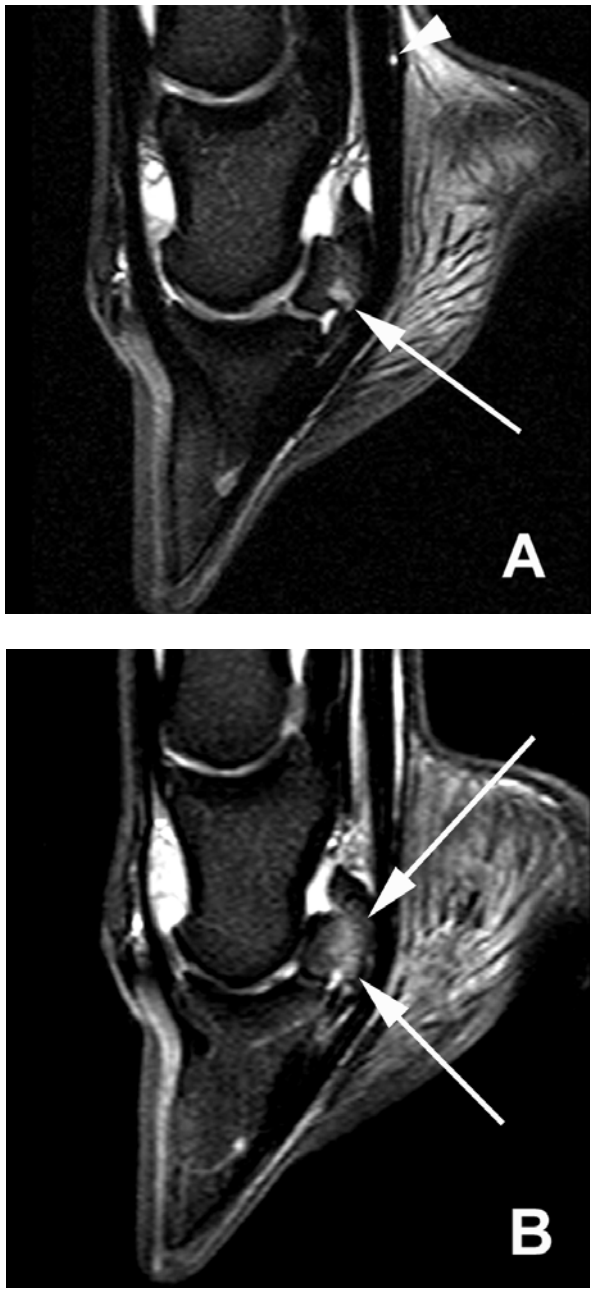

Figure 1: Sagittal short tau inversion recovery (STIR) images showing (A) abnormal hyperintensity in the distopalmar aspect (arrow) of the navicular bone near the origin of the distal sesamoidean impar ligament. There is focal hyperintense signal that extends proximally to the insertion of the collateral sesamoidean ligament. A small amount of synovial fluid is seen as focal hyperintensity at the palmar aspect of the deep flexor tendon (arrowhead). B. Abnormal hyperintensity is more diffuse and extends proximally along the palmar half of the medullary cavity (arrows) of the navicular bone. In this image, there is also hyperintensity at the proximal aspect of the distal sesamoidean ligament. The focal area of hyperintensity along the flexor cortex represents the normal crecent shaped depression in this area on many horses.

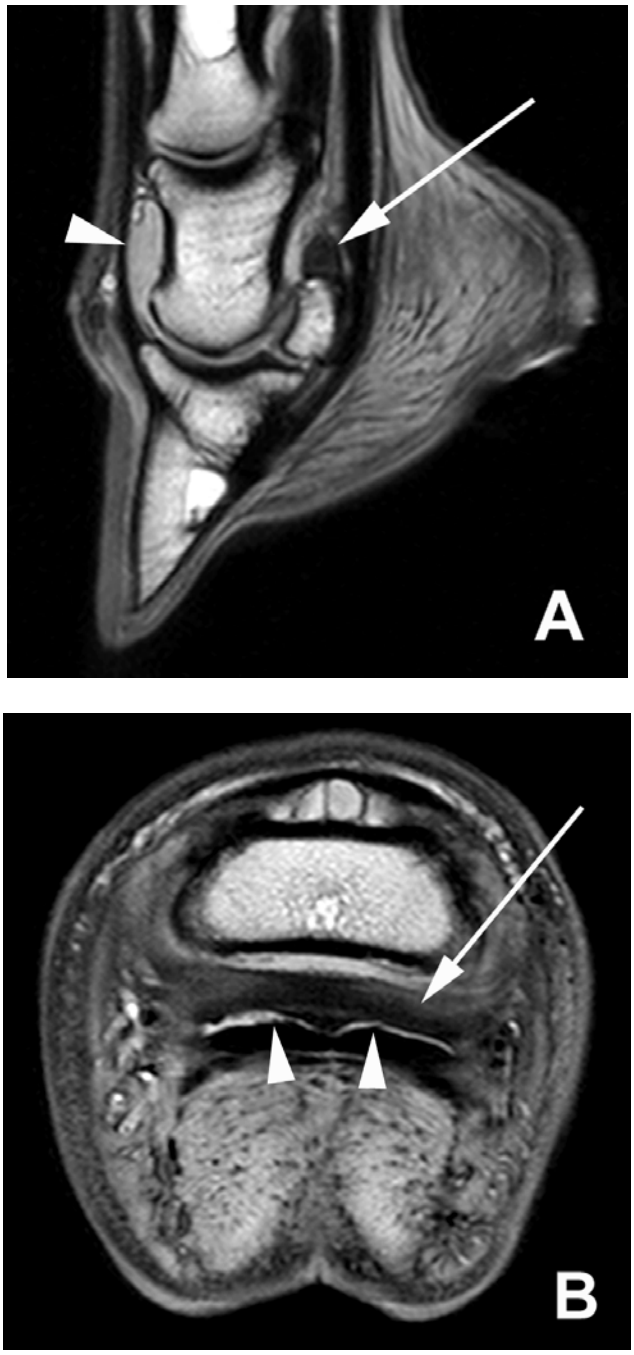

Figure 2: These are sagittal (A) and axial (B) proton density (PD) images of a horse with thickening of the collateral sesamoidean ligament (arrows). A. The distal interphalangeal joint capsule is distended due to increased synovial fluid in this space (arrowhead). There is also a focal mild hyperintensity on the palmar aspect of the flexor cortex midway between the proximal and distal aspect of the bone that represents the normal depression in this area of the flexor cortex with a focal pocket of bursal fluid within the depression. B. There is irregularity of the dorsal aspect of the deep digital flexor tendon (arrowheads) that is contrasted by the hyperintense signal of fluid in the navicular bursa between the tendon and the collateral sesamoidean ligament.

Figure 3: This is a sagittal proton density (PD) image from a horse with thickening and hyperintensity within the distal sesamoidean impar ligament (arrow). Corresponding T2-weighted images were used to rule out magic angle artifact in this ligament, which was evident in the distal aspect of the deep flexor tendon as a relative increase in signal intensity (arrowhead). Enthesopathy of the palmarodistal aspect of the navicular bone is also visible at the origin of the impar ligament.

Figure 4: These are axial proton density (PD) images of a horse with hyperintensity in the medial lobe of the deep digital flexor tendon with corresponding enlargement of this tendon lobe (arrow) at the level of the proximal middle phalanx (A). The area of hyperintensity extends proximally in the tendon into the pastern region, as high as the horse was imaged (distal third of the proximal phalanx) (B).

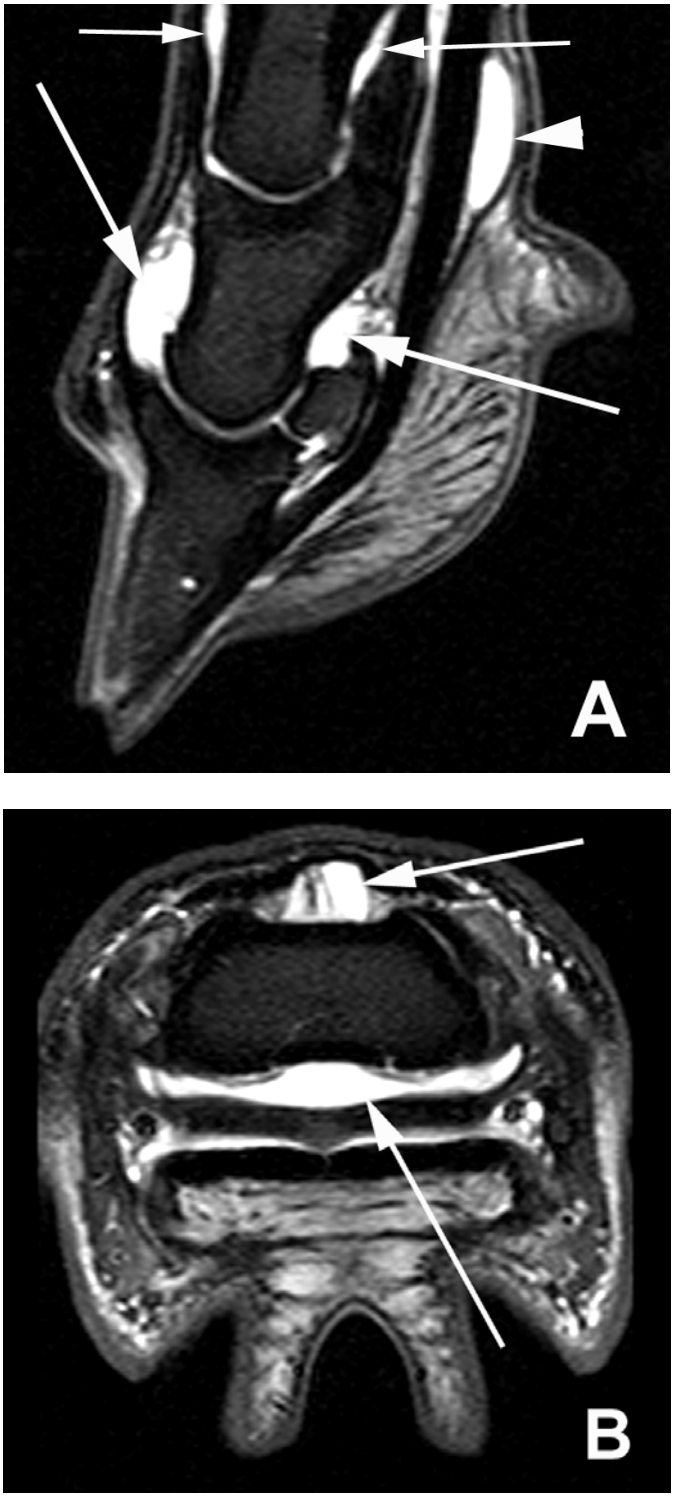

Figure 5: These are sagittal (A) and axial (B) short tau inversion recovery (STIR) images showing increased fluid in the distal (large arrows) and proximal (small arrows) interphalangeal joints. There is also increased fluid in the digital flexor tendon sheath visible on the sagittal image (arrowhead).

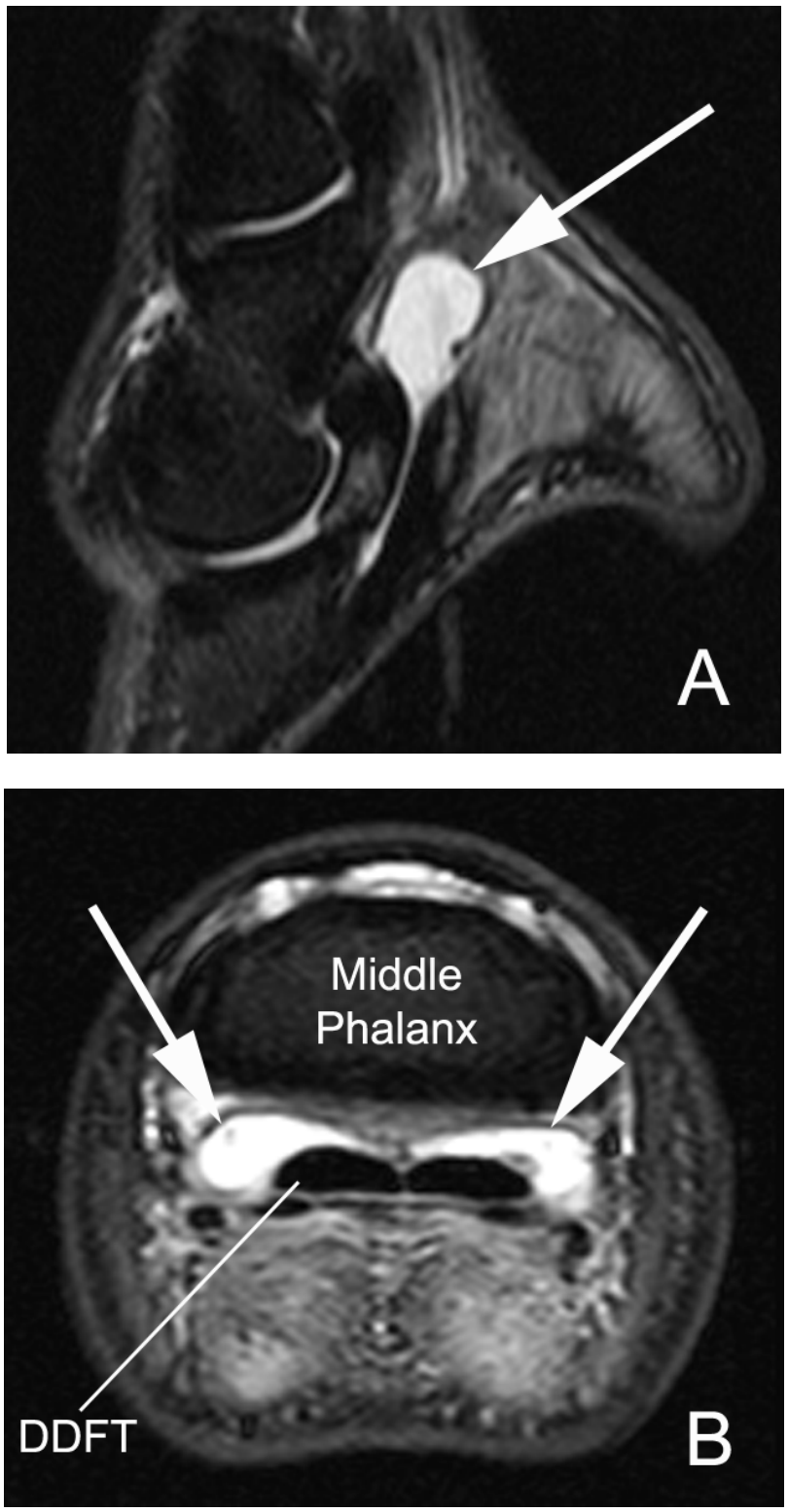

Figure 6: These are sagittal (A) and axial (B) short tau inversion recovery (STIR) images showing increased fluid in the navicular bursa in a horse in which severe effusion (arrows) of the bursa was present. DDFT, deep digital flexor tendon.

Table 1: Phillips 1 Tesla Magnetic Resonance Imaging Parameters for the Foot of the Horse

Slice Plane	Sequence	TR (msec)	TE (msec)	FA	FOV/ rFOV	Matrix Size	Slice #/ Width	Gap (mm)	Time (min)
Axial	TSE T2	2116	100	90	15/10.5	256x512	30/4mm	0.5	5:08
Axial	TSE PD	2116	11	90	15/10.5	256x512	30/4mm	0.5	**
Axial	STIR*	1725	35	90	15/10.5	192x256	30/3.5mm	1.0	4:42
Axial	3D GE	47	9	25	10/10	192x256	30/1.5mm	-1.5	3:13
Sagittal	TSE T2	3395	110	90	14/10	256x512	22/4mm	0.5	2:21
Sagittal	TSE PD	3395	14	90	14/10	256x512	22/4mm	0.5	2:21
Sagittal	STIR*	1500	35	90	14/10	256x256	22/3.5mm	0.5	5:48
Coronal	3D GE	47	9	25	10/10	192x256	30/1.5mm	-1.5	3:13

*Inversion time (TI) for STIR sequences is 140 msec
**T2 and PD sequences are collected together during the TSE scan
TSE = Turbo spin echo
STIR = Short tau inversion recovery
3D GE = Three dimensional gradient echo
TSE PD = Proton density
TSE T2 = T2-weighted
TR = Repetition time
TE = Echo time
FA = Flip Angle
FOV/rFOV = Field of view/Relative field of view
Slice # = Number of slices
Width = Thickness of slice
Gap = Space between slices
Time = Actual scanning time for each sequence

Table 2: Magnetic resonance imaging findings in structures of the navicular region

Structure	# of Limbs Affected	# of Horses Affected	Primary Lesion/Horse
NB	108 (75%)	62 (86%)	24 (33%)
DDFT	49 (34%)	32 (44%)	13 (18%)
CSL	86 (60%)	54 (75%	11 (15%)
DSIL	40 (28%)	26 (36%)	7 (10%)
NBA	58 (40%)	32 (44%)	0
NB Fragments	*15/48 (31%)	*9/24 (37.5%)	0
DIP Effusion	71 (49%)	36 (50%)	0
Multiple	NA	13 (18%)	NA

NB, navicular bone; DDFT, deep digital flexor tendon; CSL, collateral sesamoidean ligament; DSIL, distal sesamoidean impar ligament; NBA, navicular bursa; DIP, distal interphalangeal joint; NA, not applicable.
*Only 24 horses (48 limbs) were imaged with coronal slices through the navicular bone enabling complete evaluation of the distal border.

CHAPTER THREE

HORSES WITH CHRONIC SIGNS OF NAVICULAR SYNDROME

Introduction

Navicular syndrome is a common cause of forelimb lameness in many types of athletic horses.[1-4] It is defined as a chronic, progressive, bilateral forelimb condition affecting the navicular bone and it's supporting soft tissue structures in the heel of the horse's foot, with or without radiographic abnormalities.[3,5,6] Navicular syndrome causes chronic pain in the palmar region of the horse's foot that can progress to degeneration of the navicular bone and chronic lameness that forces the horse to be removed from performance.

Radiography is the first diagnostic imaging step to detect pathology in horses with navicular syndrome, but has poor correlation with clinical signs,[7] as horses affected with navicular syndrome frequently have no abnormalities on radiographs. In some cases, radiography and ultrasonography have been able to define pathologic change within the bone or soft tissues, respectively, within the horse's foot,[1,6,8-11] but negative findings are not conclusive evidence of lack of pathology.[4,12-15] Furthermore, even with findings of pathologic change using these imaging modalities, it is apparent with MRI that lesions within the horse's foot have been missed when only radiography and/or ultrasonography are used as diagnostic aids.[4,7,12,16-22] Magnetic resonance imaging has proven how little information is available from radiographs regarding the changes that are occurring in the boney structures of the horse's foot.[4,12,16,20-21,23-24]

Magnetic resonance imaging was first performed on live horses in 1997, but it has become quickly apparent how much MRI has to offer in the diagnosis of orthopedic

injury.[4,10,12-30] It has been a valuable diagnostic tool for orthopedic problems in humans, in both bone and soft tissue injury, for over 30 years.[31-33] The more recent availability of MRI for live horses has enabled detection of pathology in both bone and soft tissues in the equine foot.[4,12-13,16-21,23-27] Prior to MRI in the horse, definitive diagnosis of pathologic change within the foot was determined only at post-mortem examination.[1,6,34-40] The ability to use MRI to further define navicular syndrome in live horses has improved our understanding of disease processes in the foot that contribute to heel pain. The increasing number of horses imaged continues to improve our understanding of individual variation between horses, as well as the variety of pathologic changes that can occur.[4,12-14,16-21,23-25,27-28,41]

Based on MRI findings, navicular syndrome appears to involve multiple pathologic processes occurring in the navicular region.[4,15-16,18,20-21,23,27] Furthermore, it has been reported that horses that block to a palmar digital nerve block can have a variety of structures involved that are not directly associated with the navicular region.[4,12,16-18,27] Pathologic change has been observed in the distal digital annular ligament; the phalanges; cartilage and subchondral bone of the proximal and distal interphalangeal joints; collateral ligaments of the distal interphalangeal joint; lamina; keratomas in the laminae; and abnormalities within the digital flexor tendon sheath.[4,12,16-19,21,42] Pathologic change can occur in any of these structures as the only manifestation of disease within the foot, or multiple structures can be affected.[4] Multiple MRI studies have been performed on cadaver specimens to evaluate horses with chronic, end-stage navicular syndrome.[13-14,30,43,44] Many of the horses in these post-mortem studies have had flexor cortical erosion or other severe bone abnormalities visible on radiographs.[14]

Magnetic resonance findings in horses with recent onset of navicular syndrome have been reported.[4] Horses with chronic clinical signs of navicular syndrome may have abnormalities different from horses that have recently developed the syndrome. To fully define navicular syndrome in each individual horse, it is necessary to evaluate these horses using MRI.[4,12,16,20-24,27,29]

The objective of this study of horses with chronic signs of navicular syndrome was to determine the prevalence of injury to structures within the horses foot when lameness has been present greater than 6 months, and to compare these findings to a previous report of horses with recent onset of navicular syndrome.[4] Magnetic resonance imaging observations in a specific group of horses with chronic clinical signs restricted to those with navicular syndrome without radiographic abnormalities have not been reported. We hypothesize that horses with chronic navicular syndrome will have MRI abnormalities similar to horses with a relatively recent onset of signs.

Materials and Methods

Medical records of all horses admitted to the Washington State University Veterinary Teaching Hospital between April 1999 and November 2007 with a bilateral forelimb lameness of greater than 6 months duration that localized to the feet were reviewed. Horses were included in the study if the lameness was localized to the palmar heel region with local anesthesia and if they had undergone MRI of the front feet.

Information recorded from the medical records of horses included in the study consisted of history, physical examination findings, result of lameness examination, MRI findings, treatment, and suggested rehabilitation program. A complete lameness evaluation was performed on all horses and all horses had bilateral forelimb lameness.

Injection of 1.5-2ml local anesthetic over the medial and lateral palmar digital nerve (PDN) of the more lame forelimb caused each horse to switch to lameness in the opposite forelimb. Injection of local anesthetic over the medial and lateral PDN of the opposite forelimb eliminated the horse's lameness. Lameness was graded using a modification of the AAEP grading system.[45] Horses were evaluated at the trot over a smooth, hard surface in a straight line and in small circles in each direction. Lameness was graded in a straight line and in circles for each horse before and after PDN blocks. Lameness grades were 0- no lameness observed, 1- mild lameness without an observed head nod, 2- mild head nod observed, 3- obvious head nod observed, 4- severe head nod with less than 50% of normal weight supported on the limb, and 5- non-weight bearing on the limb. Radiographs, including a 60 degree dorsopalmar view, a palmaroproximal to palmarodistal oblique (skyline) of the distal sesamoid (navicular) bone, and a lateromedial projection of the foot were evaluated for all horses included in the study.

Magnetic resonance imaging was performed on both front feet of every horse following general anesthesia. Each horse had a complete physical exam, including an ECG and CBC, prior to anesthesia. Anesthesia was induced with ketamine and diazepam and maintained with 2 to 5% isoflurane in oxygen. All horses were placed in right lateral recumbency and their front feet positioned in a 1.0 Tesla magnet.[a] A human knee quadrature receiver coil was positioned around the foot and multiple image sequences were obtained using proton density, T2-weighted, short tau inversion recovery, and gradient echo sequences. Axial, sagittal, and coronal sections were obtained using standard MR protocols for the foot of the horse that were developed at Washington State

University.[21] All MR images were stored on magnetic optic discs for later retrieval and evaluation. All horses were rope recovered from anesthesia in a padded recovery stall.

A standardized format was used to record MRI observations and images were compared to those previously obtained from normal horses. A primary finding, based on severity and lack of other observed abnormalities, was made in horses where it was clear that one principle abnormality was present. In the other horses, a primary location of inflammation could not be identified from the multiple abnormal findings identified. Based on MRI findings, the limb with the most severe findings was recorded before lamest limb was known, and these results later compared to lameness exam findings. If MRI findings were similar between limbs, this was recorded.

The prevalence of injury to the five structures most commonly affected in this group of horses was compared to the 5 most prevalent findings in a previous report on horses with recent onset of navicular disease[4] using contingency tables (GraphPad Software, Inc., 5755 Oberlin Drive #110, San Diego, CA 92121, USA).

Results

Seventy-nine horses met the study criteria between April 1999 and November 2007. There were 51 geldings, 25 mares, and 3 stallions with a mean age of 9.4 years (median 9, range 3-18). There were 39 Quarter Horses, 20 Warmbloods, 7 Thoroughbreds, 7 Paints, 2 Arabians, 1 Appaloosa, 1 Lippizaner, 1 Paso Fino, and 1 Morgan. Twenty-eight were used in western performance events, 15 were used for dressage, 12 were used as pleasure or show horses, 9 were used for jumping or eventing, 1 was used for racing, and 1 had not yet been trained. Use was unknown in the other 13 horses. The mean lameness grade was 2 when the horses were trotted in a straight line

over a smooth hard surface (range 1 to 3). Lameness was observed on both forelimbs in 41 horses when the horse was trotted in small circles. All other horses had a unilateral lameness observed prior to the PDN block on the lame leg. The forelimb lameness was more easily observed following firm flexion of the distal forelimb for 6-8 seconds in at least 18 horses. At least fifty horses had sensitivity to hoof testers on at least one foot during the initial lameness examination.

MRI Observations

Many different abnormalities were observed on MR images of the front feet of the horses in this study. The majority of horses had multiple abnormalities surrounding the navicular region in both front feet that made it difficult to determine a primary abnormality.

Thickening, with or without abnormal hyperintensity, of the collateral sesamoidean ligament (CSL) was observed in 72 horses (137 limbs) (Figure 1). This was the most frequent abnormality observed based on the number of limbs it affected and was seen bilaterally in most of these horses. Thirty-six horses (65 limbs) had adhesions between the CSL and the deep digital flexor tendon (DDFT). Thirty-eight limbs had damage to the DDFT at the level of the CSL and 1 limb had damage to the DDFT at the level of the navicular bone. Damage to the CSL was determined to be the primary abnormality in 19 (24%) horses.

Abnormal hyperintensity was observed in the navicular bone on STIR sequences in 73 horses (133 limbs). Abnormal hyperintensity was always observed in the distal third of the bone, either as focal or diffuse hyperintensity. In many horses, the hyperintensity also extended proximally into part or all of the medullary cavity. The amount and

strength of hyperintensity on STIR sequences was graded as mild, moderate, or severe (Figure 2). Eighteen horses (26 limbs) had abnormal hypointensity on proton density and T2-weighted sequences that was located within the central medullary cavity of the navicular bone, compatible with sclerosis (Figure 3). In 7 horses, this sclerosis was associated with flexor cortical erosion (Figure 4). Hyperintensity in the navicular bone was determined to be the primary abnormality in 13 (16%) horses. Hyperintensity in the navicular bone was not significantly different between horses with chronic signs of navicular syndrome and those with recent onset of signs ($P = 0.1970$).[4]

Forty two-horses had coronal images through the navicular bone enabling definitive diagnosis of distal border fragmentation; 15 (36%) horses (19 limbs) had navicular bone fragments in this area (Figure 5). Ten horses had distal margin fragments only in one limb; 6 were medial and 4 were lateral. Four horses had distal margin fragments in both limbs; 1 horse had medial and lateral fragments in each limb, 1 horse had medial and lateral fragments in one limb and a medial fragment on the other limb, and 2 horses had lateral fragments. One horse had an avulsion fragment on the proximo-lateral aspect of the navicular bone within the body of the CSL. Fragments from the distal border of the navicular bone did not always correlate with lameness; 7 fragments were found on the most lame leg and 4 were found in the least lame leg.

Eight horses in the study had erosions in the flexor cortex of the navicular bone. All erosions involved the flexor surface in the centrodistal third of the bone. One horse had defects in both navicular bones and the remaining 7 horses had a single defect in one navicular bone (4 in the left front, 3 in the right front). The horse with bilateral lesions had small erosions on either side of the sagittal ridge on one limb. Erosions measured 3-

6mm, from medial to lateral in the horses in this study. Of the horses with unilateral erosions, 5 were found on the most lame leg, and 2 were found on the least lame leg.

Abnormal hyperintensity and/or enlargement of the distal sesamoidean impar ligament (DSIL) was observed in 50 horses (95 limbs). Twenty-five horses (36 limbs) also had abnormal hypointensity on proton density and T2-weighted sequences at the DSIL insertion onto the navicular bone, compatible with sclerosis in this area (Figure 6). Distal sesamoidean impar ligament damage was determined to be the primary abnormality in 6 horses. Two horses also had unilateral hyperintensity within the third phalanx at the insertion of the DSIL (Figure 7). Both of these horses had DSIL thickening and abnormal hyperintensity within this ligament on the same foot. Horses with chronic signs of navicular disease are 3 times more likely to have DSIL injury than horses with recent on set of navicular syndrome ($P = 0.001$).[4]

Thirty-nine horses (58 limbs) had enlargement, irregularity and/or abnormal hyperintensity within the DDFT which was graded as mild, moderate, or severe at four separate levels of the tendon within the horse's distal limb (Figure 8). Twenty-one horses (27 limbs [46%]) had damage proximal to the proximal interphalangeal joint and all of these were core lesions in one or both lobes. Thirty-eight horses (56 limbs [97%]) had damage proximal to the navicular bone of which the majority were core lesions (61%), followed by sagittal plane splits (20%), and focal dorsal border lesions (4%). The remaining 6 horses had a combination of core lesions and sagittal plane splits. Nineteen horses (24 limbs [41%]) had damage at the level of the navicular bone and all of these were sagittal plane splits. Twelve horses (12 limbs [21%]) had damage distal to the navicular bone, of which 10 (83%) were core lesions and 2 (17%) were sagittal plane

splits. Dorsal border fibrillation was only visualized at the level of the CSL, and this occurred with or without core lesions, sagittal plane splits, or focal dorsal border lesions.

Tendon abnormalities were most commonly located just proximal to the navicular bone. Of the 56 limbs that had lesions in the tendon at this level, 42 (73%) had increased fluid within the navicular bursa, 37 (64%) had adhesions to this ligament, and 26 (44%) had scar tissue within the proximal aspect of the bursa. Tendon damage distal to the navicular bone was only seen unilaterally, and was found in the lamest limb in 8 of the 12 horses (67%). Tendon damage in the pastern region was never seen without tendon damage also occurring in a more distal portion of the tendon in the same limb. In 5 horses, tendonitis of the DDFT was the primary finding observed. There was no difference in prevalence of DDFT injury between this study and a previous study on horses with recent onset of navicular syndrome ($P = 0.625$).[4]

Fifty-six horses (96 limbs) had increased synovial fluid observed in the navicular bursa, this was graded as mild, moderate, or severe (Figure 9). Twenty-eight horses (49 limbs) also had abnormal hypointense tissue, consistent with scar tissue, present in the proximal aspect of the navicular bursa between the DDFT and the CSL (Figure 10). This was considered a primary abnormality in 1 horse. Horses with chronic signs of navicular bursitis were 3 times more likely to have navicular bursitis than horses with recent onset of signs ($P = 0.0016$).[4]

Thirty-six horses (62 limbs) had increased synovial fluid observed in the distal interphalangeal joint. All these horses also had other abnormalities observed in the navicular bone or it's supporting soft tissue structures. Three horses (4 limbs) had osteoarthritis of the distal interphalangeal joint. In these horses, irregularity of the

cartilage and subchondral bone was present in some region of the distal interphalangeal joint, most obvious on the transverse images (Figure 11). One horse (1 limb) had damage to the medial collateral ligament of the distal interphalangeal joint. This horse had damage at the insertion of the ligament on the left distal phalanx with associated hyperintensity on STIR images and hypointensity on proton density and T2 images (Figure 12).

Eight horses (12 limbs) had thickening, with or without abnormal hyperintensity, in the distal digital annular ligament (DDAL) (Figure 13), of which 4 horses had unilateral injury and 4 horses had bilateral injury. Of the unilateral injuries, 3 were on the lamest leg, with one having adhesions to the digital flexor tendon sheath and DDFT. Of the bilateral injuries, 2 horses had similar injuries on both limbs, 1 had a worse injury on the lamest leg, and 1 had a worse injury on the least lame leg. Inflammation of the DDAL was not determined to be the primary abnormality in any of these horses.

Two horses (2 limbs) had hyperintensity in the middle phalanx seen on STIR sequences (Figure 14). These horses also had obvious pathologic change in the navicular region of both front feet. One horse (both limbs) had abnormal hyperintensity in the distal phalanx bilaterally along the dorsal surface of the bone, but this was not associated with laminar thickening or signal change.

Three horses (3 limbs) had irregularity of the lamina on one foot near the toe. None of these horses had rotation of the distal phalanx within the hoof capsule, but they did have focal thickening of lamina in areas near the toe. One horse had laminar irregularity in the least lame leg, and 2 horses had laminar irregularity in the lamest leg. These changes were not determined to be a primary abnormality in any horse.

Thirty-five (44%) horses had multiple abnormalities present that made determination of a primary abnormality difficult. Of these horses, 13 (38%) had involvement of the DDFT and CSL, with adhesions between these two structures. This subgroup was more likely to have navicular bursitis with scar tissue in the proximal extent of the bursa. Another subgroup of 11 (32%) had involvement of the navicular bone and CSL and/or DSIL without involving any other structures.

Correlation of MR Findings and Lamest Limb

Of the 79 horses evaluated with MRI, 13 horses (16%) had very similar findings on both limbs, and 66 horses (84%) had obvious differences in severity of pathology between limbs. In the horses with obvious differences between limbs, 90% (59/66) had the most severe and highest number of findings on the most lame leg and 10% (7/66) of the horses had the most severe and highest number of findings on the least lame leg.

Lameness Follow Up

Fifty-six horses (71%) were available for follow up evaluation by phone calls with the owner or trainer. Twenty-five (45%) of these had remained lame and out of work after diagnosis with MRI. Twenty-nine (52%) had remained in the same or lower level of work for the following 6-12 months after diagnosis. Within 1 year of diagnosis, 6 horses died of unrelated causes and 4 were euthanized because of persistent lameness.

At one year after diagnosis, 9 of the 46 horses still alive were working at a lower level than before their lameness began, and 14 were working at the same level as before their lameness began, for a total of 50% (23/46) still in work at some level. By 2 years after diagnosis, 5 horses were working at a lower level and 9 horses were working at the same level, for a total of 31% (14/46) still in work. By 3 years after diagnosis, 6 horses

remained working at a lower level and 6 horses remained at the same level, for a total of 25% (12/46) horses still in work. Follow up was available on 6 horses that remained in work for at least 6 years following diagnosis.

Discussion

This is the first report of MRI observations in a group of horses with chronic clinical signs of navicular syndrome without radiographic changes. It is clear that clinical signs of navicular syndrome can result from a variety of abnormalities.[4,12-13,16-21,23-27] Multiple abnormalities like navicular bone degeneration, CSL desmitis, DSIL desmitis, navicular bursitis, and DDF tendonitis, may be related and occur together in the same horse.

Horses with chronic signs of navicular syndrome were 3.6 times more likely to than horses with recent onset of clinical signs to have multiple structures pathologically altered in which a primary diagnosis could not be made.[4] This is evident by the large number of horses (44%) in which a primary abnormality could not be determined. Horses with multiple abnormalities had more than 2 structures moderately to severely involved, and it was not possible to determine if one pathologic change initiated another.

There are two predominant groups of horses in the multiple abnormality category. One group of horses had concurrent damage to the DDFT and CSL with adhesion between these two structures, and often navicular bursitis with scar tissue in the proximal joint pouch. This group was considered a primary soft tissue case as there was little navicular bone involvement. The second group of horses had concurrent pathologic change within the navicular bone and one or both of it's supporting ligaments which points to a combined navicular suspensory apparatus injury. Both groups of horses have

comparable pathologic change within all affected structures which may mean that in these horses, the structures are affected together and degeneration progresses at a similar rate.

It was difficult to determine the initial location of pathologic change in the horses in this study unless only one structure was affected. Aging these lesions and determining the chronological order of different pathologic changes is not possible at this time, although it may be possible in the future to use specific contrast agents to separate areas of active inflammation from chronic scar tissue. It is evident that individual horse's with similar clinical signs can have different structures or combinations of structures affected. Horses with changes to the navicular bone and it's supporting structures may go on to develop DDFT injuries as a progression of the disease process centered around the navicular bone. In other horses, primary DDF tendonitis occurs without pathologic change to the navicular bone or its ligamentous supporting structures.

In this study, the majority of horses diagnosed with navicular syndrome are Quarterhorses, followed by Warmbloods and Thoroughbreds. These horses perform in a wide variety of events which suggests that the activity itself may not be an important factor in the pathologic processes that occur. The horses in this study often had one limb that was more lame than the other limb and lameness was observed in the opposite limb sometimes only after a local anesthetic block was performed. Because of the bilateral nature of navicular syndrome, the majority of horses are seen to be moderately lame on one limb prior to nerve blocks, but this does not always indicate the actual degree of lameness in these horses since they are protecting both feet to some degree. To truly determine the lameness grade of the most lame limb, lameness would have to be

eliminated from the least lame limb, and vice versa. This is impractical in a clinical setting and was not done with the horses in this study.

Distal limb flexion did exacerbate lameness in some of these horses and this would suggest that compression over the navicular bone and its supporting structures was painful. It has been shown that extreme extension of the distal interphalangeal joint can also exacerbate lameness in navicular syndrome horses.[3] More than half the horses in this study had sensitivity to hoof testers over the middle of the frog on at least one limb, and this correlates with the location of the pathologic change in many of these horses. This area is directly under the navicular bone and its supporting structures, as well as the area of the deep flexor tendon within the foot commonly affected with pathologic change.[4]

There were more chronic horses (91%) with pathologic change in the CSL than horses with recent onset of navicular syndrome (75%),[4] and horses in the chronic group were 3.4 times more likely to have pathologic change within this ligament. Also in this study, there was a high incidence of adhesion between the CSL and the DDFT. The source of initial pathologic change in these horses is difficult to determine. Perhaps inflammation in any of these structures can result in fibrosis and adhesion between the ligament and the tendon. Some of these horses also have abnormal signal changes within the navicular bone, and it is difficult to determine whether this is related to surrounding ligament or tendon injury.

Pathologic change in the navicular bone was the second most common finding in this chronic group of horses and was present in almost as many limbs as pathologic change in the CSL (133 vs. 137 limbs, in 73 and 72 horses, respectively). More severe hyperintensity changes (compatible with edema) were observed in the lamest leg more

often than abnormal hypointensity (compatible with sclerosis). Therefore, hyperintensity on STIR sequences may be more important as a cause of pain than hypointensity on proton density sequences. Small, unilateral flexor cortical erosions were found to correlate with the more lame leg 71% (5/7) of the time. However, these small erosions (3-6mm in width) may cause less pain than larger lesions visible on radiographs, and the larger lesions may correlate better with lameness.

The prevalence of distal margin navicular bone fragments in horses with chronic navicular syndrome (36%) was comparable to findings in horses with recent onset of navicular syndrome (37.5%).[4] More often, these fragments were found in the lamest limb. It remains unknown how important these fragments are in the pain caused by pathologic change in the navicular region. All horses with distal margin navicular bone fragments had DSIL desmitis and/or navicular bone degeneration in the distal third of the bone centered over the DSIL insertion. This suggests that there may be a pathologic process occurring prior to fragmentation.

Deep digital flexor tendonitis was the primary abnormality in 5 horses (6%) in this study, which is lower than the reported prevalence in horses with recent onset of navicular syndrome[4] (18%). The overall prevalence of horses with DDF tendonitis in this chronic study, when compared to the previously reported study, is not that different (49% vs. 44%[4], respectively), but horses in the chronic study have more structures involved in the navicular region. A large number of horses with lesions in the tendon just proximal to the navicular bone had adhesions to the CSL. This indicates that horses with tendonitis in this region may be predisposed to adhesions to the CSL leading to secondary inflammation in this ligament.

When comparing the locations of DDF tendonitis in the horses in this study to the reported cases of horses with recent onset of navicular disease,[4] it is interesting to note that 50% more of the chronic horses had extension of the DDF tendonitis into the pastern region. This may be due to chronicity of the tendon pathology because tendon lesions would be more likely to progress over time.

Multiple other abnormalities were also found in the horses in this study, including DDAL desmitis, distal interphalangeal joint osteoarthritis, abnormal hyperintensity within the middle and distal phalanx, distal interphalangeal joint collateral ligament desmitis, laminar abnormalities, and adhesions of the DDFT to the digital flexor tendon sheath. It is difficult to determine in many horses that have multiple abnormalities, how these findings relate to the changes in the heel region of many of these horses. The presence of hyperintensity within the phalanges, suggestive of acute traumatic bone injury, suggests a rest and rehabilitation program may be helpful in these specific horses. Without information from a MRI evaluation, these horses are often kept in work with anti-inflammatory medication and not given a chance for bone healing to occur.

The identification of osteoarthritis and cartilage damage with MRI provides an argument for arthroscopy of the joint to debride lesions, providing a better chance for return to work in the future. Identification of collateral ligament injury would support the institution of a rest and rehabilitation program to give the ligament time to heal. It is unlikely that many of these bone, cartilage, and ligament lesions would heal if the horse continued in treatment for navicular syndrome, which supports the use of MRI to provide a definitive diagnosis.

In this study, the overall severity of MRI findings had a high correlation with the lamest leg of the horse, and this is similar to the findings reported in horses with recent onset of navicular syndrome (90% and 93%[4], respectively). The multitude of structures affected and the severity of pathology in many of the chronic horses may account for the slight decrease in accuracy in picking the limb that was most lame. These horses had more variation in the number and types of pathologic change in each limb which made it difficult to determine which changes accounted for the pain in some horses. With more cases, eventually we may be able to determine which lesions result in lameness more often or which specific groups of lesions cause lameness more frequently. Furthermore, prognosis for return to work in this study was lower than horses with recent onset of clinical signs,[4] as pathologic changes most likely progress with time and the affected horses are less likely to remain in work for extended periods.

Conclusion

There is not one pathologic process that leads to the myriad of changes present within the foot of the horse. For this reason, MRI is valuable for evaluating horses with navicular syndrome to provide a specific diagnosis that may affect new or further treatment. More horses need to be evaluated to learn more about horses with a clinical diagnosis of navicular syndrome. Correlation of MRI findings with clinical progression of lameness and response to treatment in a large number of horses will be necessary to gain further knowledge of the problems that can cause lameness in the heel of the horse.

Footnotes

[a] Philips Gyroscan, Medical Systems, Best, The Netherlands

[b] Schneider RK. Injection of the digital flexor tendon sheath as a diagnostic and treatment technique for horses with deep digital flexor tendonitis. Unpublished cases. 2001.

References

1. Ackerman N, Johnson JH, Porn CR. Navicular disease in the horse: risk factors, radiographic changes, and response to therapy. *J Am Vet Med Assoc* 1977;170:183-187.

2. Lowe JE. Sex, breed and age incidence of navicular disease and its treatment. *In Pract* 1982;4:29.

3. Stashak TS. Lameness. In: Stashak TS, ed. *Adams' Lameness in Horses.* Philadelphia: Lippinjcott, Williams, & Wilkins, 2002:664-680.

4. Sampson SN, Schneider RK, Gavin PR, Ho CP, Tucker RL. Magnetic resonance imaging of the front feet in 72 horses with recent onset of signs of navicular syndrome without radiographic abnormalities. Submitted to Vet Rad & Ultrasound 2008.

5. Wright IM, Kidd L, Thorp BH. Gross, histological and histomorphometric features of the navicular bone and related structures in the horse. *Equine Vet J* 1998;30(3):220-234.

6. Turner T, Fessler J. The anatomic, pathologic, and radiographic aspects of navicular disease. *Comp Cont Ed* 1982;4(8):350-355.

7. Turner TA, Kneller SK, Badertscher RR, Stowater JL. Radiographic changes in the navicular bones of normal horses, in Proceedings. 33rd Annu Conv Am Assoc Equine Pract 1987;33:309-313.

8. Jacquet S, Coudry V, Denoix JM. Severe tear of the collateral sesamoidean ligament in a horse. *Vet Record* 2006;159(24):818-820.

9. Dyson SJ. Radiological interpretation of the navicular bone. Equine Vet Educ 2008;20(5):268-280.

10. Dyson SJ, Murray R. Use of concurrent scintigraphic and magnetic resonance imaging evaluation to improve understanding of the pathogenesis of injury of the podotrochlear apparatus. *Equine Vet J* 2007:39(4):365-369.

11. Turner T. Diagnosis and treatment of the navicular syndrome in horses. Vet Clin N Am: Equine Pract 1989;5:131-144.

12. Sanz M, Sampson SN, Schneider RK, et al. Epidermoid cyst in the foot of a horse diagnosed with magnetic resonance imaging. *J Am Vet Med Assoc* 2006;228:1918-1921.

13. Whitton RC, Buckley C, Donovan T, et al. The diagnosis of lameness associated with distal limb pathology in a horse: a comparison of radiography, computed tomography and magnetic resonance imaging. *The Vet Journal* 1998;155:223-229.

14. Schramme MC, Murray RC, Blunden TS, et al. A comparison between magnetic resonance imaging, pathology, and radiology in 34 limbs with navicular syndrome and 25 control limbs, in *Proceedings.* 51st Annu Conv Am Assoc Equine Pract 2005;51:348-358.

15. Barber M, Sampson SN, Schneider RK, et al. Unilateral navicular bone injury diagnosed with magnetic resonance imaging in a horse. J Am Vet Med Assoc 2006;229(5):717-720.

16. Schneider RK, Sampson SN, Gavin PR. Magnetic resonance imaging evaluation of horses with lameness problems, in *Proceedings.* 51st Annu Conv Am Assoc Equine Pract 2005;51:21-34.

17. Dyson SJ, Murray RC, Schramme MC, et al. Collateral desmitis of the distal interphalangeal joint in 18 horses (2001-2002). *Equine Vet J* 2004;36(2):160-166.

18. Zubrod CJ, Farnsworth KD, Tucker RL, et al. Injury of the collateral ligaments of the distal interphalangeal joint diagnosed by magnetic resonance. *Vet Radiol Ultrasound* 2005;46(1):11-16.

19. Zubrod CJ, Schneider RK, Tucker RL, et al. Use of magnetic resonance imaging for identifying subchondral bone damage in horses: 11 cases (1999-2003). *J Am Vet Med Assoc* 2004;224:411-418.

20. Dyson S, Murray R, Schramme M, et al. Lameness in 46 horses associated with deep digital flexor tendinitis in the digit: diagnosis confirmed with magnetic resonance imaging. *Equine Vet J* 2003;35(7):681-690.

21. Sampson SN, Schneider RK, Tucker RL. Magnetic resonance imaging of the equine distal limb, in Auer JA and Stick JA, eds. *Equine Surgery,* 3rd ed. Philadelphia: WB Saunders Co, 2005;946-963.

22. Dyson SJ, Murray R. Magnetic resonance imaging evaluation of 264 horses with foot pain: The podotrochlear apparatus, deep digital flexor tendon and collateral ligaments of the distal interphalangeal joint. *Equine Vet J* 2007:39(4):340-343.

23. Dyson SJ, Murray RC, Schramme MC. Lameness associated with foot pain: results of magnetic resonance imaging in 199 horses (January 2001-December 2003) and response to treatment. *Equine Vet J* 2005;37(2):113-121.

24. Widmer WR, Buckwalter KA, Fessler JF, et al. Use of radiography, computed tomography and magnetic resonance imaging for evaluation of navicular syndrome in the horse. *Vet Radiol Ultrasound* 2000;41(2):108-116.

25. Murray RC, Dyson SJ, Schramme MC, et al. Magnetic resonance imaging of the equine digit with chronic laminitis. *Vet Radiol Ultrasound* 2003;44:609-617.

26. Zubrod CJ, Schneider RK, Tucker RL. Use of magnetic resonance imaging to identify suspensory desmitis and adhesions between exostoses of the second metacarpal bone and the suspensory ligament in four horses. *J Am Vet Med Assoc* 2004;224(11):1815-1820.

27. Dyson S, Murray R, Schramme M, et al. Magnetic resonance imaging of the equine foot: 15 horses. *Equine Vet J* 2003;35:18-26.

28. Murray RC, Schramme MC, Dyson SJ, et al. Magnetic resonance imaging characteristics of the foot in horses with palmar foot pain and control horses. *Vet Radiol Ultrasound* 2006;47(1):1-16.

29. Dyson SJ, Murray R. Magnetic resonance imaging of the equine foot. Clin Tech *Equine Pract* 2007;6:46-61.

30. Murray RC, Blunden TS, Schramme MC, et al. How does magnetic resonance imaging represent histologic findings in the equine digit? *Vet Radiol Ultrasound* 2006;47(1):17-31.

31. Moon KL, Genant HK, Helms CA, et al. Musculoskeletal applications of nuclear magnetic resonance. *Radiology* 1983;147:161-171.

32. Sabiston CP, Adams ME, Li DKB. Magnetic resonance imaging of osteoarthritis: correlation with gross pathology using an experimental model. *J Orthop Res* 1987;5:164-172.

33. Poly DW, Callaghan JJ, Sikes, RA, et al. The accuracy of selective magnetic resonance imaging compared with the findings of arthroscopy of the knee. *J Bone Joint Surgery* 1988;70(2):192-198.

34. Pool RR, Meagher DM, Stover SM. Pathophysiology of navicular syndrome. In: Yovich JV, ed. *Vet Clin of North Am Equine Pract* 1989;109-129.

35. Numans SR, van der Watering CC. Navicular disease: podotrochlitis chronica aseptica podotrochlosis. Equine Vet J 1973;5(1):1-7.

36. Ostblom L, Lund C, Melsen F. Histological study of navicular bone disease. Equine Vet J 1982;14(3): 199-202.

37. Poulos PW. Correlation of radiographic signs and histologic changes in navicular disease, in Proceedings. 29th Annu Conv Am Assoc Equine Pract 1983:241-255.

38. Ostblom L, Lund C, Melsen F. Navicular bone disease: a comparative histomorphometric study. Equine Vet J 1989;21(6):431-433.

39. Poulos PW, Brown A. On navicular disease in the horse: a roentgenological and patho-anatomic study, Part I: evaluation of the flexor central eminence. Vet Radiol 1989;30(2):50-53.

40. Poulos PW, Brown A, Brown E, Gamboa L. On navicular disease in the horse: a roentgenological and patho-anatomic study, Part II: osseous bodies associated with the impar ligament. Vet Radiol 1989;30(2):54-58.

41. Busoni V, Heimann M, Trenteseaux J, et al. Magnetic resonance imaging findings in the equine deep digital flexor tendon and distal sesamoid bone in advanced navicular disease: an ex vivo study. *Vet Radiol Ultrasound* 2005;46(4):279-286.

42. Cohen JM, Schneider RK, Zubrod CJ, Sampson SN, Tucker RL. Desmitis of the distal digital annular ligament in seven horses: MRI diagnosis and surgical treatment. Vet Surg 2008;37:336-344.

43. Blunden A, Dyson S, Murray R, et al. Histopathology in horses with chronic palmar foot pain and age-matched controls. Part 1: Navicular bone and related structures. *Equine Vet J* 2006;38(1):15-22.

44. Blunden A, Dyson S, Murray R, et al. Histopathology in horses with chronic palmar foot pain and age-matched controls. Part 2: The deep digital flexor tendon. *Equine Vet J* 2006;38(1):23-27.

45. American Association of Equine Practitioners. Definition and classification of lameness. *Guide for veterinary service and judging of equestrian events*. Lexington, KY: American Association of Equine Practitioners, 1991.

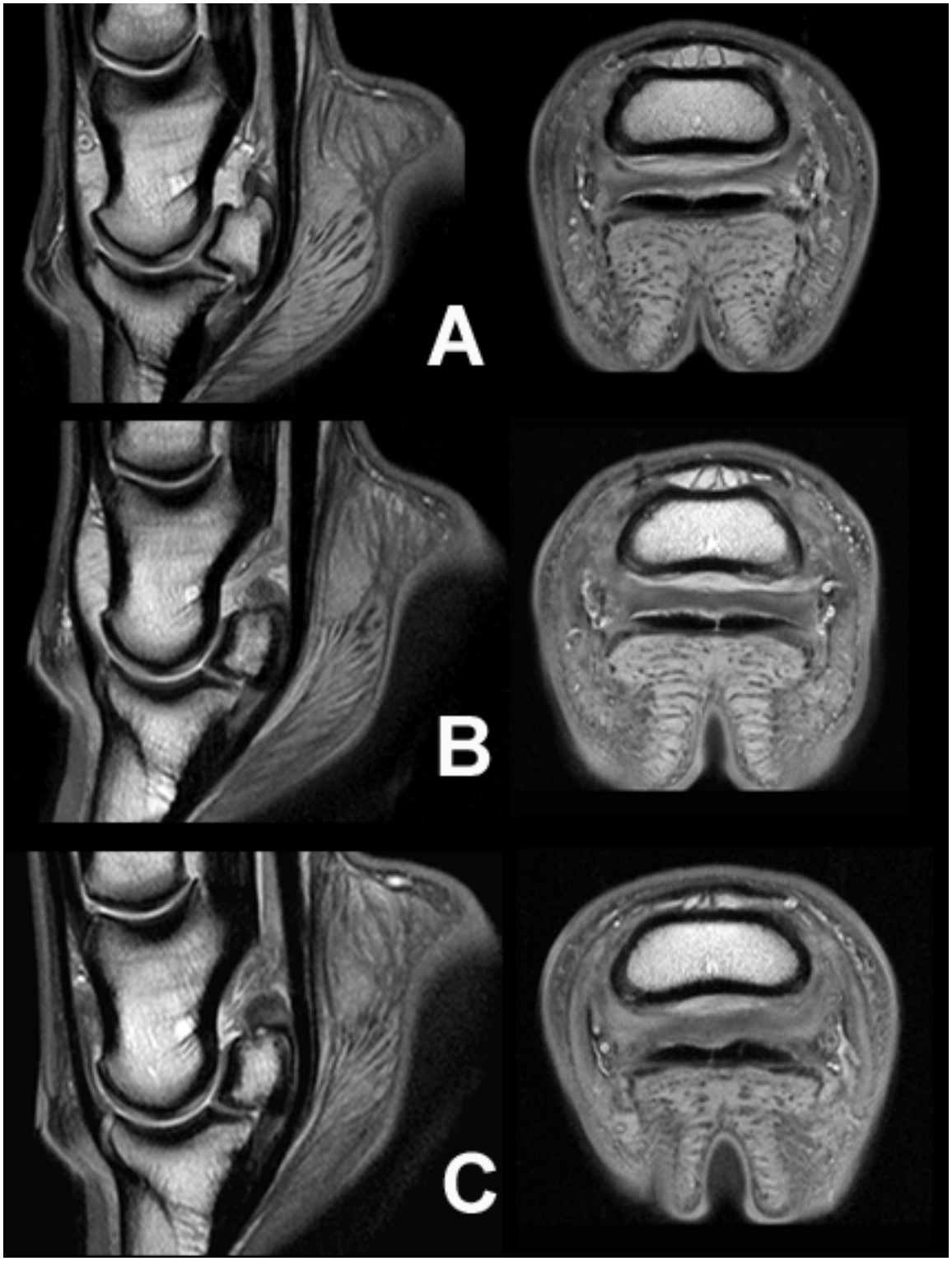

Figure 1: Sagittal (left) and axial (right) proton density images showing mild (A), moderate (B), and severe (C) enlargement of the collateral sesamoidean ligament.

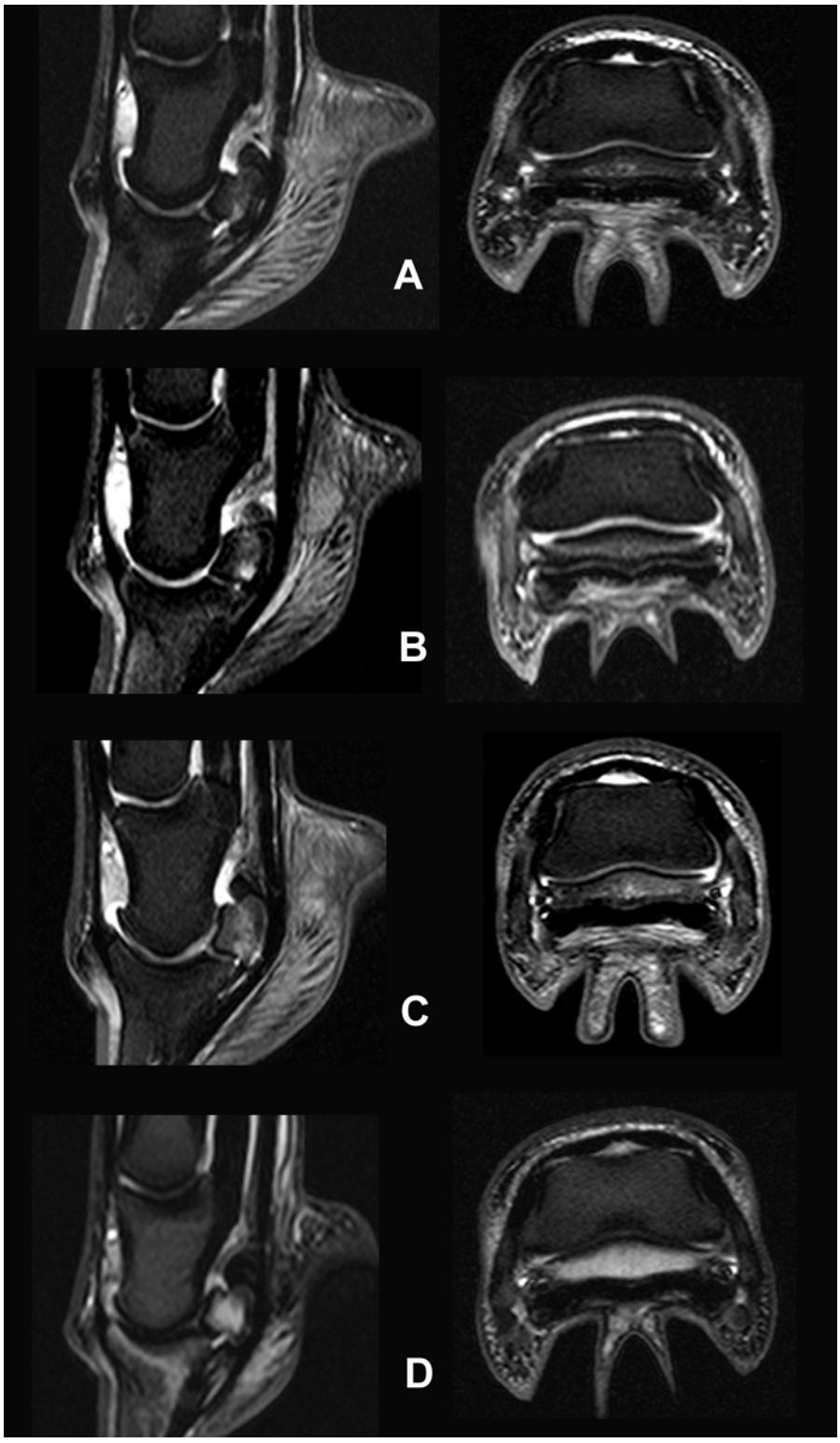

Figure 2: Sagittal (left) and axial (right) short tau inversion recovery (STIR) images showing mild (A), moderate (B), severe (C), and very severe (D) hyperintensity of the navicular bone.

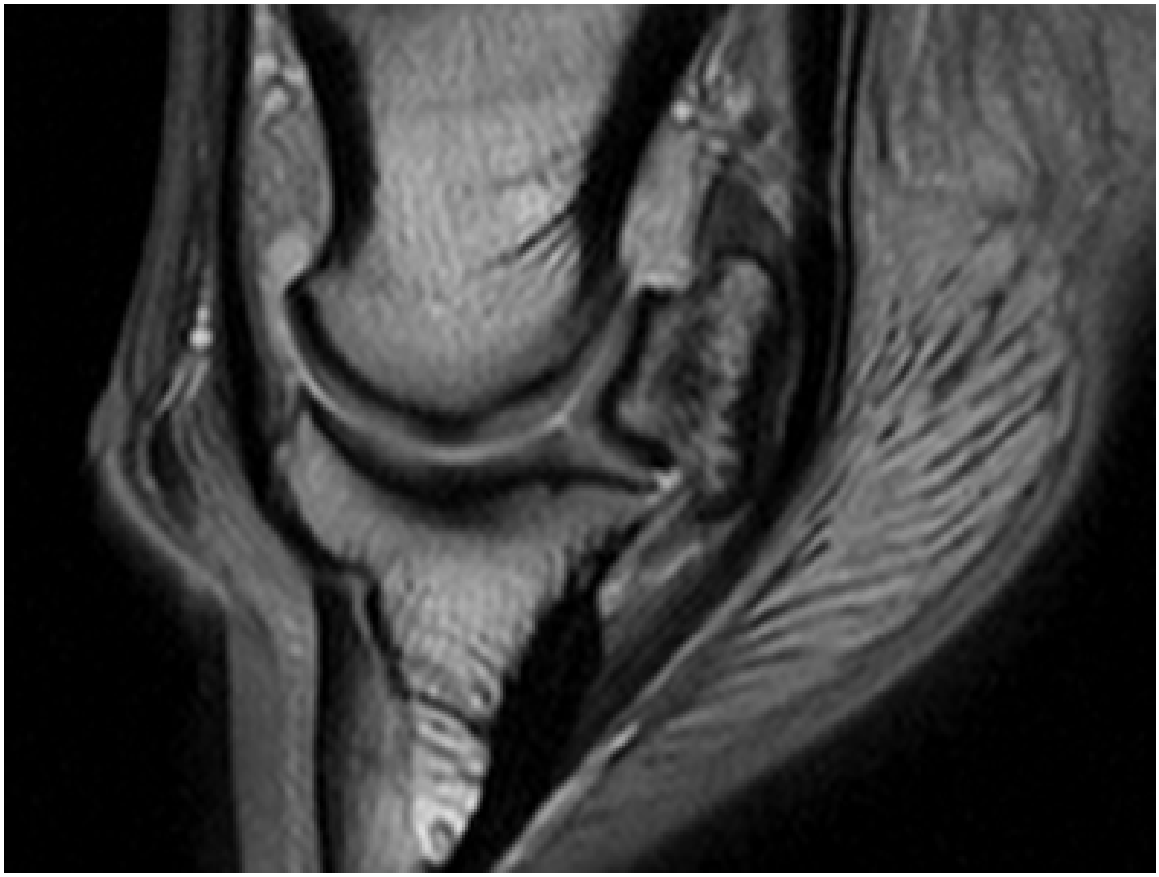

Figure 3: Sagittal proton density image from a horse with abnormal hypointensity centrally located within the navicular bone, indicating remodeling of the trabeculae resulting in sclerosis and/or fibrosis.

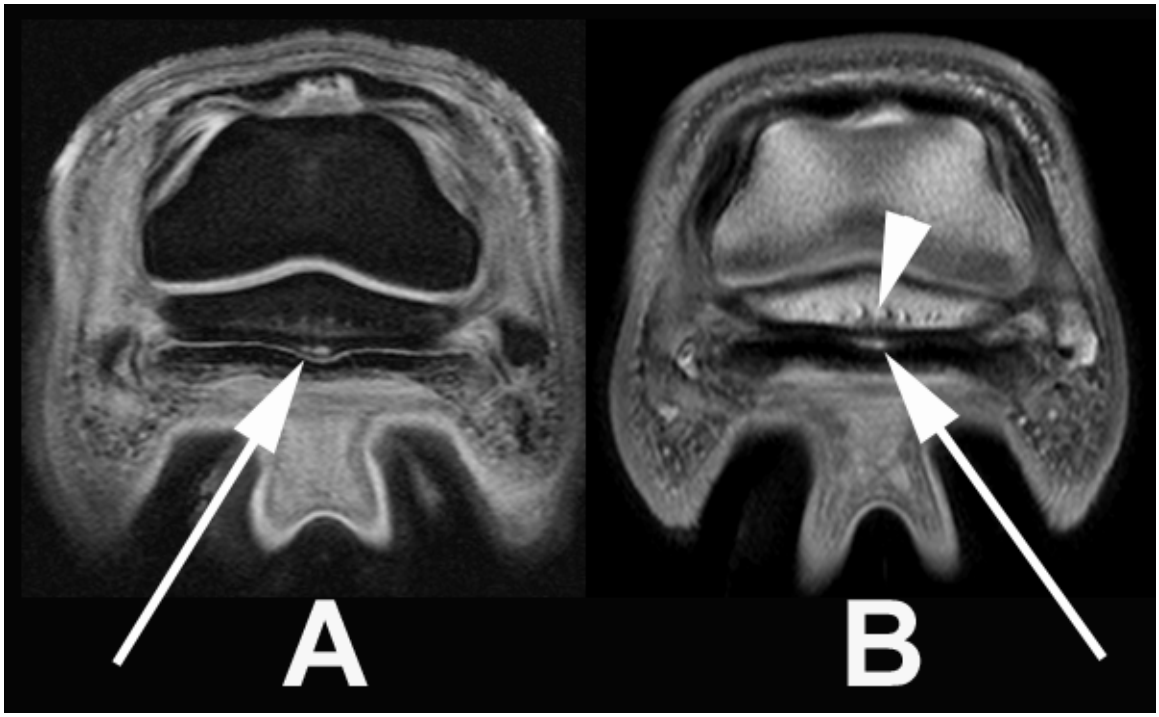

Figure 4: Axial gradient echo (A) and proton density (B) images of a horse with abnormal hyperintensity in the flexor cortex of the navicular bone at the mid-sagittal ridge (arrows). This horse also has an area of abnormal hypointensity within the medullary cavity associated with the flexor cortex defect visible on the proton density image (B) (arrowhead).

Figure 5: Coronal gradient echo image showing a distal margin fragment off the lateral angle (arrow) of the navicular bone located within the distal sesamoidean impar ligament.

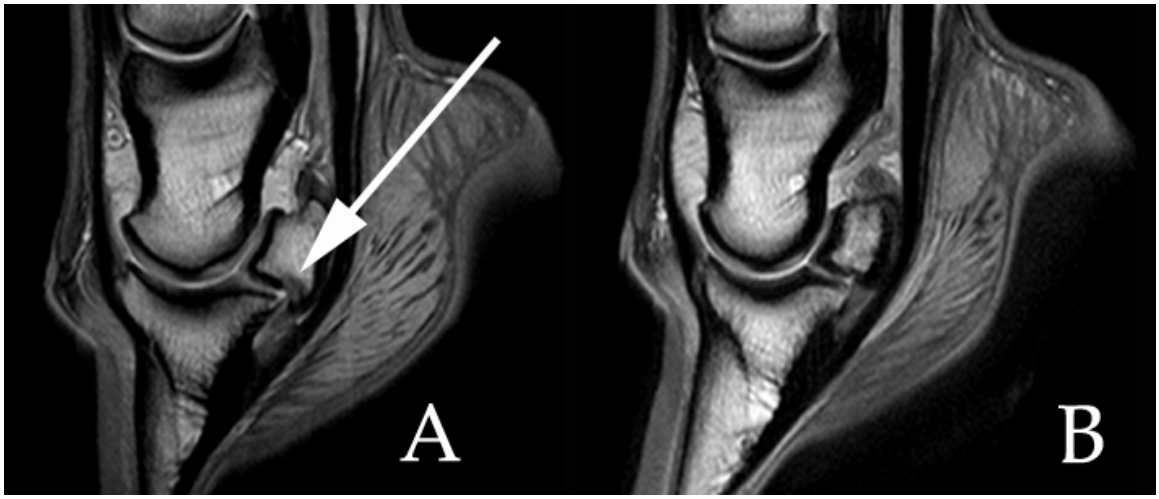

Figure 6: Sagittal proton density images showing diffuse thickening and abnormal hyperintensity of the distal sesamoidean impar ligament with (A) and without (B) abnormal hypointensity at the insertion of this ligament on the distal navicular bone (arrow).

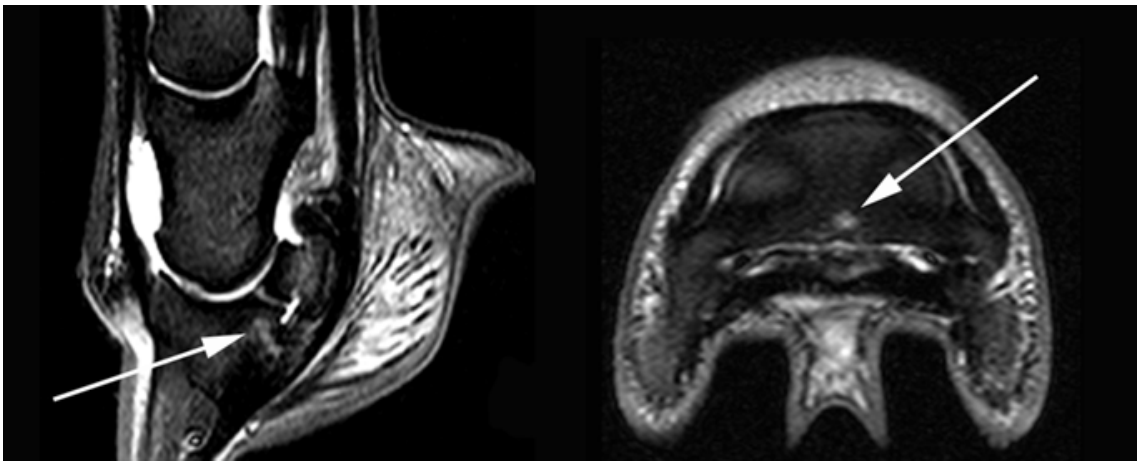

Figure 7: Short tau inversion recovery (STIR) sagittal (left) and axial (right) images of focal hyperintensity at the insertion of the distal sesamoidean impar ligament on the palmar aspect of the distal phalanx (arrows).

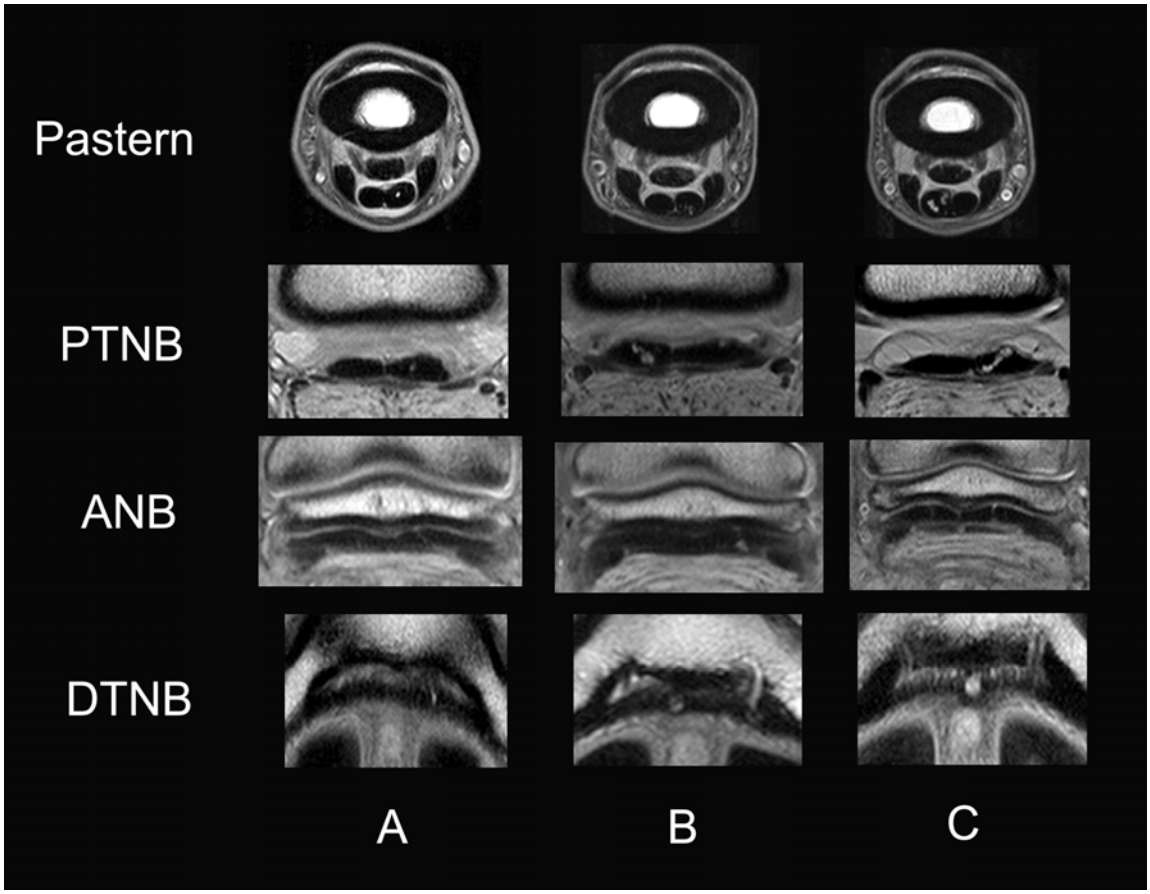

Figure 8: Axial proton density images of the pastern and foot arranged left to right showing mild (A), moderate (B), and severe (C) lesions within the deep digital flexor tendon at different levels of the limb. Pastern = above the pastern joint; PTNB = proximal to the navicular bone; ANB = at the navicular bone; DTNB = distal to the navicular bone.

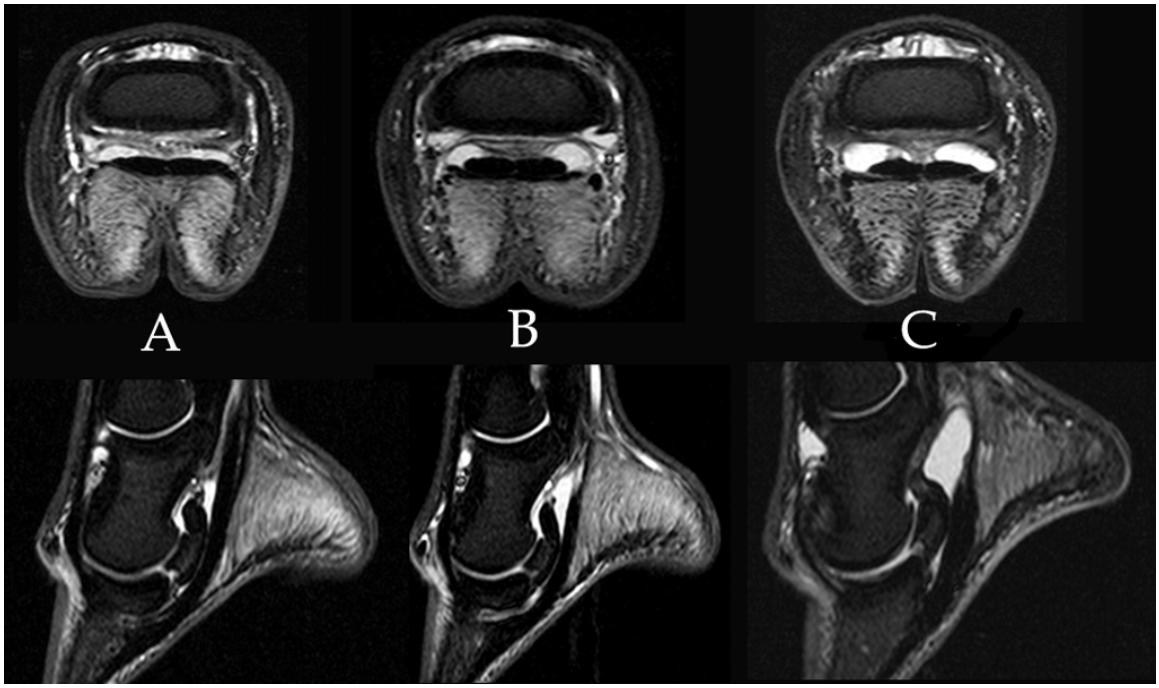

Figure 9: Axial (top) and sagittal (bottom) short tau inversion recovery (STIR) images showing mild (A), moderate (B), and severe (C) amounts of increased fluid within the navicular bursa, indicated by increased amount of signal intensity within the bursa.

Figure 10: Axial short tau inversion recovery (STIR) image proximal to the navicular bone showing abnormal low signal intensity tissue within the navicular bursa at the dorsal aspect of the deep digital flexor tendon lobes (arrows).

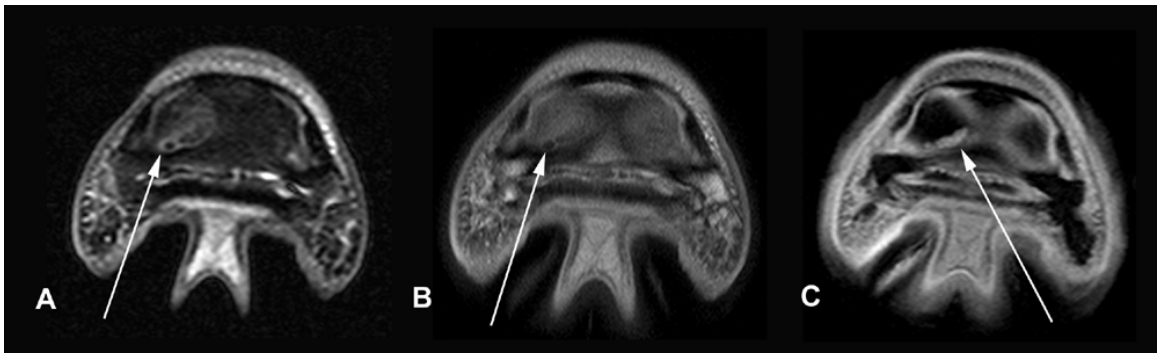

Figure 11: Axial short tau inversion recovery (STIR) (A), proton density (B), and gradient echo (C) images showing a cartilage and subchondral bone defect in the medial aspect of the distal phalanx (arrows) of the same horse.

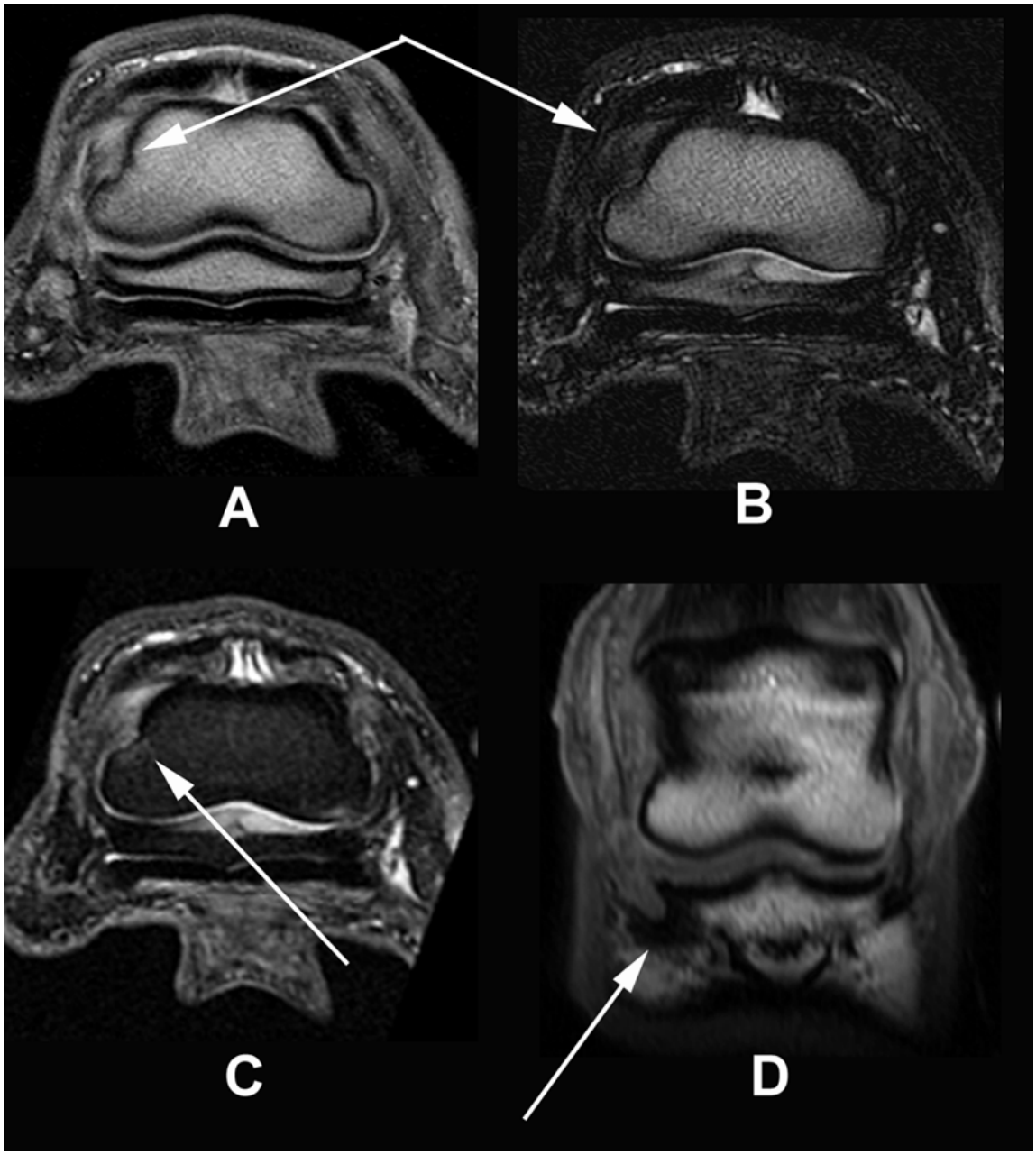

Figure 12: The top two images are axial proton density (A) and T2-weighted (B) images showing abnormal hyperintensity (arrows) within the medial collateral ligament of the distal interphalangeal joint at its insertion onto the middle phalanx. The short tau inversion recovery (STIR) image (C) shows abnormal hyperintensity within the middle phalanx at the collateral ligament insertion (arrow). The coronal T1-weighted image (D) shows the abnormal hypointensity (arrow) within the distal phalanx at the insertion of the collateral ligament, indicating sclerosis in this area.

Figure 13: Axial proton density image at the level of the proximal middle phalanx showing mild diffuse thickening of the distal digital annular ligament (arrow). There is also an area of abnormal hyperintensity (core-type lesion) present in the medial lobe of the deep digital flexor tendon.

Figure 14: Sagittal (left) and axial (right) short tau inversion recovery (STIR) images showing different areas of abnormal hyperintensity seen in horses in this study. A: diffuse hyperintensity in the navicular bone and medial half of the middle phalanx (arrows). B: focal and slightly diffuse hyperintensity within the dorsodistal middle phalanx (arrows).

CHAPTER FOUR

EVALUATION OF A SURGICAL APPROACH FOR TRANSECTION OF THE COLLATERAL SESAMOIDEAN LIGAMENT IN SIX HORSES

Introduction

Navicular syndrome is one of the most common performance limiting lameness problems in equine athletes.[1,2] A wide variety of medical treatments have been used to decrease pain and continue horses in performance[3], but there is no treatment available that provides long term relief. Navicular syndrome has been a frustrating problem to treat because it frequently progresses with degeneration of the navicular bone and re-occurring lameness to a point where horses cannot continue in performance. There have been few improvements in the treatment of this condition in the last 30 years.

The availability of MRI for live horses over the last 10 years has improved both bone and soft tissue injury diagnosis within the feet of horses with navicular syndrome.[4-23] It has become a valuable diagnostic tool that allows recognition of multiple abnormalities in horses previously grouped into one clinical diagnosis. As a result, treatments can now be based on the precise anatomical localization of the problem. Horses with navicular syndrome can have pathology in one or more of the following structures: navicular bone, distal sesamoidean impar ligament (DSIL), collateral sesamoidean ligament (CSL), navicular bursa, deep digital flexor tendon (DDFT), collateral ligaments of the distal or proximal interphalangeal joint, distal digital annular ligament (DDAL), distal phalanx, middle phalanx, or laminae.[5,7-9] Pathologic abnormalities in any of these structures has the potential to produce pain that is alleviated with a palmar digital nerve block.[5,7-9]

Many navicular syndrome horses have multiple abnormalities on MRI, but a primary abnormality can often be determined.[8,9] In some horses, the primary abnormality appears to be pathologic change in the CSL.[8-10] Magnetic resonance imaging enables evaluation of the CSL in multiple planes to accurately diagnose CSL desmitis; this has not been possible with other imaging modalities.[5,8-11] Enlargement of the body and branches of the CSL is a common finding in horses with navicular syndrome and was the primary abnormality observed in 25% of horses in one study.[9] Enlargement of the CSL is most likely a result of chronic loading that causes repetitive tearing of fibers resulting in inflammation, and a fibrotic ligament that is less elastic, causing replacement of normal ligament tissue with scar tissue.[24] Chronic tearing of a fibrotic CSL may be one source of the recurrent lameness when the ligament is under load prior to toe off. Transection of the CSL may result in a functionally longer ligament and stop repetitive damage to a fibrotic CSL, decreasing pain in these horses.

The CSL spans the proximopalmar margin of the navicular bone and attaches the wings of the proximal abaxial navicular bone to the abaxial surfaces of the middle phalanx and the distal abaxial and dorsal surface of the proximal phalanx.[25] The chondrosesamoidean ligament, an extension of the CSL, attaches the ends of the navicular bone to the axial surface of the adjacent collateral cartilage and the palmar process of the distal phalanx.[26,27] The body of the CSL is covered dorsally by the synovial membrane of the distal interphalangeal (DIP) joint pouch and palmarly by the synovial membrane of the navicular bursa. The proximal palmar joint pouch of the DIP joint forms cranial and caudal abaxial compartments that wrap around the dorsal and palmar surfaces of the distal end of each CSL branch.[26] This arrangement of proximal palmar pouch

synovial outpocketings almost completely isolates the CSL within the DIP joint.[26,28] This anatomy enables arthroscopic access to the CSL through the palmar DIP joint pouch.

Transecting the CSL has been evaluated previously in horses.[29-33] In these previous studies, horses with unilateral or bilateral forelimb heel pain had the CSL transected on the medial and the lateral aspect of the pastern at the level of the proximal interphalangeal joint. When these studies were performed, MRI was not available for live horses and the procedure was performed on all horses with clinical signs of navicular syndrome. The ability of horses to return to use in these previous studies ranged from 43-81%.[29-33] The surgical technique used in these studies did not completely transect the CSL as the CSL has multiple attachment sites on the middle and proximal phalanx that are not released through the surgical procedure employed.[25] Verification of increased movement between the navicular bone and the middle phalanx upon transection was not possible through this approach. Because of the lack of consistent improvement after surgical transection and failure to improve outcome over medical treatment and corrective shoeing, this surgery has not become popular.

The purpose of this study was to evaluate a new procedure for arthroscopic transection of the CSL in normal horses. The palmar approach to the DIP joint allows visualization of the CSL body and branches and their attachment on the middle phalanx.[34] This arthroscopic approach enables CSL transection to be visualized and increased motion between the middle phalanx and the navicular bone to be verified intra-operatively. Transection of the CSL may result in increased length in the CSL, but evaluation of this procedure in normal horses is necessary before the procedure can be recommended in clinical patients. Magnetic resonance imaging is valuable to document

complete CSL transection after surgery and evaluate healing of the CSL after arthroscopic desmotomy. Furthermore, MRI evaluations could then be compared to histomorphologic findings and results of clinical evaluation.

Materials and Methods

Horses

Six healthy adult horses free of lameness were used in this study. There were 4 mares and 2 geldings, whose mean age was 5.5 years (median 5.5, range 4-7 years). Horses were Quarterhorse (3), Paint (1), Appaloosa (1), and Arabian (1). Horses were determined to be free of front foot pathology based on clinical examination, radiographs, and magnetic resonance imaging. Horses entering the study had their feet trimmed to their natural angle and trimming was repeated every 6-7 weeks for the duration of the study. All animals in the study received immunization against Eastern and Western Equine Encephalitis, Tetanus, Influenza, Equine Herpes Virus, and West Nile Virus prior to beginning the study. They were dewormed with Ivermectin (0.22 mg/kg orally) at the beginning of the study and every 90 days during the study. All procedures described in this paper were approved by the International Animal Care and Use Committee at Washington State University.

Experimental Protocol

One forelimb was randomly assigned to be operated. The CSL was transected under arthroscopic guidance. Lameness examination was performed on all horses before surgery and monthly for 12 months (every 30 days) after surgery, resulting in 13 lameness evaluations for each horse. Bilateral front feet radiographs were taken at 0, 180 and 360 days. All lameness examinations were recorded on digital videotape. Bilateral

front feet magnetic resonance imaging evaluation was done at 0, 7, 90, 180, and 360 days. All front feet were examined at necropsy and samples collected for histologic evaluation.

Lameness Evaluation

Horses were trotted on a smooth, hard surface in a straight line and then in left and right circles. Lameness of each forelimb was graded using a modification of the AAEP grading scale:[35] 0= no lameness, 1= lame without a head nod, 2= lame with a mild head nod, 3= lame with a moderate head nod, 4= lame with a severe head nod, and 5= non-weight bearing. Lameness evaluations were videotaped for blinded evaluation at a later time. Evaluators were unaware of the limb operated and the time period of the lameness evaluation; evaluator's scores were averaged to achieve a final score for each lameness exam.

Radiography

Four radiographic projections (lateromedial, proximopalmar-distopalmar skyline of the navicular bone, 45 degree dorso-palmar of the navicular bone, and 60 degree dorso-palmar of the distal phalanx) were obtained prior to entering the study and at 180 and 360 days after surgery. Animals were sedated with 150 mg xylazine hydrochloride and 5 mg butorphanol tartrate IV.

General Anesthesia

Each horse had a complete physical examination prior to general anesthesia, including hematology and serum biochemistry, electrocardiography, and thoracic auscultation. Horses were administered butorphanol tartate (0.02 mg/kg, IV) and xylazine hydrochloride (0.85 mg/kg, IV) for sedation. Induction of anesthesia was performed

using diazepam (0.05 mg/kg, IV) and ketamine hydrochloride (2.2 mg/kg, IV) and maintained with Isoflurane, 2.0-5.0% inhaled with oxygen in a semi-closed circle system with intermittent positive pressure ventilation, for the duration of the procedure.

Magnetic Resonance Imaging

Magnetic resonance imaging was used to evaluate CSL transection and enabled measurement of the ligament at all imaging evaluations in dorsopalmar (axial images) and proximodistal (sagittal images) dimensions (Figure 1). Anatomic changes and abnormal signal intensities were evaluated using proton density, T2-weighted, gradient echo, and short tau inversion recovery (STIR) imaging sequences. Front feet images were obtained using a 1.0 Tesla MR system (Philips NT Gyroscan, Philips Medical Systems, Best, the Netherlands) using a standardized imaging protocol designed for the study (Table 1). A human quadrature receiver coil was placed on the foot and the foot positioned in the isocenter of the magnet. Transection of the CSL was verified with MRI at 7 days after surgery and healing of the CSL was monitored with MRI at 90, 180 and 360 days after surgery. Images were interpreted by 3 observers blinded to operated limb and time of examination who were experienced in equine MRI interpretation.

Surgery

Horses undergoing surgery were administered potassium penicillin (20,000 IU/kg, IV q6, two doses) and gentamicin (4.4 mg/kg, IV, one dose) on the day of surgery. Horses received phenylbutazone (4.4 mg/kg, IV) prior to surgery. After induction of general anesthesia, the horse was placed in lateral recumbancy with the operated limb uppermost. After aseptic preparation and draping, an 18 gauge, 3.5 cm needle was inserted into the dorsal pouch of the DIP joint 1.5 cm abaxial to the extensor process of

the distal phalanx and the joint was distended with 10ml of sterile saline. Joint distension was palpable axial to the palmaroproximal end of the collateral cartilage. A 5 mm incision was made with a #11 scalpel blade into the palmar pouch of the DIP joint, palmar to the neurovascular bundle and proximal to the lateral collateral cartilage. A 4mm arthroscopic obturator and cannula was inserted into the DIP joint, the obturator was removed, and a 4mm arthroscope was inserted. Entry into the DIP joint was determined by flow of joint fluid from the arthroscope sleeve when the trocar was removed, and then by direct visualization of the palmar joint pouch after arthroscope insertion. A 5 mm instrument portal was created in the same location on the opposite side of the limb using a #11 scalpel blade**.** Systematic examination of the palmar aspect of the DIP joint was performed to identify the proximal aspect of the navicular bone, the palmar aspect of the middle phalanx, and the CSL body and branches within the joint capsule. The medial collateral branch of the CSL was then located opposite the arthroscope portal and transected using a hook knife (Storz hook knife model #64146L, Karl Storz Veterinary Endoscopy, Goleta, CA 93177) with the blade edge under the dorsal aspect of the collateral branch (Figure 2).

Following complete transection of the medial collateral branch of the CSL, the arthroscope and instrument were reversed: the arthroscope was placed medially and advanced across the joint to visualize the lateral collateral branch of the CSL and the instrument was placed in the lateral portal. The lateral collateral branch was located and transected with a hook knife. Motion between the navicular bone and the middle phalanx was compared before and after transection of the CSL during surgery. Measurement of movement was based on the ability to place increasingly larger blunt trocars (2, 3, 4, 5, or

6mm) between the articular surfaces of the navicular bone and middle phalanx before and after arthroscopic transection of the CSL. Both portals were closed with 1-2 skin sutures using 0 Prolene in a simple interrupted pattern. Limbs were placed in a padded compression bandage.

Postoperative Care

Horses were recovered in a padded recovery stall. Recovery was assisted with ropes attached to the halter and tail. Phenylbutazone (4.4 mg/kg orally, once daily) was administered for 14 days. After surgery, horses were stall confined, and the operated limb bandaged with a distal limb bandage that extended distally over the heel bulbs for 14 days. Sutures were removed at 14 days and the limb rebandaged for 2-3 more days. A standard rehabilitation program was used in all horses (Table 2).

Humane Euthanasia

All animals were humanely euthanized at 360 days after surgery. They were sedated with xylazine hydrochloride (0.85 mg/kg, IV) prior to euthanasia. Animals were euthanized with 120ml of sodium pentobarbital administered IV via a 14 gauge, 3.5 cm needle as a rapid bolus.

Necropsy

After euthanasia, the distal forelimbs were removed from each horse after transection through the fetlock joint and then bisected sagittally into medial and lateral halves with a band saw. Gross observation of DIP joint extension was obtained by placing force on the proximal articular surface of the proximal phalanx and the toe to cause hyperextension of the limb. The navicular bone and middle phalanx, attached to each other by the CSL, were dissected and removed intact from each half of the foot. The

CSL collateral branch and body was measured on each half before the ligament was transected from its attachments on the middle phalanx after isolation of the middle phalanx and navicular bone from the foot. The length of the ligament on each medial and lateral side of the limb was measured from its insertion on the navicular bone wing to its first insertion on the middle phalanx. Width of the ligament was measured at 5 locations, two cross-sectional measurements through each CSL branch (measured in a medial to lateral direction at midpoint between the navicular bone and the middle phalanx), and three measurements along the body of the ligament on the proximal aspect of the navicular bone (measured in a proximal to distal direction), one at the sagittal midline (axial) and two at ½ of the distance between midline and the lateral or medial limits of the CSL, respectively. Measurements from the normal and the CSLD limb were recorded and compared. The ligaments were dissected from their attachment on the middle phalanx but left attached to the bisected half of the navicular bone and placed in 10% buffered formalin for further microscopic examination.

Histopathology

Following at least 72 hours of fixation, the CSL from both the operated and non-operated limbs was trimmed at six locations equally spaced along the entire length of the CSL from the lateral to the medial attachments to the middle phalanx. Four cross-sections of the body of the ligament and 2 long sections of the collateral branches were obtained. The trimmed CSL tissues were embedded in paraffin, sectioned at 4 microns, then stained with Hematoxylin & Eosin (H&E) for routine examination or with Trichrome stain for specific assessment of collagen.

Data Analysis

Lameness scores were compared over time using repeated measures ANOVA. Lameness scoring evaluation was separated into horses trotting in a straight line, horses trotting with the operated limb on the inside of the circle, and horses trotting with the operated limb on the outside of the circle. The average lameness grade at each time point was calculated for each lameness evaluations. Dunnett's multiple comparison post-hock test was used to determine differences between the pre-surgery and post-surgery values of each separate lameness evaluation over the 12 month evaluation period with a two-tailed significance level of $\alpha = 0.05$ for comparisons with the pre-surgery values. Measurements of the CSL from operated and non-operated limbs were compared using paired one-tailed t-tests with a significance level of $\alpha = 0.05$. Data analysis was performed using GraphPad Prism 5.01 (GraphPad Software, Inc., San Diego, CA).

Results

Surgery

Surgical transection of the CSL resulted in increased movement between the navicular bone and the middle phalanx assessed during surgery. This was determined by the ability to place larger blunt trocars (3-5mm) between the navicular bone and middle phalanx after transection, than before transection (2mm). One complication was observed during the desmotomy procedure in three horses. The palmar digital artery was partially transected during transection of the collateral sesamoidean ligament branch, most commonly on the lateral side of the limb. All horses were wrapped with a distal limb pressure bandage that extended from the proximal metacarpus to the hoof capsule and over the heel bulbs. A second pressure wrap of 4x4 gauze and elastikon was placed over the palmar pastern before the horse was moved to the recovery stall. All bandages were

changed the day following surgery and no further hemorrhage occurred. All horses were walking well after recovery and all surgical sites healed without complication.

Lameness

The average lameness score for all horses trotting in a straight line and in a circle were significantly different ($p<0.01$) from pre-surgery values for all horses at 1, 2, and 3 months post-surgery (Figure 3 and 4). The average lameness score for all the horses trotting with the operated limb on the outside of a circle was significantly different ($p<0.01$) only at 1 and 2 months post-surgery (Graph 5). All horses returned to pre-surgery lameness values when trotting in a straight line and when circling both directions by 4 months post-surgery and remained at baseline values for the 12 month duration of the study. Lameness scores were highest at the first evaluation (range 1-4) after surgery and gradually diminished to baseline values by 2-4 months after surgery. Lameness grades for each evaluator were consistent for mean lameness score.

Radiography

Radiographs of both front feet at 180 days and 360 days after surgery did not show abnormalities.

Magnetic Resonance Imaging

Complete transection of the CSL branches was verified with MRI in all horses 7 days after surgery (Figure 6). The proton density images of the operated limbs showed hyperintense signal similar to joint fluid in the gap caused by the desmotomy procedure. The signal intensity within the gap decreased over time as healing progressed, until it was the same or of similar intensity as the adjacent CSL. The transected ends of the CSL at the 7 day MR examination had increased signal intensity, but the body of the ligament

remained normal in signal intensity throughout the study. By 180 days post-surgery all horses were seen to have continuous tissue of similar intensity spanning the ligament gap (Figure 7). No changes were observed in the MRI examinations of the non-operated limbs during the study.

Gross Evaluation

Gross post-mortem evaluation of the operated front feet clearly demonstrated increased movement between the navicular bone and the middle phalanx when compared to the non-operated limb when the DIP joint was hyper-extended after sagittal transection with a band saw. The CSL branch length measurements made at necropsy at 360 days post surgery were statistically different between operated and non-operated limbs for the medial ($P = 0.0294$), but not the lateral ($P = 0.2056$), branch. There was no significant difference in the width of the body of the CSL (directly proximal to the navicular bone) between operated and non-operated horses. The average gross measurements of the non-operated and operated limbs CSL body and collateral branches are depicted in Table 3. Morphologically, the CSL of the operated limb was of irregular dorsal-palmar thickness along the lateral abaxial and medial abaxial regions, but had uniform dorsal-palmar thickness along the body (portion of ligament spanning the central, proximal navicular bone). The lateral and medial margins of the CSL (collateral branches) in the operated limbs were irregularly thinned, approximately 50% thinner in a dorsopalmar direction when compared to the non-operated CSL, giving the ligament an irregular, ragged, linearly pitted appearance (Figure 8). The attachment site of the healed transected CSL and middle phalanx varied in location proximal to the articular edge of the distal palmar articular cartilage and tended to be broader and thinner in the operated limb compared to

the non-operated limb in which the CSL attachment to the middle phalanx was thick and focal. This resulted in a heterogeneous appearance to the ligament in the operated limb and palpable differences in thickness of the ligament between the operated and the non-operated limbs.

Histopathology

The CSL collateral branches of all operated limbs had long-term reparative microscopic changes consistent with a healed surgical incision. Compared to non-operated limbs, the operated CSL had more loosely and haphazardly arranged collagen fibers, increased fibrovascular stroma between collagen bundles (fasciculi), more irregularity in size and shape of fasciculi, and intertwining instead of parallel collagen fasciculi (Figure 9). Addition pathologic changes in CSL of operated limbs included neovascularization and chondromucinous change of the collagen matrix (cartilage metaplasia) within the ligament proper (Figure 9), and synovial hyperplasia lining the distal interphalangeal joint pouch. The CSL collateral branches of all non-operated limbs, as well as the body of the CSL in both operated and non-operated limbs consisted of densely packed collagen fibers arranged in compact, parallel, uniform bundles interspersed with minimal fibrovascular stroma with slight irregularity of fasiculi size towards the medial and lateral margins of the collateral branches (Figure 9). In both operated and non-operated limbs, the loose connective tissue surrounding the CSL had small to large well-differentiated blood vessels and well-differentiated nerves.

Discussion

Surgical transection of the CSL branches caused transient lameness that resolved by 4 months in all horses. Healing of the ligament may be necessary before horses return

to soundness. Function of the palmar foot structures was similar between operated and non-operated limbs after lameness returned to pre-surgery levels. Although horses were not followed long term and were not returned to a regular performance training program, the return to soundness in all horses would support the use of this procedure in clinical patients. The initial variation in lameness scores between horses in the first 3 months may be due to differing pain tolerances of each horse.

Transection of the CSL resulted in a measurable difference in ligament length between the navicular bone and middle phalanx after healing in the medial, but not the lateral branch. Surgery also resulted in increased movement between the navicular bone and middle phalanx intra-operatively, indicating that release of the CSL branches had been achieved. Hyperextension of the digit was apparent at necropsy when compared to the non-operated limbs and this may be due to morphologic change in the operated CSL branches, as they were wider, but approximately 50% thinner than the non-operated CSL branches, as well as increased length of the medial collateral branch. This could result in less resistance to stretching during extension, resulting in a dynamic lengthening that was not apparent in static length measurements. The microscopic anatomy of healed ligaments indicates less collagen density that is more loosely spaced as well as disoriented fasciculi, and this may account for increased lengthening of the ligament under strain. The length measurements at necropsy were more difficult to perform in the operated limbs because of the diffuse nature of the new attachment sites to the middle phalanx in some horses making it difficult to choose a point from which to measure.

It is possible that even though the static ligament length was only increased in the medial branch, the dynamic length may be increased in both branches when loaded.

Measurement of this was difficult and quantitative data collection was not possible as hyperextension could not be recreated after dissection of the CSL and it's attachments from within the foot. Fibrotic ligaments that are thickened and less elastic may also be more likely to increase in length after desmotomy, resulting in increased compliance in the structures that support the navicular bone.

Magnetic resonance imaging was able to confirm complete transection of the CSL branches one week after surgery in all horses as hyperintense DIP joint fluid delineated the CSL branches and their margins. Follow-up evaluation with MRI revealed progressive healing as the gap between the transected ends of the CSL branches decreased over time and filled with increasingly dense tissue. Healing visualized with MRI correlated with a gradual decrease in signal intensity of the transected branches. Complete continuity of both CSL branches occurred after lameness returned to pre-surgery levels in all horses. Post-mortem (360 day) MRI findings of the thickness and variation in attachment of the CSL to the middle phalanx corresponded to morphologic evaluation of these findings at necropsy.

Previous studies have looked at healing of desmotomy of the accessory ligament of the deep digital flexor tendon (ALDDFT) in horses. The histomorphologic findings in this study were similar to experimental desmotomy of the ALDDFT in which an increased number of blood vessels, irregular size and shape of up to 100% of the collagen bundles, and decreased collagen density at 6 months post-surgery were seen.[36] It was shown that desmotomy can result in scar tissue of inferior quality, having a material strength of approximately one third that of normal ligaments.[36] Similar to ALDDFT desmotomy, CSLD results in transected ends maintained in axial alignment in the

direction of force. This results in an increase in gap between the ligament ends, but theoretically, not mediolateral instability. Axial alignment increases the probability that the ends would heal together, even within a synovial fluid environment which may physically slow or inhibit repair of ligaments. After ACL rupture in humans, synovial tissue forms over the ruptured surface and expresses the contractile actin isoform gene, α-smooth muscle actin, which differentiates into myofibroblasts.[37] A similar event may have occurred in this study, as multiple horses had synovial hyperplasia within the axial aspect of the transected ligaments that was incorporated into part of the gap where healing occurred.

The arthroscopic technique for CSLD enabled visualization of the palmar DIP joint pouch and CSL branch transection, as well as verification of increased movement between the navicular bone and the middle phalanx. Bleeding from the surgical site was observed in some horses which occurred as the hook knife transected the CSL branch continued palmarly through a part of the palmar digital artery. This hemorrhage did not affect arthroscopic visualization. It also occurred more commonly when the hook knife handle was directed abaxially. There can be difficulty entering the palmar pouch because of the complex anatomy in this area,[34] but this became easier with experience. The operative incisions were small and post-operative care was uncomplicated.

One of the limitations of the study was the difficulty in accurately measuring the length of the healed CSL post-mortem. The variation of the diffuse CSL attachments to the middle phalanx seen with MRI and at necropsy made accurate length measurements less precise. It is also possible that due to the small number of horses in this study, and the variation in breeds of horses in this group, there was enough variation between

normal horses that a significant length difference post-surgery could not be identified. This variation may account for the trend towards increased length in the medial collateral branch not being statistically significant, although it is unknown why there was a difference between medial and lateral branches. A second limitation in the study was the inability to work horses under saddle to simulate a more normal rehabilitation program. A more strenuous exercise program in which the horses were returned to a regular training and riding regimen may have resulted in increased lameness that lasted a longer period of time.

Conclusion

To date, this is the only study evaluating the effects of CSLD in horses. The results of this study would support the use of this procedure for horses with clinical signs due to chronic CSL injury. The efficacy of this procedure can only be determined by transection of the CSL in clinical cases with CSL injury. Magnetic resonance imaging was able to accurately assess healing of the ligament in the horses in this study.

References

1. Ackerman N, Johnson JH, Dorn CR: Navicular disease in the horse: risk factors, radiographic changes, and response to therapy. JAVMA 170:183-187, 1977.

2. Lowe JE: Sex, breed, and age incidence of navicular disease and its treatment. In Practice 4:29-31, 1982.

3. Madison JB, Dyson SJ: Treatment and prognosis of horses with navicular disease, in Ross M, Dyson SJ (eds): Diagnosis and Management of Lameness in the Horse. St.Louis, MS, Saunders, 2003, pp 299-303.

4. Mehl ML, Tucker RL, Ragle CA, et al: The use of MRI in the diagnosis of equine limb disorders. Equine Pract 20:14-17, 1998.

5. Schneider RK, Gavin PR, Tucker RL: What MRI is teaching us about navicular disease. Proc Am Assoc Equine Practnr 49:210-218, 2003.

6. Dyson SJ, Murray RC, Schramme MC, et al: Magnetic resonance imaging of the equine foot: 15 horses. Equine Vet J 35:18-26, 2003.

7. Dyson SJ, Murray RC, Schramme MC, et al: Magnetic resonance imaging in 18 horses with palmar foot pain. Proc Am Assoc Equine Practnr 48:145-154, 2002.

8. Sampson SN, Schneider RK, Gavin PR, et al: Magnetic Resonance Imaging of the front feet in 72 horses with recent onset of signs of navicular syndrome without radiographic abnormalities. Vet Radiol Ultrasound (in press)

9. Sampson SN, Schneider RK, Gavin PR, et al: Magnetic Resonance Imaging of the front feet in 79 horses with chronic signs of navicular syndrome without radiographic abnormalities. Vet Radiol Ultrasound (in press)

10. Sampson SN, Schneider RK, Tucker RL: Magnetic resonance imaging of the equine distal limb, in Auer JA, Stick JA (eds): Equine Surgery (ed 3). Philadelphia, PA, Saunders, 2005, pp 946-963.

11. Schneider RK, Sampson SN, Gavin PR: Magnetic resonance imaging evaluation of horses with lameness problems. Proc Am Assoc Equine Practnr 51:21-34, 2005.

12. Zubrod CJ. Barrett MF: Magnetic resonance imaging of tendon and ligament injuries. Clin Tech Eq Pract 6:217-229, 2007.

13. Kofler J, Kneissl S, Malleczek D: MRI and CT diagnosis of acute desmopathy of the lateral collateral semoidean (navicular) ligament and long-term outcome in a horse. Vet J 174:410-413, 2007.

14. Mair TS, Kinns J, Bolas NM: Magnetic resonance imaging of the distal limb of the standing horse: technique and review of 40 cases of foot lameness. Proc Am Assoc Equine Practnr 49:29-41, 2003.

15. Dyson S, Murray R, Schramme M, et al: Lameness in 46 horses with deep digital flexor tendonitis in the digit: diagnosis confirmed with magnetic resonance imaging. Equine Vet J 35(7):681-690, 2003.

16. Murray R, Roberts BL, Schramme MC, et al: Quantitative evaluation of equine deep digital flexor tendon morphology using magnetic resonance imaging. Vet Radiol Ultrasound 45(2):103-111, 2004.

17. Martinelli MJ, Rantanen NW: Relationship between nuclear scintigraphy and standing MRI in 30 horses with lameness of the foot. Proc Am Assoc Equine Practnr 51:359-365, 2005.

18. Mair TS, Kinns J: Deep digital flexor tendonitis in the equine foot diagnosed by low-field magnetic resonance imaging in the standing patient: 18 cases. Vet Radiol Ultrasound 46(6):458-466, 2005.

19. Dyson SJ, Murray R, Schramme MC: Lameness associated with foot pain: results of magnetic resonance imaging in 199 horses (January 2001-December 2003) and response to treatment. Equine Vet J 37(2):113-121, 2005.

20. Mitchell RD, Edwards, RB, Makkreel LD, et al: Standing MRI lesions identified in jumping and dressage horses with lameness isolated to the foot. Proc Am Assoc Equine Practnr 52:422-426, 2006.

21. Sherlock CE, Kinns J, Mair TS: Evaluation of foot pain in the standing horse by magnetic resonance imaging. Vet Record 161:739-744, 2007.

22. Dyson SJ, Murray R: Magnetic resonance imaging evaluation of 264 horses with foot pain: the podotrochlear apparatus, deep digital flexor tendon and collateral ligaments of the distal interphalangeal joint. 39(4):340-343, 2007.

23. Dyson S, Murray R: Magnetic resonance imaging of the equine foot. Clin Tech Equine Pract 6:46-61, 2007.

24. Smith RKW, Goodship AE: Tendon and ligament physiology, in Hinchcliff KW, Kaneps AJ, Geor RJ (eds): Equine Sports Medicine and Surgery. London, UK, Saunders, 2004, pp 1211-1212.

25. Bowker RM: Functional anatomy of the palmar aspect of the foot, in Ross M, Dyson SJ (eds): Diagnosis and Management of Lameness in the Horse. St.Louis, MS, Saunders, 2003, pp 282-286.

26. Bowker RM, Linder K, van Wulfen KK, et al: Anatomy of the distal interphalangeal joint of the mature horse: relationships with navicular suspensory ligaments, sensory nerves and neurovascular bundle. Equine Vet J 29(2):126-135, 1997.

27. Furst AE, Lischer CJ: Foot, in Auer JA, Stick JA (eds): Equine Surgery (ed 3). Philadelphia, PA, Saunders, 2005, pp 1211-1212.

28. Bowker RM, Rockershouser SJ, Linder K, et al: A silver-impregnation and immunocytochemical study of innervation of the distal sesamoid bone and its suspensory ligaments in the horse. Equine Vet J 26(3):212-219, 1994.

29. Wright IM: Navicular suspensory desmotomy in the treatment of navicular disease: technique and preliminary results. Equine Vet J 18(6):443-446, 1986.

30. Wright IM: A study of 118 cases of navicular disease: treatment by navicular suspensory desmotomy. Equine Vet J 25(6):501-509, 1993.

31. Bell BTL, Bridge IS, Sullivan STK: Surgical treatment of navicular syndrome in the horse using navicular suspensory desmotomy. New Zealand Vet J 44:26-30, 1996.

32. Watkins JP, McMullan WM, Morris EL: Navicular suspensory desmotomy in the management of navicular syndrome: a retrospective analysis. Proc Am Assoc Equine Practnr 39:261-262, 1993.

33. Diehl M: Desmotomy of the navicular collateral ligaments in horses with navicular disease. Proc Eur Soc Vet Surg 16:53-56, 1986.
34. Vacek JR, Welch RD, Honnas CM: Arthroscopic approach and intra-articular anatomy of the palmaroproximal or plantaroproximal aspect of distal interphalangeal joints. Vet Surg 21(4):257-260, 1992.

35. American Association of Equine Practitioners Definition and classification of lameness: Guide for Veterinary Service and Judging of Equestrian Events. Lexington, KY, American Association of Equine Practitioners, 1991, p19.

36. Becker CK, Savelberg HHCM, Buchner HHF, et al: Effects of experimental desmotomy on material properties and histomorphologic and ultrasonographic features of the accessory ligament of the deep digital flexor tendon in clinically normal horses. Am J Vet Res 59(3):352-358, 1998.

37. Murray MM, Martin SD, Martin TL, et al: Histological changes in the human anterior cruciate ligament after rupture. J Bone Joint Surg 82A(10):1387-1397, 2000.

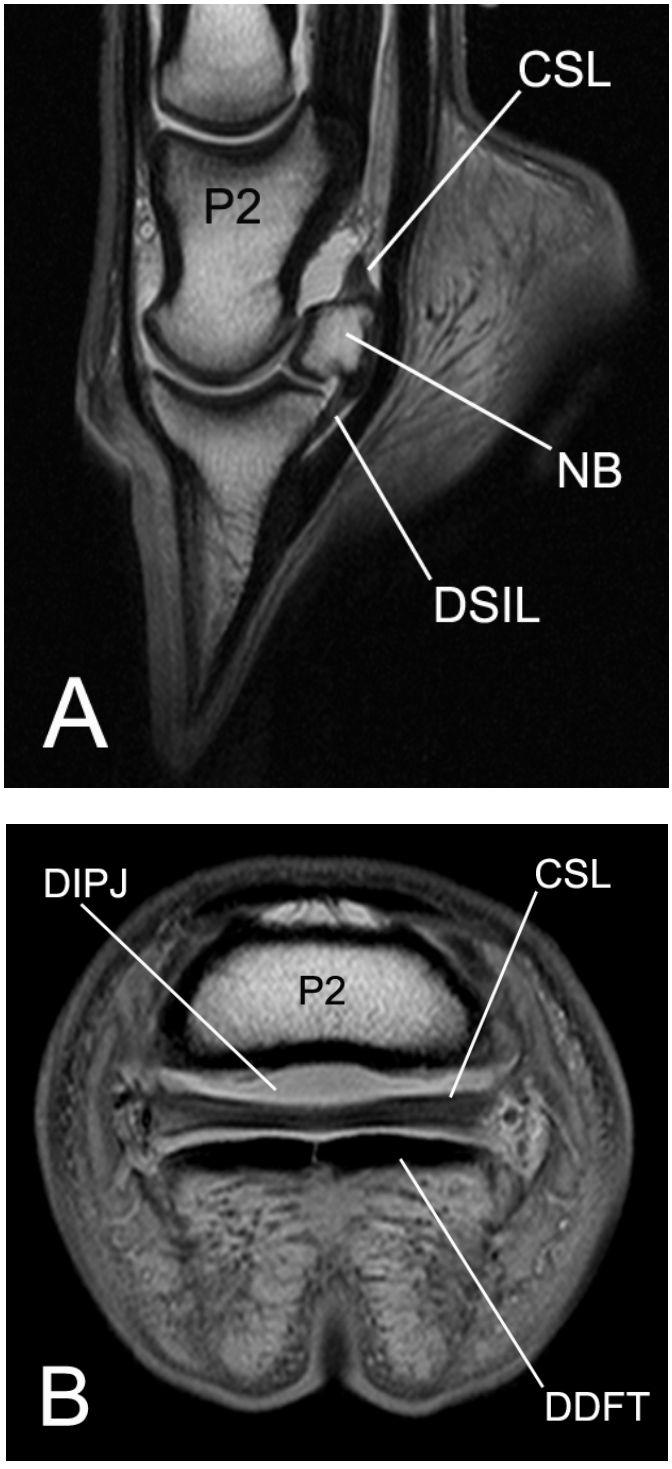

Figure 1: Sagittal (A) and axial (B) proton density images of a normal foot. The sagittal image (dorsal is to the left) is on midline and the axial image (dorsal is to the tope) is at the level of the body of the collateral sesamoidean ligament (CSL). NB, navicular bone; DSIL, distal sesamoidean impar ligament; P2, middle phalanx; DDFT, deep digital flexor tendon; DIPJ, distal interphalangeal joint pouch.

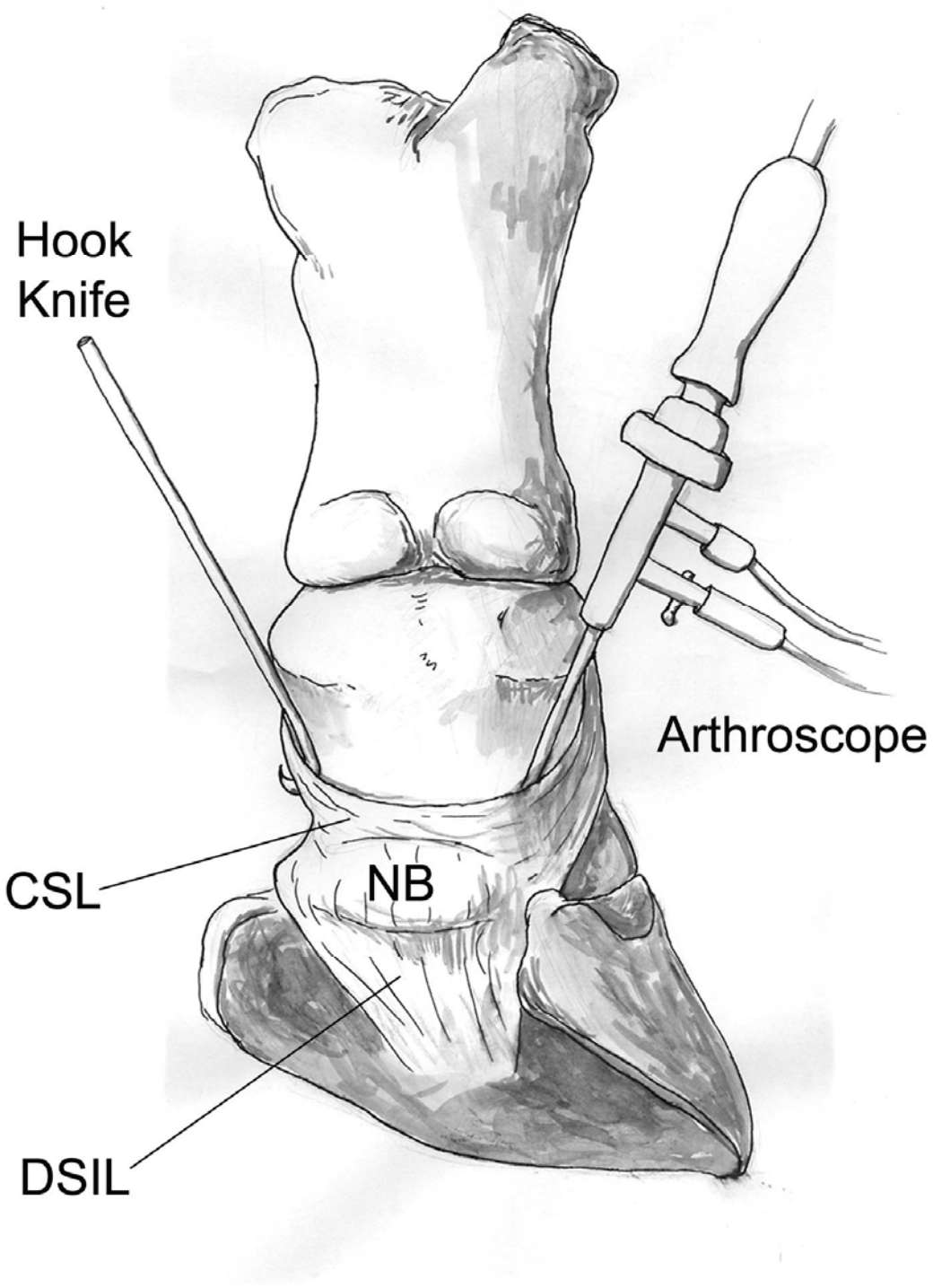

Figure 2: Diagram of arthroscope and hook knife placement in the palmar distal interphalangeal joint pouch to transect one branch of the collateral sesamoidean ligament (CSL). NB, navicular bone; DSIL, distal sesamoidean impar ligament.

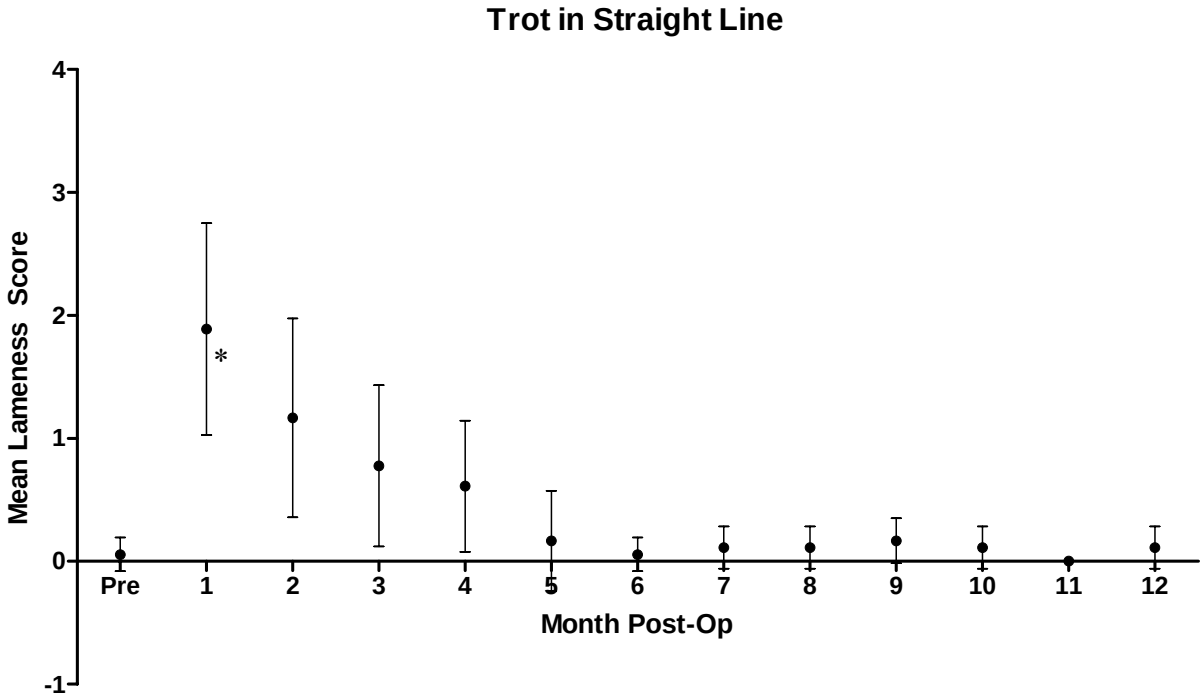

Figure 3: Lameness scores of horses trotting in a straight line (* significantly different than baseline, p<0.01).

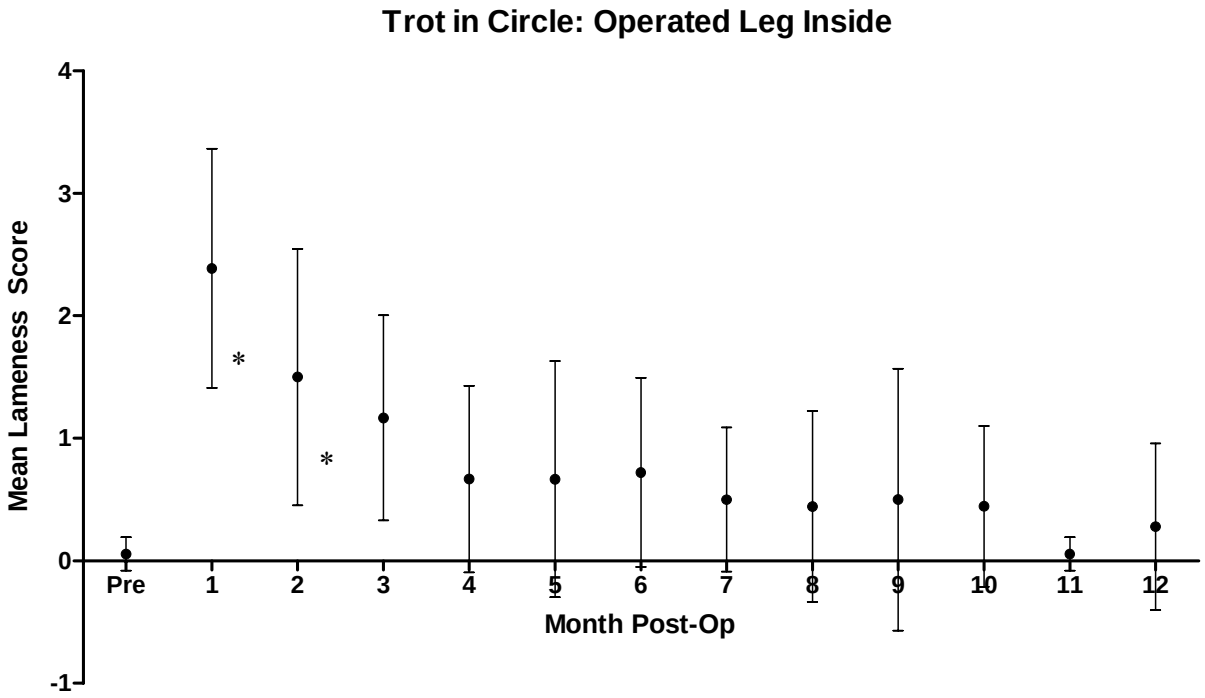

Figure 4: Lameness scores of horses with operated limb on inside of circle (* significantly different than baseline, p<0.01).

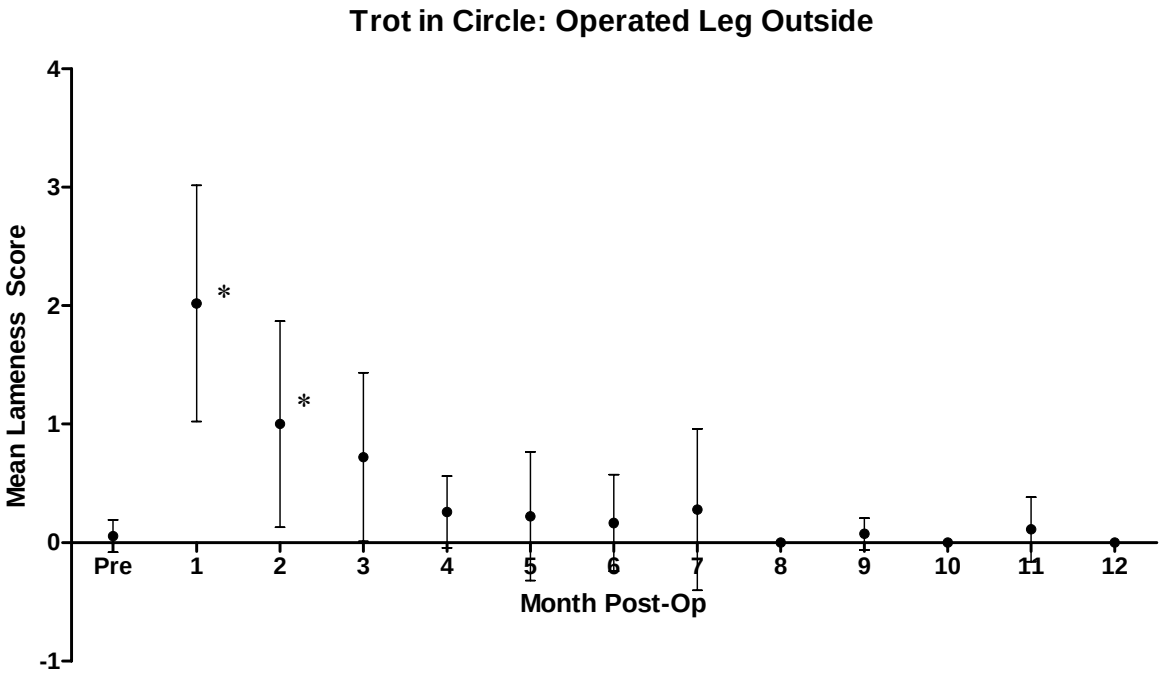

Figure 5: Lameness scores of horses with operated limb on outside of circle (* significantly different than baseline, p<0.01).

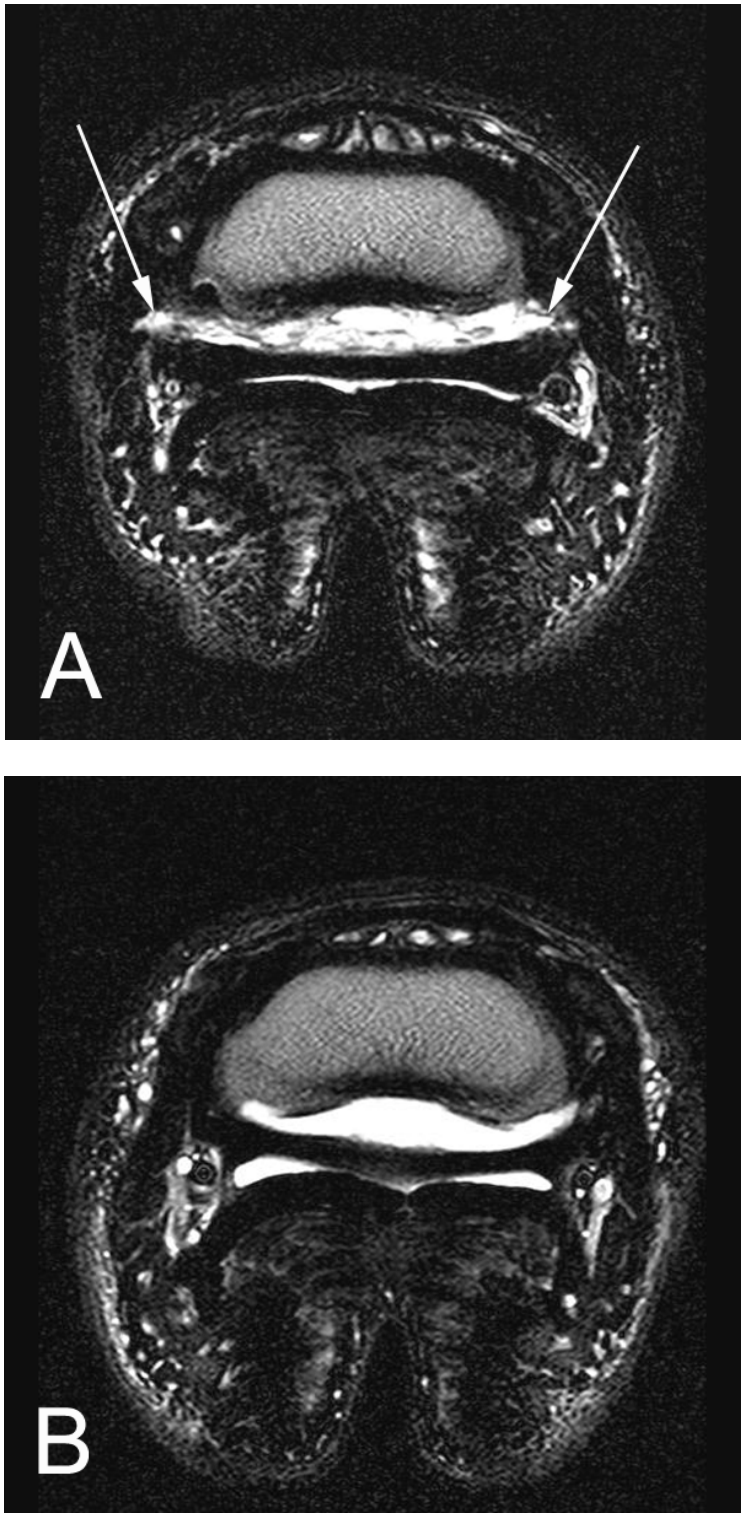

Figure 6: Axial T2-weighted images at the level of the collateral sesamoidean ligament (CSL). The left front foot (A) CSL was transected through both branches (arrows) 7 days previously and loss of continuity of the branches can be seen where hyperintense joint

fluid has replaced the hypointense ligamentous tissue. The normal right front foot (B) can be used for comparison.

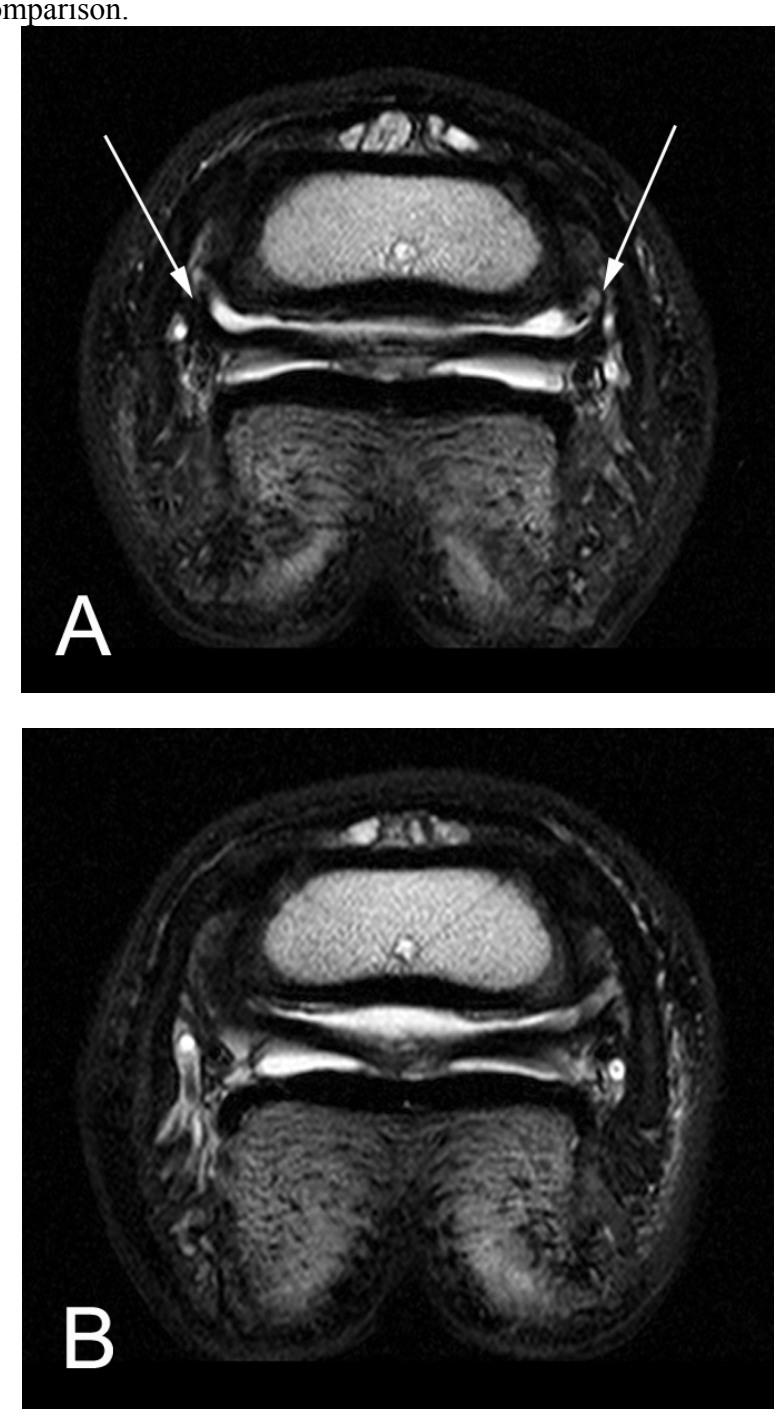

Figure 7: Axial T2-weighted images at the level of the collateral sesamoidean ligament (CSL). The left front foot (A) CSL was transected through both branches (arrows) 180 days previously and continuity of the branches can be seen as hypointense ligamentous tissue. The normal right front foot (B) can be used for comparison.

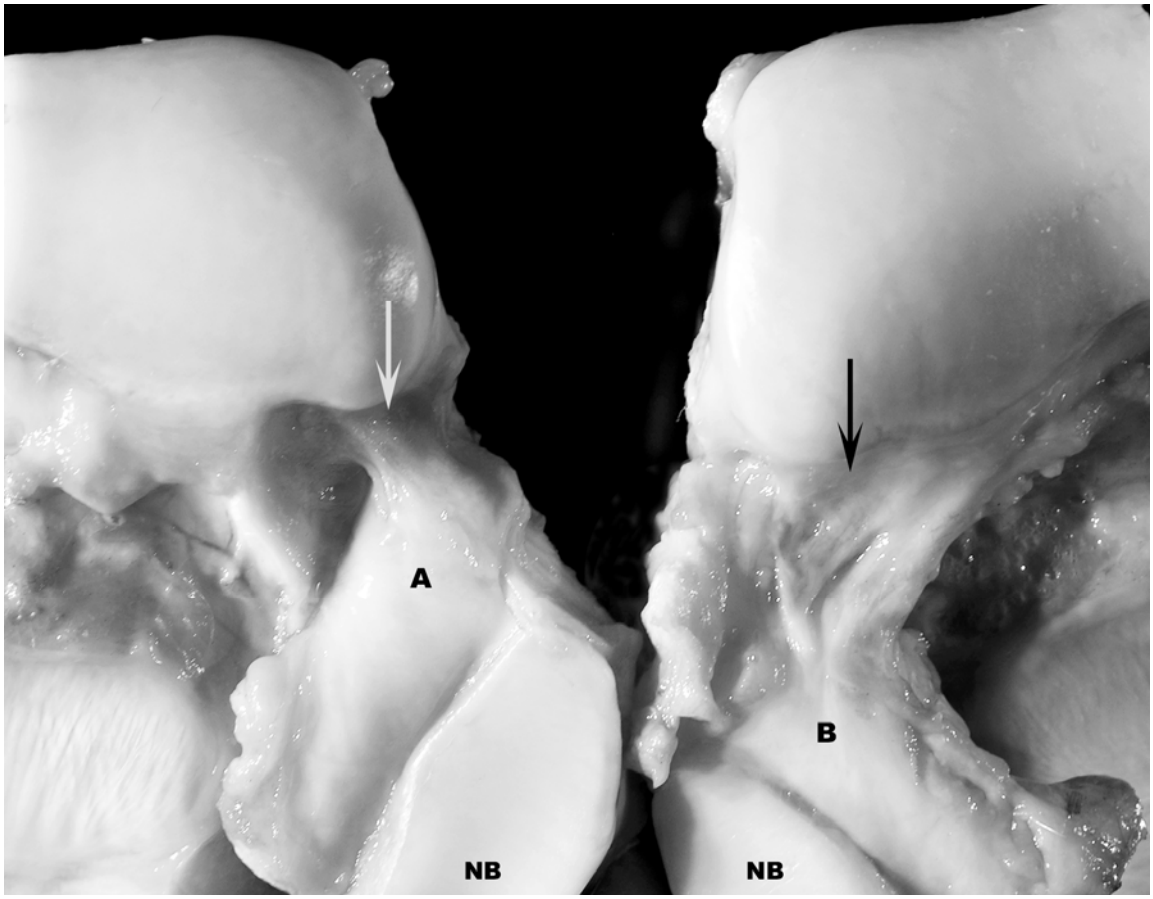

Figure 8: Macroscopic comparison between non-operated (A) and operated (B) collateral sesamoidean ligament (CSL) 360 days post-surgery. Collateral branch of operated CSL (black arrow) is thinner, more irregular and has a broader, dispersed attachment to middle phalanx compared to the collateral branch of the non-operated CSL (white arrow) of the same horse. NB = Navicular bone.

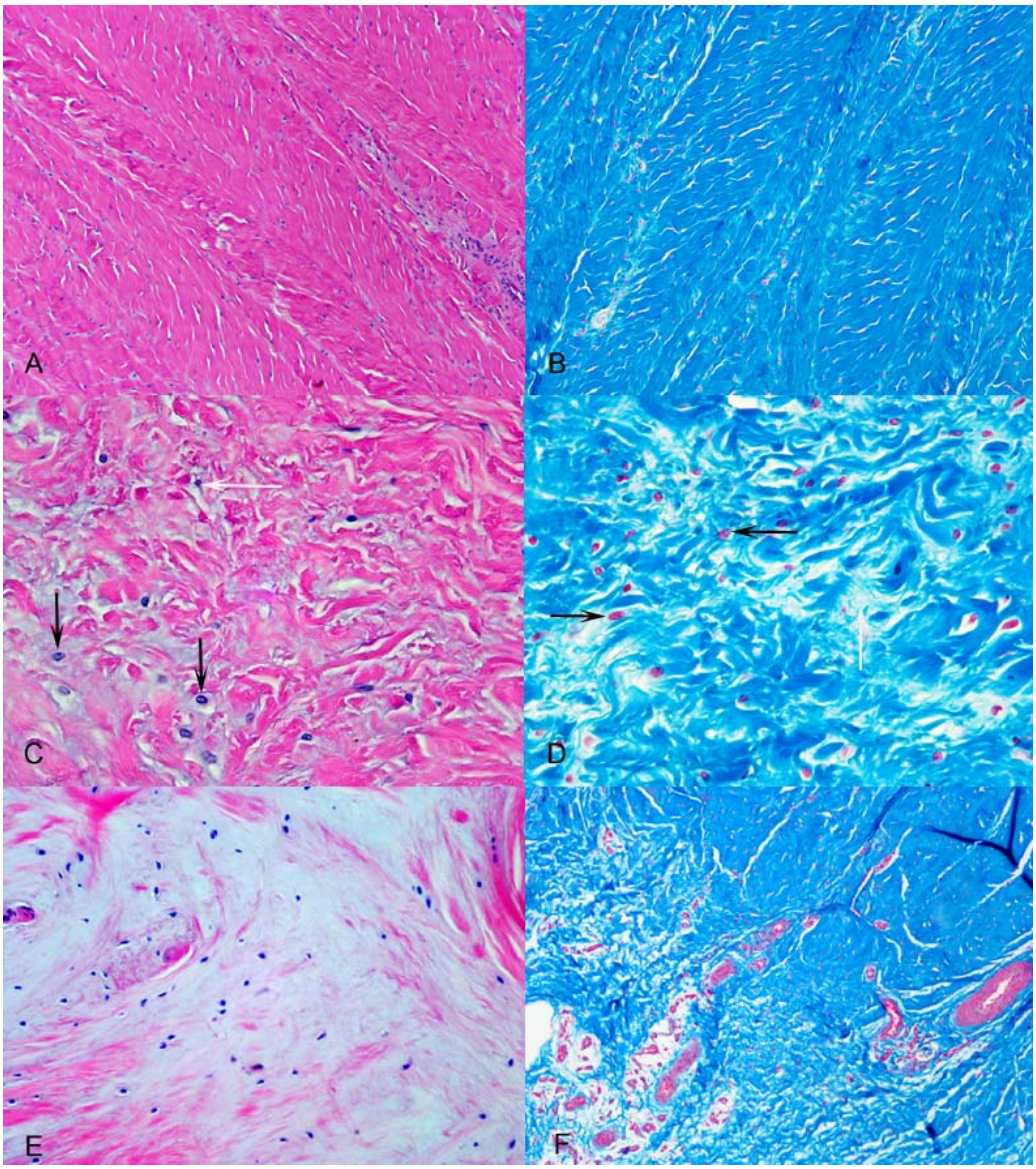

Figure 9: Comparison of microscopic changes in the collateral branch of the collateral sesamoidean ligament (CSL) between non-operated (A, B) and operated (C – F) limbs at 360 days post-surgery (Left: Hematoxylin and Eosin, Right: Masson's trichrome).

A, B.) Non-operated CSL branch. Densely packed collagen fibers arranged in compact, parallel, uniform bundles (fasiculi).

C, D.) Operated CSL branch. Collagen fibers arranged in loose, haphazard, interweaving pattern with no formation of fasciculi. Increased cellularity, fibroplasia (black arrows) and immature wavy collagen fibrils (white arrows).

E.) Operated CSL collateral branch. Collagen fibers (pale red) widely dispersed and replaced by pale basophilic chrondromucinous and cellular matrix (cartilage metaplasia). F.) Operated CSL collateral branch near transection site. Neovascularization and loose arrangement of collagen fibers in repaired ligament (lower left) compared to normal, resident ligament (upper right).

Table 1: Phillips 1 Tesla magnetic resonance imaging parameters for evaluation of the equine forelimb digit.

Slice Plane	Sequence	TR (msec)	TE (msec)	FA	FOV/ rFOV	Matrix Size	Slice #/ Width	Gap (mm)	Time (min)
Transverse	TSE T2	2116	100	90	15/10.5	256x512	30/4mm	0.5	**5:08
Transverse	TSE PD	2116	11	90	15/10.5	256x512	30/4mm	0.5	**5:08
Transverse	TSE PD	2000	30	90	15/15	512x512	20/2mm	0.2	2:54
Transverse	*STIR	1725	35	90	15/10.5	192x256	30/3.5mm	1.0	4:42
Transverse	3D GE	47	9	25	10/10	192x256	30/1.5mm	-1.5	3:13
Sagittal	TSE T2	3395	110	90	14/10	256x512	22/4mm	0.5	2:21
Sagittal	TSE PD	3395	14	90	14/10	256x512	22/4mm	0.5	2:21
Sagittal	*STIR	1500	35	90	14/10	256x256	22/3.5mm	0.5	5:48
Dorsal	3D GE	47	9	25	10/10	192x256	30/1.5mm	-1.5	3:13

*Inversion time (TI) for STIR sequences is 140 msec
**T2 and PD sequences are collected together during the TSE scan
TSE = Turbo spin echo
STIR = Short tau inversion recovery
3D GE = Three dimensional gradient echo
TSE PD = Proton density
TSE T2 = T2-weighted
TR = Repetition time
TE = Echo time
FA = Flip Angle
FOV/rFOV = Field of view/Relative field of view
Slice # = Number of slices
Width = Thickness of slice
Gap = Space between slices
Time = Actual scanning time for each sequence

Table 2: Post-Operative Exercise Protocol

Week	Exercise Protocol
3-8	Stall rest, 10 minutes hand walking daily
9-16	Small paddock turnout, 20 minutes walking daily
17-20	Small paddock turnout, 10 minutes walking, 20 minutes trotting 3 times weekly
20-26	Small paddock turnout, 10 minutes walking, 30 minutes trotting 3 times weekly
27-38	Pasture turnout, 20 minutes trotting, 20 minutes cantering 3 times weekly
39-52	Pasture turnout, 20 minutes trotting, 30 minutes cantering 3 times weekly

Table 3: Collateral sesamoidean ligament gross pathology measurements of non-operated and operated limbs at 360 days post-surgery.

CSL	Non-Operated Limb		Operated Limb	
Location	**Average Width ± SEM**	**Average Length ± SEM**	**Average Width ± SEM**	**Average Length ± SEM**
Medial Branch	1.6 ± 0.15	1.8 ± 0.12	1.5 ± 0.20	2.3 ± 0.17*
Mid-Medial	1.0 ± 0.0	NA	1.0 ± 0.05	NA
Midline	0.9 ± 0.07	NA	0.9 ± 0.07	NA
Mid-Lateral	1.0 ± 0.0	NA	1.1 ± 0.04	NA
Lateral Branch	1.4 ± 0.16	1.8 ± 0.14	1.6 ± 0.20	2.1± 0.13

*Significantly different from normal limb ($p < 0.05$)
CSL, collateral sesamoidean ligament; Mid-Medial, half way between midline and medial CSL branch; Mid-lateral, halfway between midline and lateral CSL branch.